Behavior of Tungsten under Irradiation and Plasma Interaction

Michael Rieth[1*], Russell Doerner[2], Akira Hasegawa[3], Yoshio Ueda[4], Marius Wirtz[5]

[1] Karlsruhe Institute of Technology, Institute for Applied Materials, Hermann-von-Helmholtz-Platz 1,76344 Eggenstein-Leopoldshafen, Germany, michael.rieth@kit.edu
[2] University of California at San Diego, Center for Energy Research, 9500 Gilman Drive #0417, La Jolla CA 92093, USA, rdoerner@ucsd.edu
[3] Tohoku University, Department of Quantum Science and Energy Engineering, Graduate School of Engineering, 6-6-01-2, Aramaki-aza-Aoba, Aoba-ku, Sendai 980-8579, Japan, akira.hasegawa@qse.tohoku.ac.jp
[4] Osaka University, Division of Electrical, Electronic and Information Engineering, Graduate School of Engineering, 1-1 Yamadaoka, Suita, Osaka 565-0871, Japan, yueda@eei.eng.osaka-u.ac.jp
[5] Forschungszentrum Jülich, Institut für Energie- und Klimaforschung, 52425 Jülich, Germany, m.wirtz@fz-juelich.de
[*] corresponding author

Keywords: tungsten, neutron irradiation, plasma interaction, high heat flux, surface modification, tritium retention

1 Introduction

In 1959 the Journal of Nuclear Materials (JNM) was founded and is now celebrating its Diamond Anniversary year. The present paper is part of a series in which single JNM-characteristic topics are reviewed both from a scientific as well as a historical point of view.
Tungsten is a body-centered cubic lattice structured transition metal with unique properties. It has the largest cohesive energy of all elements, including diamond (carbon), and thus not surprisingly, the highest melting and boiling point (3695 K and 5828 K) as well as the lowest vapor pressure ($8.15 \cdot 10^{-8}$ Pa at 2000 °C and 10^{-1} Pa at 3000 °C) of all metals. Its anisotropy coefficient is very close to one (A=1.010 at room temperature), which means that with regard to elasticity, tungsten behaves nearly isotropically. With a Young's modulus of 411 GPa, tungsten is one of the stiffest metals exceeded only by Iridium (582 GPa), Osmium (560 GPa), Rhenium (463 GPa), and Ruthenium (447 GPa). Nevertheless, severe drawbacks like a catastrophic oxidation behavior or a rather low toughness prevented tungsten from its use in most structural applications.
In any case, as a functional material, tungsten is well-known for many high-temperature applications (in inert atmosphere or vacuum, as a matter of course) in the lighting industry, cathode ray tubes, X-ray tube cathodes and anodes, furnace heaters and shields, glass fiber production, but also for armor penetrating ammunition, and to some extent in aerospace engineering. Due to its high density (19250 kg/m^3), tungsten is a very effective X-ray absorber material and thus plays an important role in radiation shielding. It is a maybe less known coincidence that the density of gold matches nearly the density of tungsten (but not the price), which frequently leads to speculations of a vast conspiracy that the world's gold supplies are being debased by filling gold ingots with tungsten (e.g. business insider, Sep. 19, 2012). However, about 66 % of the global tungsten consumption is allotted to cemented carbide products, and about 17 % to the alloying of steel and other materials. This means that world-wide only 11 % is used for mill products and 6 % for other applications (International Tungsten Industry Association, London, 2011).
Historically, a significant part of tungsten-related research was and still is dedicated to chemistry. With its use as filaments in incandescent lamps, tungsten-associated research in materials science rapidly increased and led to some astonishing achievements – even though unintentionally in the one or other case. Today, oxide dispersion strengthening (ODS) is an important practice in physical metallurgy. In the case of thoriated tungsten, this technology was applied already in 1913, that is, long before the ODS mechanism was known. Also, the discovery of high-temperature creep strengthening by soft dispersoids goes back to materials processing in the period of 1910-1925. Tungsten materials that were processed in certain clay crucibles turned out by a fluke to be extraordinary stable. Consequent chemical analysis showed a pick-up

of potassium, aluminum, and silicon during powder processing, but mainly potassium remained in the sintered material, which formed tiny bubbles. Ongoing materials research led later on to the strongest man-made refractory alloy (i.e. at temperatures above 2000 K): precipitation hardened W-Re-HfC [1].
Beside the invention of the modern design of x-ray tubes by William Coolidge in 1913, other important tungsten-related scientific and technological discoveries during the early 20th century are closely related to the work of the Nobel Prize laureate Irving Langmuir (see Section 2). Since the late 1950s, tungsten was used in neutron irradiation experiments for various basic material studies. Later on, proton irradiations were investigated with a focus on the use as spallation target. But tungsten never gained much importance as a nuclear power material, that is, it never played a significant role in commercial fission reactor technology. However, it was considered as candidate material for advanced technologies, like for example, in space nuclear power systems. Therefore, many design-relevant engineering and technological data on tungsten were produced already in the early 1960s [2–4]. This work was continued and finally compiled within the SP-100 Program – a cooperation among the NASA, the DOE, and the DARPA [5]. Without any doubt, tungsten materials have achieved by far the highest interest in nuclear fusion research. Especially the International Thermonuclear Experimental Reactor (ITER) project and the decision for tungsten as an armor material was the main driver for an amazing increase in tungsten-related publications regarding irradiation and plasma interaction. Moreover, the world-wide ambitions towards a fusion demonstration reactor (DEMO) have recently initiated comprising irradiation projects and plasma experiments. Therefore, the interest in tungsten materials from a technological as well as a scientific viewpoint is currently as high as probably never before.
The following Section 2 provides an overview on the history of tungsten research. It starts with the area before 1959. Some statistics on tungsten publications since the foundation of JNM highlight the main topics and stakeholders. The chapter ends with a brief literature survey. Section 3 gives an overview on tungsten materials, which are relevant for this paper. In the succeeding Sections 4-7 the following topics are reviewed: neutron irradiation, plasma surface interaction, synergistic effects of neutron irradiation and plasma interaction, and high heat flux effects.

2 Historical Development

2.1 Tungsten-related publications before the foundation of the Journal of Nuclear Materials

In 1564, Johann Mathesius – a German priest and teacher – was the first to mention the mineral wolframite in literature [1,6]. The mineral Scheelite was mentioned by A. F. Cronstedt in 1757 and in 1783 metallic tungsten was first prepared by Don Juan Jose de Elhuyar and his brother Fausto by reduction of tungstic acid with powdered charcoal as proposed by T. Bergmann two years earlier. Finally, R. Oxland can be considered as the real founder of systematic tungsten chemistry in 1841. He gave procedures for the preparation of sodium tungstate, tungsten trioxide, and tungsten metal. Oxland also patented procedures for ferrotungsten production in 1847 and 1857, which is the basis for high speed steels (sources and more details are given in [1]).
According to the Scopus database, scientific publications on tungsten date back to 1860 when the first article on “tungsten steel” appeared in the Journal of the Franklin Institute [7]. During the 19th century there were only 19 tungsten-related publications, which mainly treated the effect of tungsten in steels (ferrotungsten) [8–11], its atomic weight [12–15], and of various chemical reactions [16–18].
At the beginning of the 20th century tungsten was mainly used as alloying element in steels and for electric lamp filaments. During the industrialization in the following 40 years the number of tungsten-related inventions and applications increased significantly. Cemented carbides or hard metal (tungsten carbide plus cobalt), stellite, tungsten heavy alloys (W-Cu, W-Ag, W-Ni/Fe), x-ray cathodes, electronic tubes and welding rods are just a few examples (a detailed overview is given in Wah Chung’s “tungsten tree” in [1]). Therefore, it is not surprising that the number of publications on tungsten increased to a few hundred in the period from 1900 until the early 1940s. Nevertheless, this period was dominated by all kind of studies related to lamp applications. More than one third of the articles were about recrystallization and sagging of incandescent tungsten wires, filaments, high temperature phenomena as well as reactions with gases, carbon, water vapor and alkali metals. During that time, obviously the main driver for applied tungsten research was the lifetime extension of light bulbs, which led to the development of doped tungsten – first

by thorium-oxide (thoriated tungsten) and later on by other refractory oxides (e.g. hafnium, zirconium or cerium oxide) and by potassium.
It is very interesting that Irving Langmuir (Nobel Prize laureate in Chemistry in 1932) made his first scientific contributions in the area of incandescent light bulbs during that period [19–26]. Further, he improved the diffusion pump, he discovered the lifetime extension by filling the bulb with inert gases and he increased the bulb efficiency by twisted filaments. Langmuir also discovered that molecular hydrogen introduced into a tungsten-filament bulb dissociated into atomic hydrogen and formed a monoatomic layer on the surface of the bulb. Moreover, he studied the emission of charged particles from hot tungsten filaments (thermionic emission). He gave these ionized gases the name "plasma" [27–29]. Together with Tonks [30–32], Langmuir discovered electron density waves in plasmas that are now known as Langmuir waves. He introduced the concept of electron temperature and in 1924 invented the diagnostic method for measuring both temperature and density with an electrostatic probe, now called a Langmuir probe and commonly used in plasma physics [33]. It is remarkable that some important fundamentals of today's nuclear fusion research (e.g. diagnostics, high temperature behavior of pure and doped tungsten, plasma physics, surface chemistry) are connected to Irving Langmuir and date back to the period from about 1910-1930. But the story doesn't end there. Langmuir put his discovery of atomic hydrogen to use by inventing the atomic hydrogen welding process – the first plasma weld ever made [34–40]. Plasma welding has since been developed into tungsten inert-gas welding (TIG) [41].
From 1940 to 1959 (the foundation year of JNM), several hundred scientific articles on tungsten were published of which about one-half fall into the category chemistry and the other half into physics and engineering. Within this period there were still many publications on light bulb applications ([42] provides one of the first reviews) and surface chemistry, but also on tungsten deposits, ore and production. Also during that time, the first articles on neutron interactions with tungsten (activation analysis, isotopes, decay, neutron resonances) were published [43–58]. Since 14 MeV neutrons play an important role in nuclear fusion, it is interesting that for the first fission cross-section studies on tungsten [59] a neutron source was used, which utilized the T+D→He+n reaction – the Los Alamos Van de Graaff. Before 1960, there were only three publications on neutron irradiation damage in tungsten. The first entry in the Web of Science database on neutron irradiation and its effect on the mechanical properties (in this case tensile properties) appears in 1957 [60]. Two irradiation damage and recovery studies were published in 1958 [61,62].
In summary, before the foundation of JNM, the estimated number of tungsten related publications ranges in the order of 1000 and only very few were about irradiation while the topic "plasma" was still in its infancy. The main subject areas of these papers were physics (25 %), chemistry (24 %), biochemistry (9 %), and engineering (9 %) (see Fig. 1, left). Note: According to the Scopus database with "tungsten" explicitly mentioned in the title of the article there were about 900 articles before 1960, but numerous other types of publications like specialist workshops, books or proceedings might not be considered by this simple approach. In addition, there are publications on this subject without the word "tungsten" in the article title. Therefore, the presented numbers have to be considered as a rough estimate – especially for the early 1960s and before.

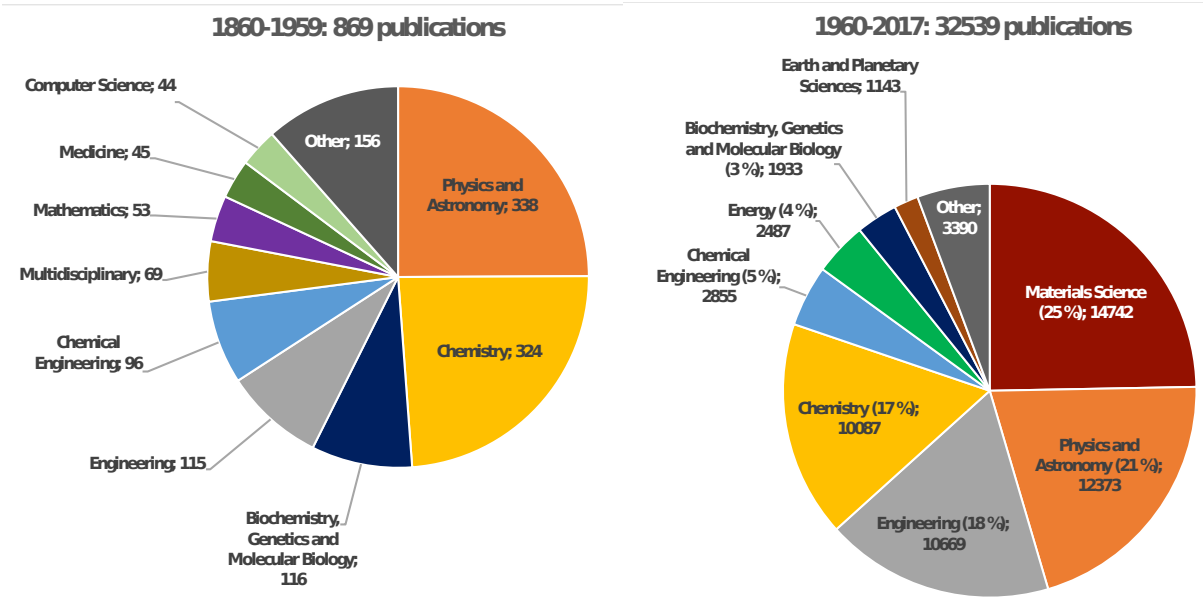

Fig. 1: Subject areas of publications from 1860-1959 (left) and from 1960-2017 (right) with "tungsten" in the article title (Scopus database, note: an article can be listed in several areas).

2.2 Some statistics on tungsten-related publications after the foundation year of the Journal of Nuclear Materials

From 1960 to 1987 the number of tungsten related publications steadily increased from 60 to roughly 600 per year. This level was more or less kept until 2003 and increased again from 650 articles in 2004 to more than 1500 papers per year in 2017. Since the foundation of JNM more than 32000 documents on tungsten have been published mainly in the subject areas materials science (25 %), physics (21 %), engineering (18 %), chemistry including chemical engineering and biochemistry (25 %), and Energy with 4 % (see Fig. 1, right). Due to the fact that each article can be listed in different areas, it is not possible to derive clear trends from the distribution in terms of key topics. In summary, the tungsten related publications from 1960-2017 can be divided into two main topics: materials/physics/engineering (64 %) and chemistry including chemical engineering and biochemistry (25 %).

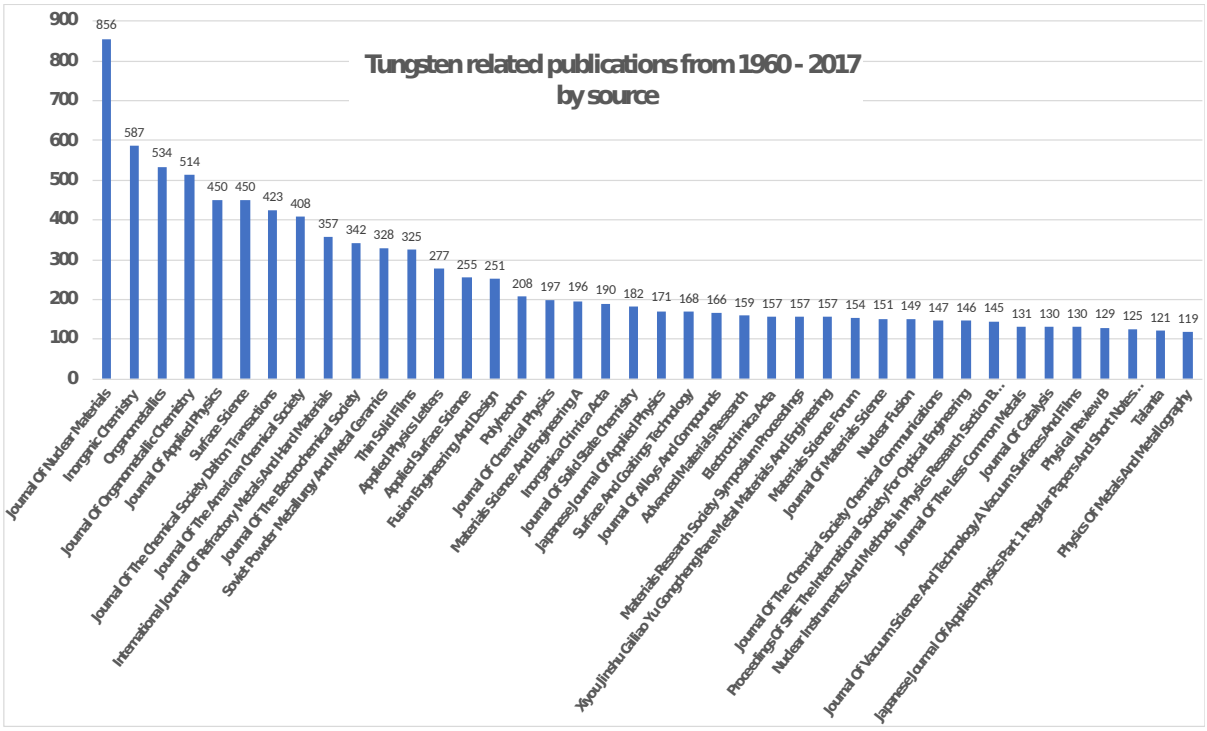

Fig. 2: Number of tungsten related publications ("tungsten" in the article title) in the period from 1960-2017. Only the leading 40 sources according to the Scopus database are listed.

A ranking of 40 journals with the highest number of tungsten related articles in the period from 1960-2017 is given in Fig. 2. This selection covers about 10200 documents, which correspond to 1/3 of the total tungsten publications from 1960-2017. With more than 850 publications (8 % within this top 40 list) JNM printed by far the highest number of articles per journal on tungsten.

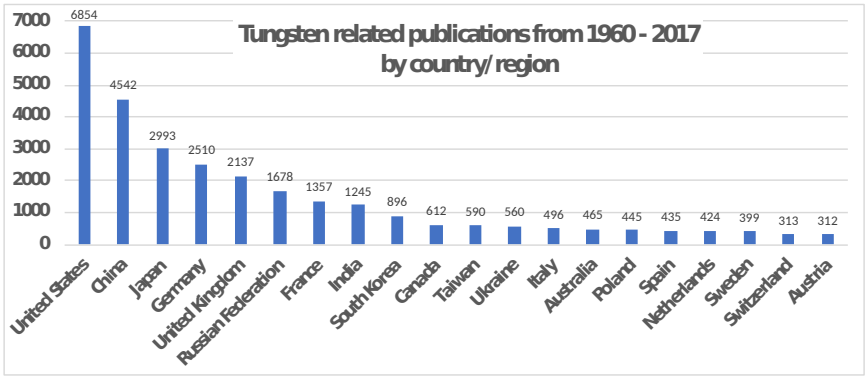

Fig. 3: Number of tungsten related publications ("tungsten" in the article title) in the period from 1960-2017. Only the leading 20 countries according to the Scopus database are listed. The average over a total of 125 countries is 260 publications per country.

The ranking of tungsten related publications by countries (also for the period 1960-2017) is plotted in Fig. 3. With over 6800 publications (21 %) the USA is clearly leading the list, followed by China with more than 4500 publications (14 %), Japan (3000, 9 %), Germany (2500, 8 %), the UK (2100, 7 %), and Russian Federation, France, and India (each less than 1700, 4-5 %), South Korea (900, 3 %) and Canada (600, 2 %). The number of publications decreases rather steeply in this ranking: the top ten countries (that are only 8 % of all ranked countries) published more than 76 % of all tungsten associated papers.

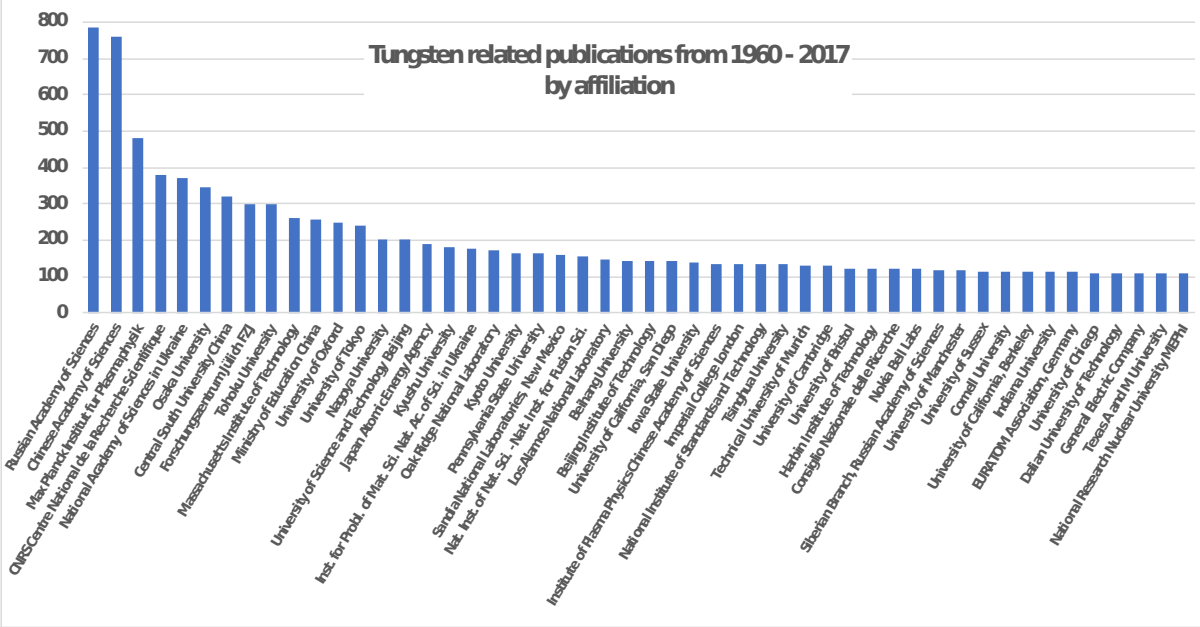

Fig. 4: Number of tungsten related publications ("tungsten" in the article title) in the period from 1960-2017. Only the leading 50 affiliations according to the Scopus database are listed.

The ranking of tungsten related publications by affiliation is shown in Fig. 4. It is a top 50 list that comprises 1/3 of all publications. The complete list of the Scopus database includes 160 affiliations, which contribute to 58 % (18840) of all publications (32713) with an average of 118 articles per affiliation. That is, the actual average for all affiliations (these are much more than 160) is certainly below 100 publications per affiliation, which highlights at least the top 10-15 in this ranking. With 783 and 758 publications, the Russian Academy of Sciences and the Chinese Academy of Sciences are clearly leading the list followed by the Max Planck Institute for Plasma Physics (479). In summary, the top five affiliations in the world regarding tungsten related publications are national academies or national institutions or national laboratories.

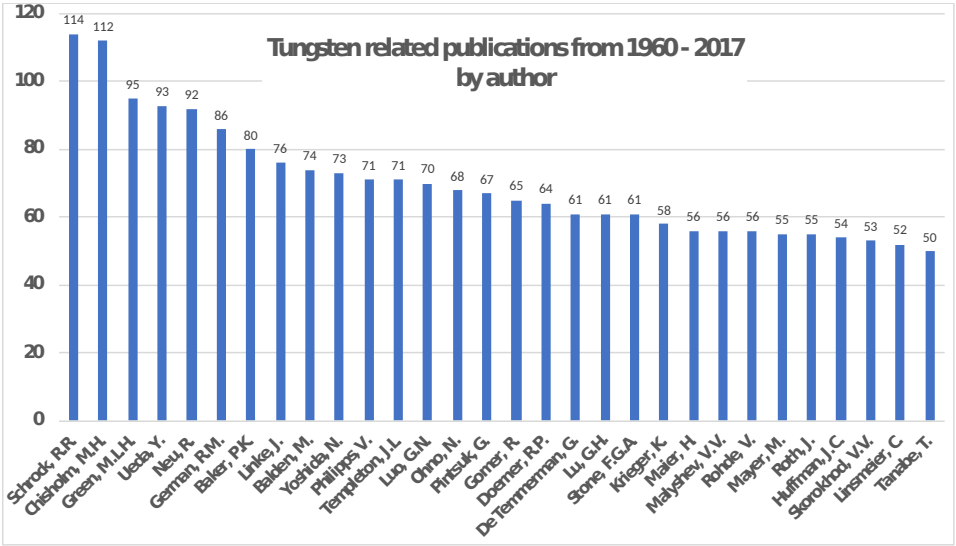

Fig. 5: Number of tungsten related publications ("tungsten" in the article title) in the period from 1960-2017. Only the leading 30 authors according to the Scopus database are listed.

In the tungsten related publications ranking by author (see Fig. 5) 18 authors out of the top 30 list published their tungsten related research work in the area of nuclear fusion (of which a substantial part is covered by JNM). This clearly demonstrates the important role of tungsten research for this topic. Moreover, nine authors contributed to the area chemistry (including surface chemistry) and three authors published in the

area materials science (including modelling). It is remarkable, that 12 of the 18 nuclear fusion focused authors are working at two German affiliations.
Important note: Whenever preparing, analyzing or citing statistics on publications, it is essential to indicate the underlying database. In this section, all statistics are based on the Scopus database (query: “tungsten” in document title and publication year 1960-2017). A comparison with other databases, like for example Web of Science, leads to similar general results, but the particular ranking sequences deviate from each other due to individual categorization in the different databases. This is especially true for Figs. 1 and 5. Nevertheless, the trends and over-all conclusions are still in good agreement, independent of the database.

2.3 Publications on the effect of irradiation and plasma interaction on tungsten

In the case of tungsten, macroscopic irradiation effects are typically caused by neutron or high-energy proton irradiation while ion irradiation only shows effects near to surfaces or in thin films. The interactions of tungsten with high-energy electron and laser beams can be restricted mainly to thermal effects.
A “side-effect” of electron irradiation is the generation of bremsstrahlung using tungsten as a target material, which has been studied more intensively by means of energy spectra and angular distribution since the 1970s (e.g. [63–72]). Bremsstrahlung is electromagnetic radiation produced by deceleration of electrons (or more generally of charged particles), in the present case, due to deflection by the tungsten lattice nuclei. The main application in connection with tungsten is the X-ray tube [73–84], in which electrons are accelerated in a vacuum by an electric voltage onto a tungsten anode.
Inelastic scattering of high-energetic protons (in the order of 1 GeV) with heavy nuclei (e.g. tungsten) leads to the production of neutrons during deexcitation of the target (tungsten) nuclei. This process is called nuclear spallation and is used in neutron sources that are not based on nuclear fission. The European Spallation Source (ESS) is a most recent international project example. Transmutation (isotope and gas production), microstructural damage, and surface modification are typical topics that have been studied since the early 1970s (e.g. [85–99]).
In connection with neutron irradiation, the setup or refinement of nuclear databases for neutronic calculations and related validation experiments is another area where tungsten materials are involved. Decay, activation, and displacement cross-sections are typical results of benchmark experiments that have been published since the 1990s (e.g. [100,101,101–113]).
Beside the three above mentioned topics, the main field in which irradiation and plasma interaction with tungsten come into play is nuclear fusion. In all current power reactor concepts (demonstration reactor, DEMO) the in-vessel components are foreseen to be protected by a tungsten armor layer or by massive blocks (see [114–116] and references therein). The problem in the related component design and materials development is the unique operating scenario in such future fusion reactors: the load on the tungsten armor parts is a multi-dimensional dynamic overlay of (i) neutron irradiation, (ii) impacting particles (plasma surface interaction), and (iii) extreme thermal stresses (or high heat flux effects). Since there is no test device in which this specific scenario could be simulated (such a device would be the reactor itself), the effects have to be studied separately. And even this single effect studies require costly large-scale facilities.
Neutron irradiation effects are mainly studied by nuclear fission materials test reactor experiments, even though the neutron spectra differ significantly. High flux neutron spallation sources to produce a fusion typic neutron spectrum are still in the planning stage (IFMIF, DONES). Investigations on the damage mechanisms, damage recovery, defect types, and microstructural changes have been continuously performed since the late 1950s ([117–143]). The same is true for studies on the neutron irradiation induced change of mechanical and physical properties ([144–160]) as well as the volumetric change – the so-called swelling ([161,162]). Transmutation is also a typical effect of neutron-nuclei interaction, which changes the chemical composition of materials. As a result, gas bubbles (e.g. hydrogen, helium) or rhenium-osmium precipitations may form in tungsten and lead to further material degradation. Corresponding studies are, for example, published in [163–180]. Due to the expensive fission reactor experiments, a few attempts have been made to simulate neutron damage by the use of proton beams [181,182]. But much more effort has been spent on the use of ion irradiation (see below).
Investigation on plasma surface interactions with tungsten are mainly based on experimental fusion (reactor) facilities (e.g. JET/CCFE, ASDEX upgrade/MPI-IPP), plasma generators (e.g. PISCES/UCSD, Magnum

PSI/DIFFER), helium/hydrogen beam facilities (e.g. GLADIS/MPI-IPP), or ion accelerators. The topic can be subdivided into three areas: (1) lattice defects, recovery, microstructure change (e.g. [183–226]), (2) surface modifications (e.g. [191,206,209,222,225,227–278]), (3) diffusion and retention of hydrogen (deuterium, tritium) and helium (e.g. [279–308]). With the steady increase in computing power and progress in micro/nano-mechanical testing and microscopy, a new research area has been established: the simulation of neutron irradiation damage in tungsten by ion irradiation and/or ion implantation in combination with various kinds of modelling approaches. The computational studies were also extended to plasma-surface interaction and other general irradiation effects. An overview on the progress of recent years in the different research directions can be obtained by [309–354].

High heat flux effects in tungsten or extreme local thermal stresses are closely related to the so-called divertor armor parts in nuclear fusion reactors (see [355–358]), but also to X-ray anodes, nuclear spallation targets or to the thermal management of high power semiconductors. In many studies the extreme heat load is generated (or simulated) by electron beams on water-cooled (e.g. JUDITH/FZJ) or helium-cooled targets (e.g. HELOKA/KIT). Especially in fusion research, neutral hydrogen/helium beams, plasma generators, experimental tokamaks or lasers are also deployed for heat flux tests. A selection of investigations on extreme heat and thermal shock tests with tungsten from the past 5 years is given in [359–407] and references therein.

From the high number of publications, it can be clearly seen that the interest in plasma surface and high heat flux effects has been dramatically heightened in the past two decades due to the International Thermonuclear Experimental Reactor (ITER) project. During this period the decision has been taken to use tungsten as the armor material for one of the main in-vessel components, the water-cooled divertor [362,408–437]. In addition, this triggered the setup of various test facilities and comprising international mock-up testing programs.

A literature survey on the present subject “Behavior of Tungsten under Irradiation and Plasma Interaction” based on the Scopus database (see Fig. 6) leads to more than 700 articles (note: the survey doesn’t claim completeness, but should show the correct trend). As mentioned above, the area “ion irradiation”, “high heat flux tests”, “modeling” and “divertor” became rather popular in the last 2 decades due to their impact on nuclear fusion. Publications of the other topics are more or less equally distributed over the whole period of interest. In any case, JNM is the most important source for the subject. More than 30 % of the papers were published in the JNM while all nuclear fusion related journals (Fusion Engineering & Design, Nuclear Fusion, Fusion Science & Technology, etc.) together printed only about 20 % of the articles.

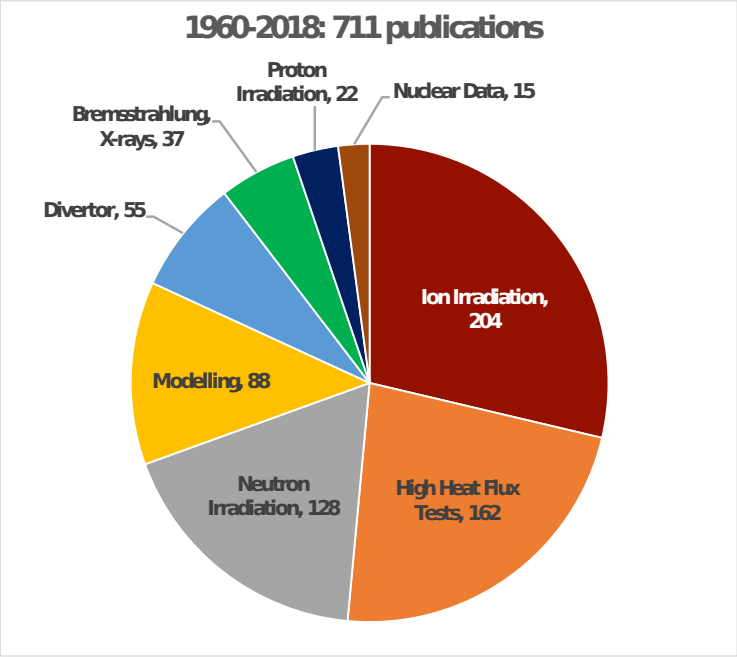

Fig. 6: Subject areas of publications on tungsten irradiation and plasma interaction from 1960 until July 2018, investigated by the Scopus database. Remarkably, more than 30 % of the articles were published by the JNM.

The progress in nuclear fusion technologies also gave rise to numerous tungsten materials development and characterization activities as well as to technological studies in which also fabrication processes play an important role. From 1960 to July 2018, more than 280 papers in these areas have been identified in the Scopus database. Since the majority of tungsten applications are within the nuclear field, it is not so surprising that JNM is the leading source here, too. JNM published about 20 % of all articles that are associated with tungsten materials development, characterization, and fabrication. For comparison, second and third are Fusion Engineering & Design (12 %) and the International Journal of Refractory Metals and Hard Materials (7 %). In the following section, the past and current trends in tungsten materials development are reviewed in more detail.

3 A brief overview on tungsten materials

Since the early 19th century, the principal production route of tungsten and tungsten alloys is by powder metallurgy. Melting technology has never reached industrial significance due to the required high temperatures and also due to the resulting coarse microstructure of the "as cast" tungsten materials [1]. The main production steps are powder fabrication, powder compacting, and sintering. To reach full density or a certain shape of the semi-finished products, final forming processes have to be applied.

Ammonium Paratungstate ($(NH_4)_{10}(H_2W_{12}O_{42})\cdot 4H_2O$, APT) is the most important and almost exclusively used precursor for tungsten powder. Other intermediate powder products, such as tungsten trioxide (WO_3), tungsten blue oxide (WO_{3-x}, TBO), tungstic acid (H_2WO_4), and ammonium metatungstate ($(NH_4)_6(H_2W_{12}O_{40})\cdot xH_20$) are derived from APT. The most important starting materials for the production of tungsten powder are tungsten trioxide, tungsten blue oxide or tungstic acid. The actual powder fabrication relies on hydrogen reduction according to the overall equation $WO_3 + 3\ H_2 \rightarrow W + 3\ H_2O$ at temperatures between 600-1100 °C in a streaming hydrogen atmosphere [1].

Due to its high hardness, tungsten powder is not easy to compact. Nevertheless, in most cases compaction is performed without lubricant to avoid contamination. The main routes are uniaxial pressing in rigid dies and hydrostatic pressing in flexible molds. Depending on the applied pressure, particle size, size distribution, particle shape, and size of the compact, the green density is in the range of 55-65% of the theoretical density (75% at most) [1].

During tailored sintering processes, the green compacts are densified to a degree that is sufficient for subsequent thermomechanical processing. Sintering of tungsten is commonly carried out between 2000 and 3000 °C under flowing hydrogen, either by direct sintering (self-resistance heating) or indirect sintering (resistance element heating systems). The final density is commonly in the range between 92 and 98% [1].

With few exceptions, tungsten is used in the form of pore-free preforms ("wrought" P/M tungsten). To obtain a fully dense material with certain mechanical properties, a complex, multistage, hot and cold forming process is required. The most important forming techniques for tungsten are rolling (for rods and sheet products), round forging (for large diameter parts), swaging (for rods), forging (for large parts), and drawing (for wires) [1,438].

Alternative tungsten production processes are plasma spraying, chemical vapor deposition, sputtering (physical vapor deposition), arc melting, and electron beam zone melting (for the production of larger single crystals). Powder or metal injection molding (PIM, MIM) is another alternative process, which enables the mass fabrication of near net-shaped parts [372,439–450].

Cemented carbides compose a very important and large group of tungsten materials, but they are rarely of interest in connection with irradiation or plasma interaction. This leaves, beside pure tungsten, four classes of tungsten materials (see Fig. 8): (i) doped tungsten (alternative terms: dispersion strengthened, grain stabilized tungsten), (ii) solid solution (or substitutional) tungsten alloys, (iii) ternary and multi-component alloys, and (iv) tungsten composites (tungsten heavy metals, two-phase tungsten alloys).

Pure tungsten has a melting point of 3695 K (3422 °C), a low coefficient of thermal expansion (4.5 µm/m/K), a high thermal conductivity (173 W/m/K), and a high Young's modulus (411 GPa). One of the main draw-backs of tungsten for most structural, but also many functional applications, is its severe brittleness with rather high ductile-to-brittle transition temperatures (DBTT). Its mechanical properties strongly depend on the microstructure (in particular, grain size and texture), and therefore, on its production history. For example, recrystallized tungsten shows a typical hardness of only about 300 HV30 and a DBTT of more than

1000 °C (measured by Charpy tests), compared to fine-grained worked tungsten with values up to 650 HV30 [584] and a DBTT of 500-600 °C. On the other hand, recrystallization depends strongly on the deformation degree (cold working) and can be as low as 900-1000 °C. Therefore, the basic objective in tungsten materials development and fabrication is to produce a tailored microstructure that provides the desired properties and to stabilize this specific microstructure with respect to high temperatures or other loads (e.g. irradiation interactions).
In the case of solid solution tungsten alloys in principle both goals may be met: a finer microstructure (this leads to a better high temperature strength) and an increased recrystallization temperature. However, as indicated in Fig. 7, there are only few elements (Ti, V, Nb, Mo, Ta, Re), which are soluble in sufficient concentrations in the tungsten lattice, and unfortunately, all of them – with the exception of rhenium – either increase the DBTT or reduce toughness [451]. Thus, none of these binary (but also ternary) tungsten base alloys has attained commercial importance and so the only significant solid solution tungsten alloy today is tungsten rhenium [1]. Rhenium additions increase the ductility of wrought products at low temperatures and also improve their high-temperature strength and plasticity. Furthermore, rhenium additions stabilize the grain structure, increase the recrystallization temperature, reduce the degree of recrystallization embrittlement, and significantly improve the weldability. Finally, W-Re alloys also exhibit superior corrosion behavior than unalloyed tungsten. The only drawback of rhenium is its high price (they are more expensive compared to tungsten by about two orders of magnitude). The most important alloy compositions are W-(3-5)Re, W-10Re, and W-(25-26)Re. Alloys with 5% rhenium exhibit the hardness minimum and highest creep strength while alloys with >8% rhenium show good workability and have significantly better welding properties. The 3-10% rhenium range is extremely resistant against alternating thermal stresses, which for example, occur in X-ray anodes with high-energy electron beams [1].

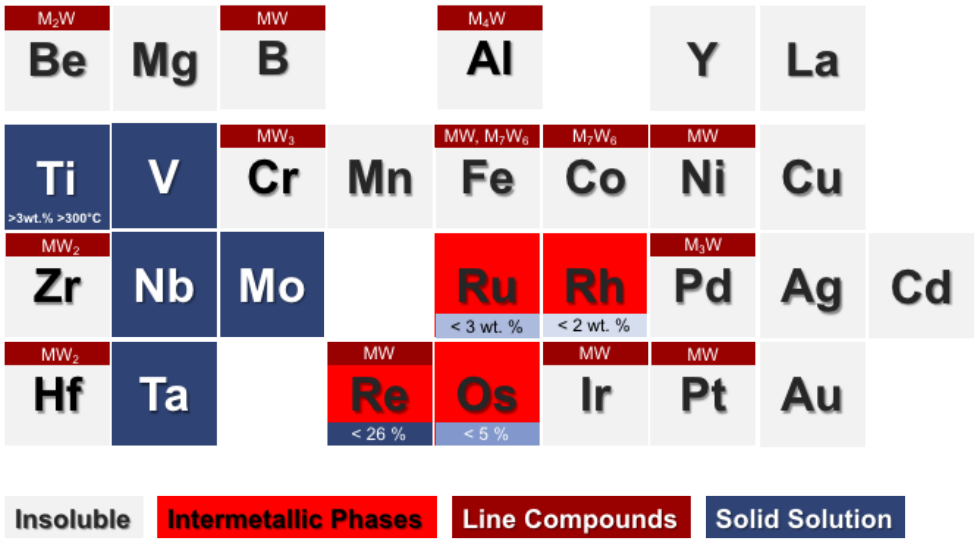

Fig. 7: Overview on typical metallic two-component tungsten phases at lower temperatures. The elements are either insoluble, form intermetallic phases in an extended concentration range, form stoichiometric (line) compounds with indicated ratios, or form solid solutions (in some cases just within certain limits).

The main effect of doping tungsten by an insoluble second phase consists in stabilizing the microstructure, that is, the recrystallization temperature is increased. Depending on the specific dopant, strength and creep resistance is improved while the elastic and physical properties remain almost unchanged. Potassium doped tungsten wires (also referred to as AKS doped, non-sag, or WVM tungsten in lamp industry) show an outstanding creep resistance due to rows of potassium-filled bubbles (they are gaseous at working temperatures), which are aligned in rows parallel to the wire axis. These bubbles act as barriers for grain boundary migration in the radial direction. This can shift the recrystallization temperature to over 1800 °C. Wire drawing with intermediate recrystallization steps forms an interlocking long-grained microstructure, which gives the lamp wire its so-called non-sag properties (sagging due to its own weight). Potassium doping can also be applied to plate and foil production. More details on the fabrication steps, properties and applications are given in [1,452] and references therein. Historically, oxide dispersion strengthening

(with the “side effect” of stabilizing the grain boundaries) in tungsten refers to the use of ThO_2, which was later on replaced by La_2O_3, Y_2O_3, CeO_2, or ZrO_2 as a second phase. Like potassium doped tungsten, the formation and distribution of ODS particles are a result of multi-step deformation and annealing processes. Since thoria and lanthana additions lower the electron work function, these materials are used in X-ray tubes, discharge lamps and as electrodes for tungsten inert-gas (TIG) welding [1]. As an alternative to oxide dispersion strengthening, the use of carbide dispersoids like TaC, NbC, TiC, or ZrC has also been investigated [453], but proved to be much less effective above 1900 °C compared to HfC. Unfortunately, HfC cannot be doped by powder metallurgy due the oxygen affinity of hafnium [1].

The so-called tungsten heavy metal alloys are composite materials consisting of tungsten particles (typically 90-98 wt.%) embedded in a binder matrix of Ni-Fe or Ni-Cu-(Fe). Due to the binder matrix, these alloys are ductile and easy to machine. They have a much higher elasticity modulus than steel and show a high absorption for X-rays and gamma-rays but have limitations on their upper use temperature due to the moderate melting point of the binder material.

More recent research focuses on tungsten-fiber reinforced tungsten composite materials with unique properties regarding high temperature strength and pseudo-plasticity [454–463]. Other composite developments make use of the special ductility of tungsten foils (ultra-fine-grained tungsten). Laminating tungsten sheets with binding layers (e.g. Cu, CuAg, V, Zr, Ta) enables the fabrication of composite parts (plates, pipes) that combine the beneficial properties of both phases [464–468].

A rather specific class of tungsten alloys – self-passivating alloys - addresses another major draw-back, which is the catastrophic oxidation behavior of tungsten. These are ternary and quaternary alloys that form a stable surface layer in the case of an (possibly accidental) oxygen contact. This layer prevents then the contamination of the environment by highly volatile tungsten oxides. Otherwise, i.e. under operational conditions in vacuum or inert atmosphere, the alloys keep their properties – thus the alternative denomination “tungsten smart alloys” [469–476].

Yet another composite material class was derived by the use of tungsten wires, fiber, and meshes as a reinforcement of copper base alloys: the copper-tungsten composites (e.g. [460,477–489]). Also tungsten particle reinforcement was applied to copper materials including the production of functionally graded parts (e.g. [490–496]). These copper base composites could play an important role in nuclear fusion technology and thus have some significance to the given topic.

An overview of the various tungsten materials is given in Fig. 8.

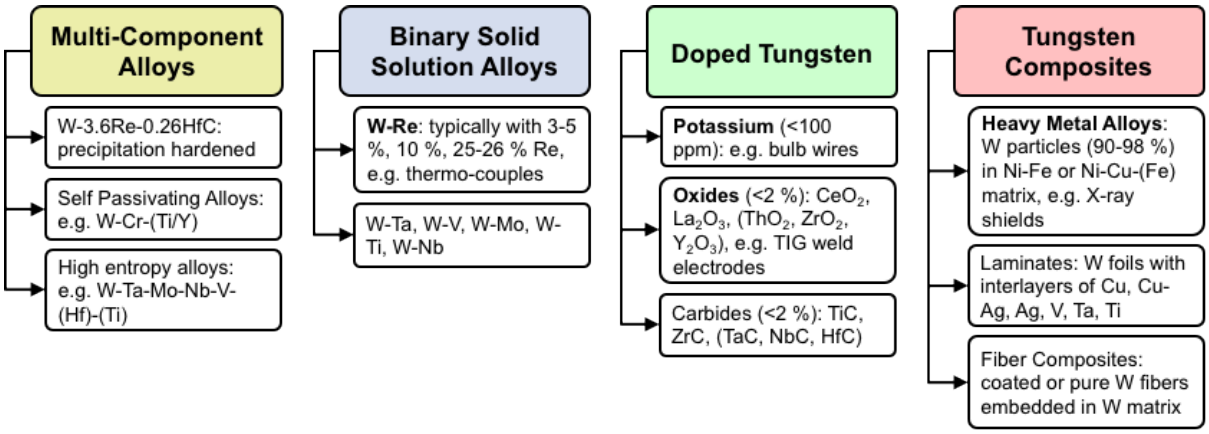

Fig. 8: A classification of tungsten materials. Multi-component alloys are typically produced by melt metallurgy (sometimes by mechanical alloying/sintering). Binary solid solution and doped tungsten alloys are produced by sintering. Tungsten composites are most often fabricated by liquid phase sintering or by a combination of CVD and PVD. Only the highlighted (bold) materials are of commercial relevance.

Note: Within the recently fashionable group of high entropy alloys there is a special class of refractory high entropy alloys that often contains a significant amount of tungsten. But so far, no compositions with promising properties regarding nuclear applications have been reported [497–500].

4 Neutron Irradiation

Neutron irradiation study of tungsten (W) started around the end of the 1950s to elucidate the point defect and radiation hardening behavior of refractory metals including molybdenum (Mo). Makin and Gillies published the effect of neutron irradiation on the mechanical properties [60] and Kinchin reported the damage recovery behavior of these metals after neutron irradiation at 30 ℃ and -196 ℃ in the British Experimental Pile (BEPO) [501]. The neutron doses in this study were up to 2×10^{19} neutrons/cm^2 (fast neutron; denoted hereafter as n/cm^2). Information regarding the defect recovery stage was expected to obtain by comparing BCC metals with FCC metals, which were used for point defect and irradiation damage studies in the early 1950s. Electrical resistivity measurement was primarily used to obtain activation energy of the defect recovery.

Kinchin reported the activation energy of three recovery peaks of neutron irradiated W, at -150 ℃ with an activation energy of 0.25 eV, and at -80 ℃ and 320 ℃ with activation energies of 0.48 eV and 1.7 eV, respectively [501]. Thompson reported the damage recovery of W after neutron irradiation at 4 K (-269 ℃) and 77 K (-196 ℃) and suggested that vacancies in W migrated at 400 ℃ with an activation energy of 1.7 eV, and recovery above -170 ℃ was attributed to the release of interstitials from traps associated with impurity atoms and dislocation [117]. The free interstitial in W was assumed to become mobile below -170 ℃. Schultz reported a vacancy formation energy of 3.3 eV in W based on vacancy recovery experiments introduced by quenching without irradiation [502].

The point defect and defect cluster images in metals could be directly observed using field ion microscopy (FIM). To obtain an image of the arrangement of atoms at the surface of a sample material using FIM, an exceedingly sharp tip was required that could tolerate the high electrostatic fields in FIM; refractory metals with high melting temperature (W, Mo, and Pt) were conventional objects for the FIM experiment. Muller reported the direct observation of defects of ion irradiated W using FIM [503]. Brandon et al. also reported similar results via ion irradiation [504]. Bowkett et al. reported vacancy and vacancy clusters of neutron irradiated W (5×10^{17} n/cm^2) [505]. Attardo irradiated W wires in the Brookhaven National Laboratory graphite reactor with a dose of 10^{18} n/cm^2 at 70 ℃ and 400 ℃ and reported direct observation of defects recovery using FIM. They concluded that isolated vacancy can be removed above 700 ℃, which corresponded to stage IV recovery [506]. Based on these studies, Jeannotte concluded that vacancies were responsible for the recovery stage at 870 ℃ in irradiated tungsten and their energy of motion was 3.3 eV [507]. Keys et al. demonstrated the effect of impurities, including Rhenium (Re) transmuted from W by (n,γ) reaction, on the point defect recovery stage III and other regions [508]. Keys et al. also reported vacancy clusters annihilation in the temperature range of approximately 300 ℃ to 900 ℃ in fast neutron reactor irradiated W at 70 ℃ [118,129,509,510]. While indicating the Re effects on the recovery behavior, they also reported recovery behavior of neutron irradiated W-25% Re alloys. They reported shift in recovery peak temperature of 0.17 T_m and 0.31 T_m and concluded that lattice weakening effects of Re altered the migration energy for defect recovery at least at the higher Re concentration [511]. Jeannotte reported kinetics of vacancy removal in neutron irradiated W using FIM and concluded that the activation energy for self-diffusion was consistent with a vacancy mechanism [512]. The point defect behavior of various BCC metals including W were summarized by Schultz in 1968 based on electrical resistivity and FIM [513].

In and around the 1960s, research regarding point defect behavior in metals started using electron beam irradiation. Subsequently, they also expanded the use of neutron irradiation in fission reactors. Since the 1960s, transmission electron microscopes (TEM) were used to characterize defect clusters, as a part of a research series on defects in refractory metals. The first report on TEM of neutron irradiated W was published by Lacefield [514]. The W single crystals were irradiated from 0.46 to 7.3×10^{19} n/cm^2 in ORR (Oak Ridge Research Reactor, USA) at reactor ambient temperature (70 ℃) [514]. Moteff et al. studied radiation behavior of refractory metals that primarily included W and Mo using fission reactors from the late 1960s [145,515–521]. Rau et al. reported the comparison of microstructure obtained via TEM observation with mechanical properties of neutron irradiated W irradiated from 10^{18} n/cm^2 to 1.2×10^{20} n/cm^2 (E_n > 1 MeV) at reactor ambient temperature in ORR and ETR (Engineering Test Reactor) in Idaho. They reported severe hardening and brittleness tested at 400 ℃ and obtained defect cluster images using TEM. The as-processed W exhibited brittle fractures after neutron irradiation, and the fracture stress was reduced to approximately 1/10 of that prior to neutron irradiation. While a tendency toward increased

strength due to neutron irradiation was observed, the same brittle fractures were observed in the heat-treated as well as un-treated W [145]. They also conducted characterization of observed dislocation loops in irradiated and 1100 °C annealed W, and reported that these were all vacancy type [515]. For irradiation at higher temperatures, where vacancies are mobile and voids grow, an increase in volume by void formation can also occur. This is called void swelling. In the case of W, Rau et al. conducted microstructural observation of neutron irradiated W from 1.3 to 1.8 × 10^{20} n/cm^2 at 1000 °C (0.35 T_m) and 1300 °C (0.43 T_m) in ETR, and reported void formation via neutron irradiation [516]. Sikka et al. conducted microstructural observation of fast reactor irradiated pure W. The W samples were irradiated in EBR-II (Experimental Breeder Reactor II, in Idaho, USA) to 1 × 10^{22} cm^2 at 550 °C (0.22 T_m). The EBR-II was a fast breeder reactor and it had high neutron flux and hard a neutron energy spectrum, therefore transmutation of W to Re by neutron capture reaction was expected to be below 1/10 of water-cooled fission reactors. It was the first report regarding void superlattice structure in neutron irradiated W [517], and they analyzed the superlattice parameters and compared them to that of other metals including Mo and Ta. Sikka et al. also conducted microstructural observation of relatively low temperature irradiated (430 °C and 530 °C) pure W in EBR-II. The irradiated fluence was approximately 1 × 10^{22} cm^2 (E_n > 1 MeV). They reported the presence of raft, which is a cluster of black spots and/or a cluster of small loops present on the habit planes. Voids were also observed but the presence of void lattice was not reported [22]. Steichen et al. performed neutron irradiation at 371–388 °C, under the conditions of 0.4–0.9 × 10^{22} n/m^2 (E > 0.1 MeV) in EBR-II, and conducted an evaluation of the post irradiation yield stress and elongation temperature dependence. Steichen observed an increase in the W yield stress, a decrease in the elongation, and an increase in DBTT after neutron irradiation from 65 °C to 230 °C [522]. Similar results were obtained by Moteff ([523], p. 114). However, the dose dependency on the irradiation hardening behavior of tungsten is given in Fig. 9. It can be clearly seen that the hardening depends not only on the neutron fluence, but also on the neutron spectrum. Since the cross-section for Re transmutation is much higher for low energy neutrons, the observed hardening is significantly lower in specimens that were irradiated in a fast reactor.

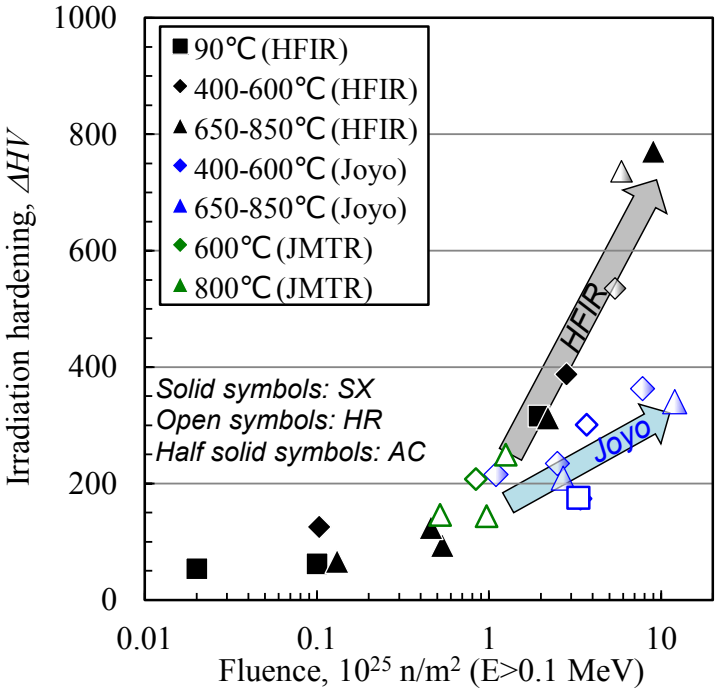

Fig. 9: Typical dose effect on hardening of tungsten after neutron irradiation. Compared to the neutron fluence, the irradiation temperature (from 90 °C to 850 °C) as well as the microstructure of the samples (SX: single crystal; HR: hot rolled and annealed; AC: produced by arc melting) have a minor effect on hardening. However, since the Re transmutation cross-section shows a maximum for thermal neutrons, irradiation hardening strongly depends on the reactor type in which the specimens are irradiated. Compared to the Japanese test reactor Joyo, the High Flux Isotope Reactor (HFIR, at Oak Ridge National Laboratory, USA) has a high peak in the low energy range of the neutron spectrum. Therefore, the formation of Re rich precipitations is much higher in samples that were irradiated in the HFIR, which leads to the observed additional increase in hardening [524]. This different behavior is indicated in the diagram by arrows.

To elucidate the neutron irradiation effects of W in fission reactors, Re effects on microstructural development, mechanical properties, and physical properties have to be considered. It is well known that W shows brittle behavior at room temperature and that this low temperature embrittlement can be improved using thermo-mechanical treatments and Re addition. Therefore, Re effects on radiation response of W have been studied. William et al. conducted neutron irradiation of W-5, 11, 25% Re alloys in the EBR-II reactor in the temperature range of 600 to 1500 ℃. The irradiation doses were between 4.3 and 37 × 10^{21} n/cm^2 (E > 0.1 MeV). They observed the microstructure using TEM and measured and reported the suppression of void formation and irradiation induced precipitation of Re_3W (χ-phase) [163]. The atomic scale resolution study regarding the radiation-induced precipitation of W-10 and 25% Re alloys was conducted using FIM by Herschitz [164,525]. The irradiation was performed up to 4x10^{22} n/cm^2 (E_n > 0.1 MeV) at 575, 625, and 675 ℃ in EBR-II. Williams suggested the formation mechanism of the precipitates. W and W-Re alloys were used as thermocouples in the reactor core area to measure the temperature of the fuel in fission reactors. Measurable drift during service in a reactor were reported and this behavior was believed to be caused by composition changes of the alloys constituting the thermocouple (TC) as a consequence of nuclear reactions. The compositional variation induced a decrease in the thermoelectromotive force; this means that the temperature was lower than the actual temperature. Vintanza et al. corrected the actual data of the reactor irradiated TC and proposed a recalibration correlation as a function of thermal neutron fluence [526].
In the 1990s, the effects of neutron irradiation on mechanical properties of W and other refractory metals continued to be studied. Gorynin et al. reported the mechanical properties of various types of W and Mo based alloys for fusion application irradiated to 0.1–2 × 10^{22} n/cm^2 at 100 to 800 ℃ in SM-2 and BOR-60 (Russia). They reported radiation embrittlement of the W and Mo alloys [527]. Krautwasser et al., used W and W-10%Re alloys in the material testing reactor FRJ2 (Julich) and HFR (Petten) up to a fluence of 5.6 × 10^{21} n/cm^2 (E_n > 0.1 MeV) at RT and 252 ℃ for neutron spallation target applications. They measured DBTT of the irradiated alloys using 3-point bending test, and reported DBTT of W to be approximately 880 ℃ after 4.4–5.6 × 10^{21} n/cm^2 [154].

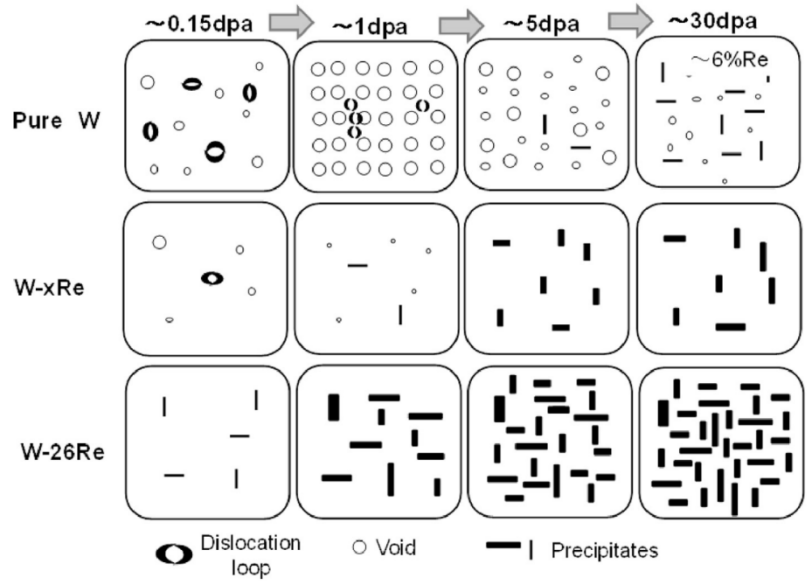

Fig. 10: Irradiation microstructure map [168]. *The schematic of the evolution of the visible damage structure of neutron irradiated pure W and We-Re alloys.*

In the 2000s, Hasegawa et al. performed irradiation of various W and W-xRe-yOs alloys [126–128,130,131,165,168,175,176,528–532]. Nemoto reported microstructure development and hardening of W-26%Re in FFTF (Fast breeder reactor at PNL, USA) in the range from 3.2 to 9.6 × 10^{22} n/cm^2 (E_n > 0.1 MeV) [32]. Further, irradiation of various types of W and W alloys were performed in JMTR (Japan Materials Testing Reactor, JAEA, Japan) and HFIR (High Flux Isotope Reactor, ORNL, USA), which are thermal neutron reactors with high nuclear transmutation rates, and also in Joyo (JAEA, Japan), which is a fast breeder

reactor with low transmutation rates. Comparing the results of JMTR, HFIR, and Joyo, the relationship between neutron irradiation hardening, microstructure change, electrical resistivity, and nuclear transmutation elements up to the irradiation temperature of 800 °C was explained for the low fluence range from 3.7 × 10^{20} n/cm^2 (E_n > 1 MeV) to 1.2 × 10^{22} n/cm^2 (E_n > 0.1 MeV). Based on these works and previously obtained data from the 1960s, Hasegawa proposed an irradiation microstructure map of W and W-Re [168]. The results of a survey regarding microstructural analysis and hardening after neutron irradiation, performed at 600 °C and 800 °C, demonstrated that size and number densities of the formed voids decreased owing to the addition of Re (see Fig. 10). Therefore, in W containing 3, 5, and 10% Re, the degree of irradiation hardening was lower compared to pure W [168]. Re in W also affects thermal conductivity. Fujitsuka et al. conducted thermal diffusivity measurements of W-Re alloys and studied the effects of neutron irradiation. They irradiated W and W-Re alloys in JMTR at approximately 60 °C. The irradiation dose was 1 × 10^{20} n/cm^2 (E_n > 1 MeV). After irradiation, they measured thermal diffusivity and reported that decrease in thermal diffusivity of pure-W and changes in that of W-Re alloys depended on the Re concentration [533,534].

In the 2010s, fission reactor irradiation of W for fusion application gained attention because ITER decided to use W for divertor materials. Neutron irradiation experiments using HFIR were conducted in ORNL [134,535,536] with irradiation doses of 0.1 to 5.9 × 10^{21} n/cm^2 (E_n > 0.1 MeV) in the temperature range of 90 to 800 °C [536]. Garrison also reported neutron irradiation results of W-Cu composites in HFIR under similar irradiation conditions [467]. Renterghem irradiated W in the Belgian Reactor (BR2) at 300 °C for 1.47 and 4.74 × 10^{20} n/cm^2 (E_n > 1 MeV). These irradiated samples were exposed to electron beam in the Judith at FZ to study material response in high-heat-flux conditions in fusion reactors [537].

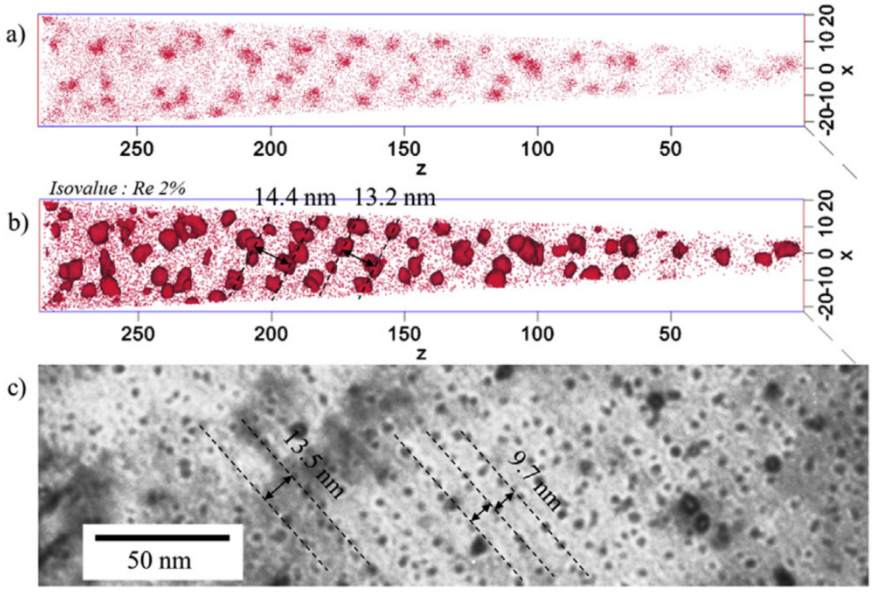

Fig. 11: Comparison of atomic probe tomography (APT) images and transmission electron microscopy (TEM) micrographs of pure W after irradiation to 0.96 dpa at 538 °C in the fast reactor Joyo. a) Re enriched area observed by APT. b) Iso-concentration representation (>2 % Re) of a). c) TEM micrograph of pure W from [175].

New and sophisticated microanalysis methods were developed for microstructure observation and results of precise analysis of correlation between damaged structure and transmuted Re from W during reactor irradiation were reported. Klimenkov et al. reported Re segregation at void surface in W after irradiation in HFR (Petten) at 900 °C [136]. W. Koyanagi et al. reported results of pure W irradiation in HFIR from 0.1 to 14.1 × 10^{21} n/cm^2 (E_n > 0.1 MeV) in the temperature range of 90 to 800 °C. Using precise analysis via TEM, Koyanagi suggested Re- and Os-rich precipitation dependence on irradiation temperature and neutron spectrum in the reactor [170]. Hwan reported Re and Os behavior in previously irradiated W and W-10%Re by Joyo and HFIR at approximately 500 °C irradiated to 6 and 7.8 × 10^{21} n/cm^2 (E_n > 0.1 MeV) to explain the segregation behavior of Re and Os in different transmutation rates caused by the neutron

spectrum [172]. The segregation behavior and damage structure were demonstrated via comparison of TEM images and results of atom probe tomography (APT) as shown in Fig. 11.
One of the reasons why W was selected as a divertor material of ITER is its low hydrogen retention behavior. To elucidate the hydrogen trapping behavior of neutron irradiated W, hydrogen retention behavior of neutron irradiated W was conducted by Hatano et al. [286,288,538]. They performed neutron irradiation to 1.1×10^{20} n/cm^2 ($E_n > 0.1$ MeV) at approximately 50 °C in HFIR and exposed high flux deuteron plasma to the irradiated sample and measured deuteron retention behavior. They reported deuteron trapping by vacancies and vacancy clusters [56, 57]. Toyama et al. performed a precise analysis of the defect cluster characterization using positron life time measurement [58].
To elucidate the above-mentioned material behavior of W under high energy and high dose neutron irradiation conditions, fission reactor irradiation with a thermal neutron shield was performed in HFIR under the Japan-US collaboration program PHENIX. Various advanced W and W-alloys including single crystal W and W-Re alloys were irradiated at 500, 800, and 1100 °C and neutron doses were up to 4×10^{21} n/cm^2 (E_n > 0.1 MeV). Within the European Fusion Project (EUROfusion) several neutron irradiation campaigns (also shielded from thermal neutrons) have been started in the BR2 reactor, which include various tungsten materials (ITER type W, PIM W grades, W composites, etc.) and specimen types (fracture mechanics, tensile, bending, high heat flux, plasma-surface-interaction, and multi-purpose, and others). The irradiation temperatures are in the range from about 500-1200 °C and the doses range from 0.1-1 dpa (in W). Some post irradiation experiments have already been started, that is, a variety of new and very interesting data on tungsten materials behavior after neutron irradiation can be expected in 2019.

5 Plasma Surface Interaction

5.1 Surface Modifications by light ion irradiation

5.1.1 Plasma material interaction (PMI) of tungsten in fusion devices

Interactions of fusion plasmas with tungsten are dominated by ion bombardment including sputtering, ion reflection, ion implantation, retention (diffusion and trapping), and material modification through these processes. Electrons in plasmas mainly bring thermal energy to materials. Although ion and material interactions are studied in a large variety of fields, these interactions in fusion devices (magnetic confinement concepts) have several notable features. Ion bombardment energy is relatively low typically from a few eV to several keV with a very low number of alpha particles with a MeV energy range. Particle flux in a steady state would reach about 10^{24} m^{-2}s^{-1} (an ion energy of a few eV in this case) for ITER near the strike point of vertical targets[539]. On the first walls, ion flux ranges down to about 10^{19} m^{-2}s^{-1} [540]. The highest steady-state heat flux in ITER is roughly 10 MW/m^2 near the strike point. This heat flux even in a steady state are roughly comparable to those in rocket nozzles, which is used only for a short time (an order of 100 sec). But plasma facing walls in fusion devices are used for a much longer duration (the cumulated discharge time for ITER is in the order of 10^7 seconds) and need to be sound during the lifetime of the divertor components. Therefore, it is important first to understand plasma material interactions during long time and high fluence ion irradiation, and then to optimize edge plasma conditions or material properties. These are new challenges, which appear only in the field of Nuclear Fusion. Moreover, the steady-state heat flux is superimposed by heat flux pulses during transients (disruptions and edge localized modes, ELMs). These pulses can be in the order of several GW/m^2 with a pulse length in the milliseconds range, which causes melting and surface morphology changes. In general, significant surface morphology changes by repeated melting or recrystallization should be avoided.
Reliable databases of ion physical sputtering of metallic materials with the energies down to about 40 eV and ion flux up to about 10^{21} m^{-2} were obtained after the 1950's by using plasma devices (discharge tubes etc.) and ion beam devices. A comprehensive review is found in [541]. The energy regimes roughly correspond to those of plasma-facing materials (PFMs) in fusion applications and these databases are useful to estimate physical sputtering yields of metallic materials (including tungsten). Sputtering yields by hydrogen isotopes and helium ions, which are dominant for components in fusion plasmas, are included in the database, indicating presence of sputtering thresholds at normal incidence of 230 eV for D and 120 eV for He for the case of tungsten (as shown in Fig. 12).

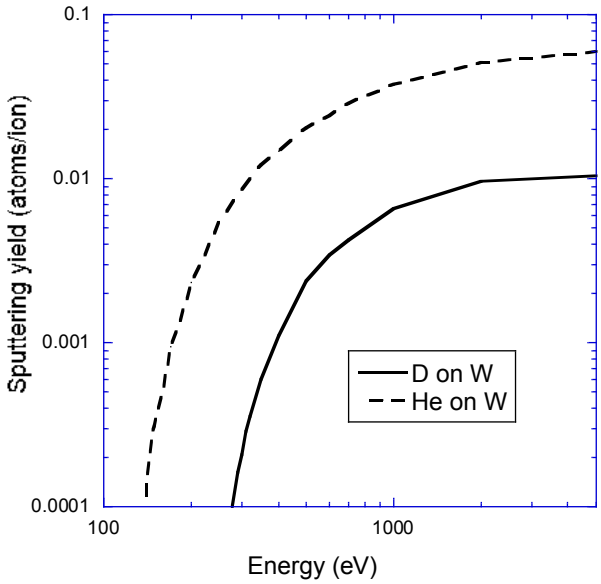

Fig. 12: Sputtering yield for deuterium and helium ions on tungsten at normal incidence.

Hydrogen isotope behavior in metals has been also studied for a long time. It is known that tungsten is an endothermic metal and its hydrogen solubility is low compared to tantalum, for example, which is an exothermic metal and the hydrogen solubility is very high. Since tungsten has a low hydrogen solubility, basic hydrogen isotope behavior in tungsten is expressed by diffusion and trapping at defects. But as described in Sec. 5.2, high flux (high fluence) ion irradiation, one of unique features for PMI in fusion devices, causes oversaturation and associated increase in hydrogen isotope retention is observed.
Surface morphology changes by light ion bombardment with a fusion-relevant low energy and high flux (high fluence) have been studied intensively after high density linear plasma devices became main tools for PMI research for fusion materials during and after the 1980's. In fact, tungsten is presently a leading PFM candidate for fusion devices because of its high melting temperature, high thermal conductivity and low sputtering yield. But during the 1970s and 1980s, graphite based wall materials played an important role in fusion designs because metallic PFMs posed serious problems such as accumulation of sputtered wall materials in the core of hot plasmas, which caused unacceptably high radiation cooling [542]. To avoid this serious problem, low Z materials such as carbon-based materials were mainly used for plasma confinement devices because its impact on core plasma performance is much lower than metallic materials (especially high Z materials). After detailed studies on PMI of carbon-based materials (mainly chemical sputtering and retention) in the 1990s, tungsten came into the focus of PMI studies after the year 2000 due to serious concerns over erosion, tritium retention, and degradation of mechanical properties by neutron irradiation of carbon-based materials.
Concerning surface morphology changes by light ion bombardment (hydrogen isotopes and helium), blistering and He induced surface modification, for example, formation of surface He holes and nano-fibers are typical for plasma facing materials. In this section, the surface He holes and nano-fibers induced by He bombardment are described in detail in the following section by referring to [543–546]. Hydrogen induced blistering will be described in the following section (Sec. 5.2).

5.1.2 Surface modification of tungsten by high flux He irradiation

He atoms implanted in metallic materials are strongly trapped by several types of defects such as vacancies, grain boundaries, dislocations, and voids [547,548]. For example, the trapping energy for a He atom by a mono-vacancy in tungsten without any further He atoms is about 4.5 eV [549], which is much higher than that for hydrogen (~1.2 eV, one atom trapped) [550]. Additional He atoms can be trapped by He-vacancy complexes which increases their size. Even in defect-free tungsten material, He atoms can aggregate at interstitial sites. Surface morphology changes start from this He cluster formation in tungsten.
He-bubble dynamics is different for the conditions with and without displacement damage. Microstructure changes of W under He plasma exposure (in the PISCES-A facility, UCSD) with an ion impinging energy of

~50 eV and He^+ irradiation at 3 keV were systematically studied by varying ion fluence and temperature [551]. In 3 keV He^+ irradiation, it is expected that vacancies and interstitial atoms are directly formed by knock-on processes within a projected range of He^+, while no vacancies were formed by the knock-on process for the He plasma exposure. For the He plasma exposure, the layer thickness (>30 nm) of He bubbles largely exceeds the ion implantation range of a few nm (similar results were also reported in [552,553]), because the diffusion length of He atoms is longer than the implantation range. The size of He bubbles is found to increase with increasing sample temperature; the He bubble size is around 10 nm at 973 K, while only small He bubbles of 1–3 nm diameter are observed at <773 K. Furthermore, regardless of the sample temperature, the saturation of the He bubble density starts at a He^+ ion fluence of 5 x 10^{23} m^2, which is higher than that of the 3 keV He irradiation (in the order of 10^{22} m^{-2}). A temperature-fluence diagram for He bubbles produced by 3 keV He^+ irradiation is shown in Fig. 13 [551]. The He bubbles became visible after a fluence of 10^{19} - 10^{20} m^{-2}, depending on temperature. At the temperature of 1250 K, He-vacancy complexes become mobile and coalesce to large He bubbles, see Fig. 13. These He bubbles show a saturation in concentration at fluences roughly larger than 10^{22} m^2.

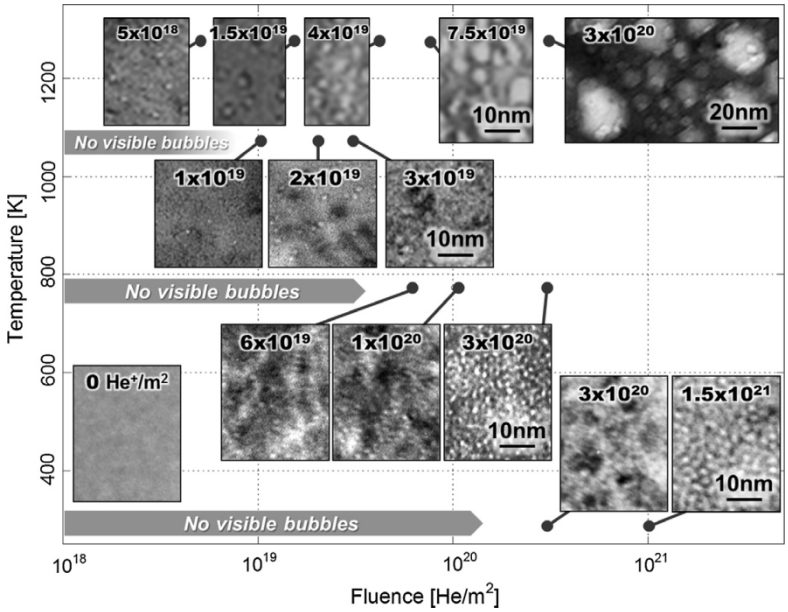

Fig. 13: The microstructural evolution of W under irradiation at constant temperatures of 293, 773, 1073, and 1273 K [551].

Differences in He bubble formation in tungsten with and without pre-damaging was also studied and reported in [554]. High-energy (260 keV) He+ pre-damaged and undamaged polycrystalline tungsten samples were irradiated with low-energy (220 eV) and high-flux (~10^{21} ions/m^2s) He^+ at a sample temperature of 873 K to a fluence of 1.0 x 10^{25} ions/m^2. A large number of nanometer-sized protuberances of irradiated tungsten samples results from the extreme internal pressure of nanometer-sized helium bubbles. For tungsten without pre-damaging, ordered and nanostructured helium bubbles with the same diameter and average spacing can be formed due to the self-trapping and self-organizing of helium atoms in the tungsten materials. In the case of pre-damaged tungsten, a random distribution of nanostructured helium bubbles are formed, indicating that high-energy He^+ implantation results in irradiation damage of tungsten materials, acting as nuclei for helium bubbles.

After the following paragraphs, surface modification of tungsten by high flux and high fluence He plasma exposure will be described. At first one comment on the technical term describing nano-fibers should be noted. There have been several names for the newly observed nano-fiber structure such as “nano-structure [555]”, “fuzz [556]”, “nano-tendril [557]”, etc. To avoid confusion, the term “nano-fiber” is used in this paper to indicate the structure shown in Fig. 14 and later.

Surface modifications of tungsten by helium plasma exposure (nano-fibers and He holes, etc.) have been investigated in detail only in the field of fusion research so far for about 20 years. The first observation of surface modification of tungsten by He plasma exposure was reported in 1997 by the Takamura group from Nagoya University [558]. In this experiment, a tungsten plate was exposed to high flux He plasma (flux of

~2 x 10^{22} $m^{-2}s^{-1}$) at 3200 K by using the NAGDIS linear plasma device [559]. The exposed surface became black and dense He holes formed with a typical size in the μm range. This surface morphology was not formed by H plasma exposure. They continued this work to investigate detailed formation conditions of the He holes. They found that the He hole formation strongly depends on ion bombarding energy [278]. There is a threshold energy (between 10 and 5 eV) below which He holes are not formed. This threshold energy is well correlated with a surface barrier potential energy (~ 6 eV) for He [549]. Therefore, at least, He ions need to be implanted into the tungsten lattice by overcoming the surface barrier for the He hole formation.

After several years of He hole experiments, nano-fiber formation was firstly observed on W coating layer on graphite at 1250 K, which was lower than the typical He hole formation conditions (~2000 K) by Takamura [555]. Then the Nagoya [560–562] and UCSD group [563] made extensive research on nano-fiber formation conditions. These results were well summarized by Kajita [564]. In addition to a temperature window (1000 K ~ 2000 K) for nano-fiber formation, an important suggestion of this study is the role of ion energy, which needs to be above 20 eV. As described, He hole formation is observed when the ion energy exceeds the surface barrier potential of about 6 eV. But nano-fiber formation needs more ion energy (~20 eV). Although the role of the ion energy is not well understood yet, it is known that the threshold energy for nano-fiber formation becomes high at a low flux condition (e. g. 10^{21} $m^{-2}s^{-1}$) [546]. One possible explanation is that the dynamic retention of He just beneath the surface is higher for higher ion fluxes. Some amount of dynamic retention of He could be a prerequisite for the formation of nano-fibers.

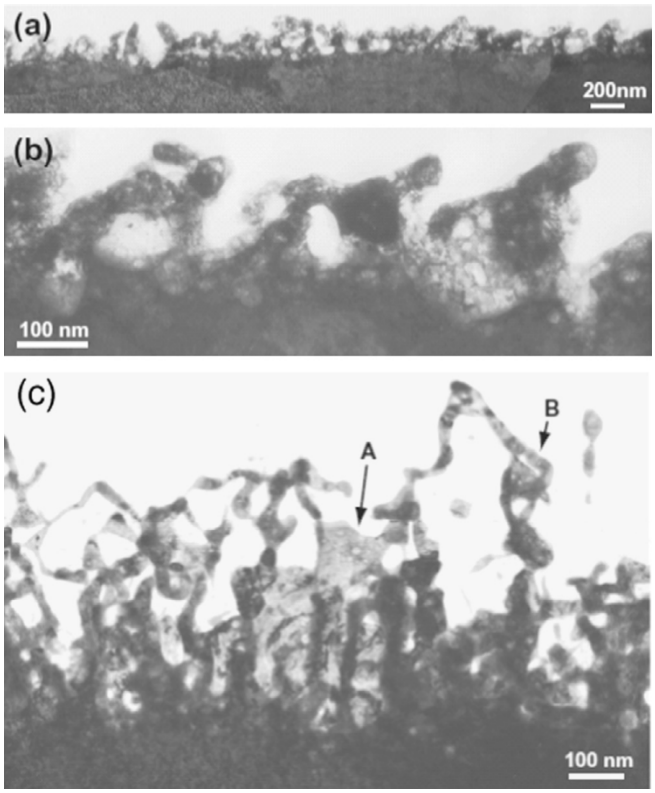

Fig. 14: He irradiated W in NAGDIS-II at 1400 K and 50 eV. He fluences are (a), (b)1.1 x 10^{25} m^2 and (c) 2.4 x 10^{25} m^2. [565]

Initial formation processes of nano-fibers were observed in detail by TEM by Kajita et al. [564,565]. Fig. 14 shows the cross sectional TEM micrographs of polycrystalline tungsten irradiated by He plasmas with a fluence of 1.1 x 10^{25} m^{-2} and 2.4 x 10^{25} m^{-2} at 1400 K [565]. Initially, many nanometer sized helium bubbles are formed on the surface. With the help of an active surface diffusion, pinholes, dips, and protrusions are formed on the surface, see Fig. 14 (a) and (b). The structure shape may become complex. As an example, a plate-like structure (A) or a ring-like structure (B) can be recognized in Fig. 14 (c). In the formation processes, the growth of the highly pressurized helium bubbles in the surface region can lead to protrusions, where the protrusion size depends on the bubble's size. Moreover, blister-like structures are formed by the development of the helium bubble growth in some locations. It is assumed that active

surface diffusion of tungsten atoms plays a key role in the formation of protrusions and fine structures, because surface diffusion is in general much faster than lattice diffusion. It is likely that surface diffusion contributes to heave tungsten together with the bubbles and, therefore, changes the surface morphology. The nature of the growth of nano-fibers at a He flux of (4–6) x 10^{22} m^{-2} s^{-1} at 1120 K in PISCES is revealed by the SEM images in [563], see Fig. 15. As the exposure time is increased, the nano-fiber layer grows in thickness to more than 5 μm for the exposure time of 2.2 x 10^4 s. Layer thickness data are shown for exposure temperature regimes of 1120 and 1320 K. For both exposure temperatures, the data are well characterized by a square root dependence on time, suggesting the diffusion-like process dominates the growth of the nano-fibers. Similar dependence was also observed in NAGDIS with an incubation He fluence of about 4 x 10^{24} m^{-2} [565]. In addition, formation of the nano-structure is hardly affected by simultaneous D implantation [566].

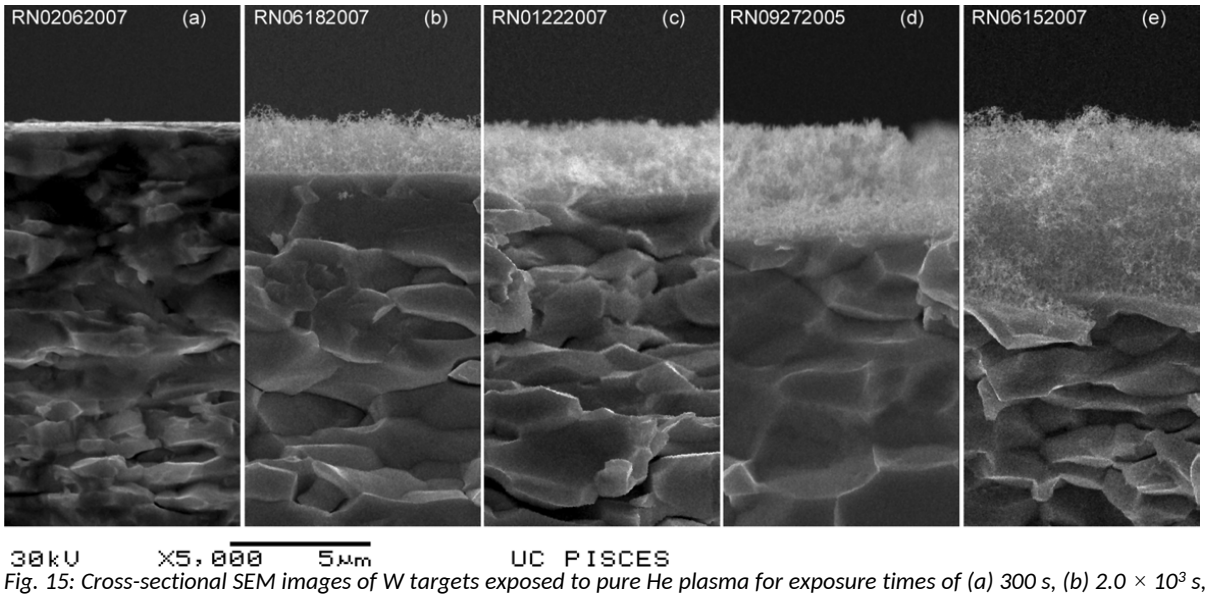

Fig. 15: Cross-sectional SEM images of W targets exposed to pure He plasma for exposure times of (a) 300 s, (b) 2.0 × 10^3 s, (c) 4.3 × 10^3 s, (d) 9.0 × 10^3 s and (e) 2.2 × 10^4 s. The targets were exposed at a fixed temperature of 1120 K. The plasma properties varied slightly in the parameter ranges n_e = 4 × 10^{18} m^{-3} and T_e ~ 6–8 eV, He^+ = (4–6) × 10^{22} m^{-2} s^{-1} in order to maintain the constant fixed target temperature [563].

In ITER, heat and particle flux at the outer strike point in a steady state would be about 10 MW/m^2 and 10^{24} $m^{-2}s^{-1}$[539]. In NAGDIS and PISCES, the highest He flux is about 10^{23} $m^{-2}s^{-1}$, which would be about the same as the highest He flux to divertor plates in ITER, because He concentration in burning plasmas would be 5-10%. The heat flux to W specimens in the abovementioned devices, however, is about an order of magnitude lower than in ITER. He irradiation with comparable heat and particle flux to ITER divertor has been performed in MAGNUM-PSI [567] and Pilot-PSI [568]. Fig. 16 shows surface morphologies after high flux He plasma exposure in Pilot-PSI [568]. From Fig. 15 and Fig. 16, it is found that similar surface morphologies as produced in NAGDIS and PISCES were observed. With increasing surface temperature the thickness of the nano-fibers increases, which is also similar to the NAGDIS results [564]. A correlation between bubble size and helium-induced nanostructure scale was clearly seen. From these results, the He induced surface morphologies could appear at much higher particle (heat) fluxes, which are comparable to those in ITER, though more detailed studies are required to examine the flux effect on the nano-fiber formation.

Formation of nano-fibers is a universal phenomenon observed in any linear plasma device. A remaining question was whether a similar structure would be formed in magnetic confinement devices. Several conditions in terms of plasma loading are different in linear plasma devices and magnetic confinement devices. The differences to magnetic confinement devices are: (i) an oblique incidence of impinging ions to the walls, (ii) the ion energy distribution - usually with a high energy component (CX neutrals, etc.), (iii) the inclusion of various types of impurities (non-volatile wall materials, volatile cooling gases, etc.) which could make mixed surfaces or deposition layers (which would inhibit nano-fiber growth [566]) or could enhance erosion (reducing the thickness of the nano-fiber layer [569]).

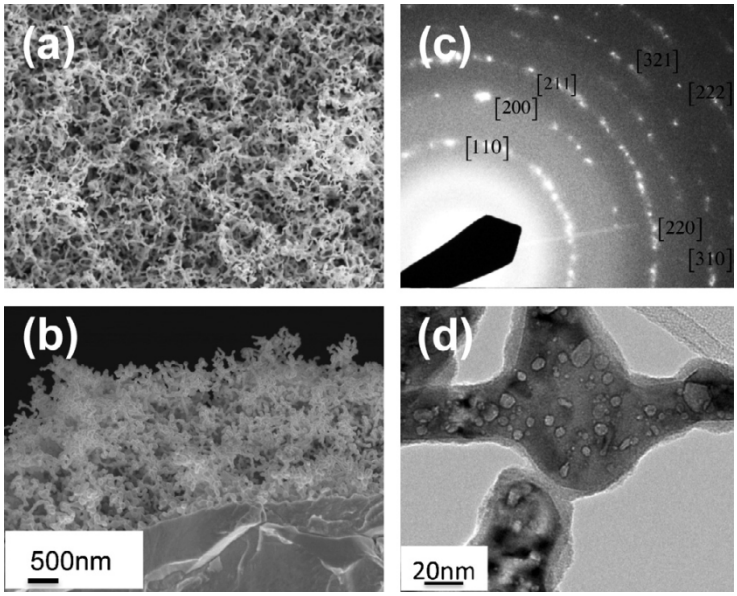

Fig. 16: Characteristics of the fiber nano-structure formed under irradiation of a tungsten surface at 1000 ºC by low-energy helium ions (50 eV) for a duration of 500 s. (a and b) Top-view and cross-section images. (c) Electron diffraction patter from the tungsten filaments of (a). (d) High-resolution TEM image of the structure of a tungsten filament [568].

The Alcator C-Mod group tried to produce He induced structures on wall materials [557,570]. After careful preparation, the Alcator C-Mod created the necessary plasma conditions for the formation of nano-fibers (they called them nano-tendril) at the outer strike point. The plasma density was kept high to achieve high power flux in the divertor but with a relatively low electron temperature at the edge (20 – 25 eV) to minimize sputtering erosion. They repeated discharges of about one second 14 times, which gave enough He fluence to form the structure. A tungsten probe and Mo ramped tiles were installed. Heat fluxes to the W probe and the Mo tiles were 30-40 MW/m^2 and ~10 MW/m^2. Averaged surface temperatures (14 shots) reached at the end of discharges were about 2300 K for W and 1000 K for Mo.
Nano-fibers were fully formed on the tungsten probe surface exposed to heat fluxes of 30-40 MW/m^2, see Fig. 17. The surface of the W probe became optically black, indicating that the thickness of the nano-fiber layer is at least ~400 nm. The thickness of individual fibers is 50-100 nm, which is thicker than the nano-fibers grown in linear devices (20-30 nm), which could be attributed to the relatively high surface temperature (>2000 K). On the ramped Mo tiles, however, no structure was observed. The reason is due to the different sputtering threshold of W compared to Mo.
The behavior of nano-fiber W surfaces in fusion plasma environments has been studied in several magnetic confinement devices [571–574]. In TEXTOR, the nano-fibers prepared with the linear high density plasma NAGDIS were exposed to D/He (1:1) mixed edge plasmas to investigate formation and erosion of the structure, and C deposition [571]. Initial specimen temperatures were ~300 ˚C and 800 ˚C, which were increased by about 200 ºC during plasma exposure. Ion flux and edge electron temperature were estimated to be about 3 x 10^{21} m^{-2}s^{-1} and ~40 eV. The nano-structure was either completely eroded or covered by C deposit. There was no clear indication of nano-fiber growth under the present conditions, mainly due to high carbon concentration in the edge plasma (~4%). On the nano-structured surface, C deposition was enhanced compared to the flat surface, probably due to a reduction of effective re-sputtering of C deposit and due to the effective reflection coefficient of carbon ions, similar to roughness effects [575].
In fusion reactor environments, enhanced erosion of the nano-fiber is a matter of concern because it would reduce the lifetime of tungsten walls. In addition, core plasma contamination and dust formation would be enhanced. Three main erosion processes so far studied are (i) sputtering erosion, (ii) erosion by pulsed load (including melting and droplet ejection), and (iii) unipolar arcing. Recent research results on these processes are summarized in the following.

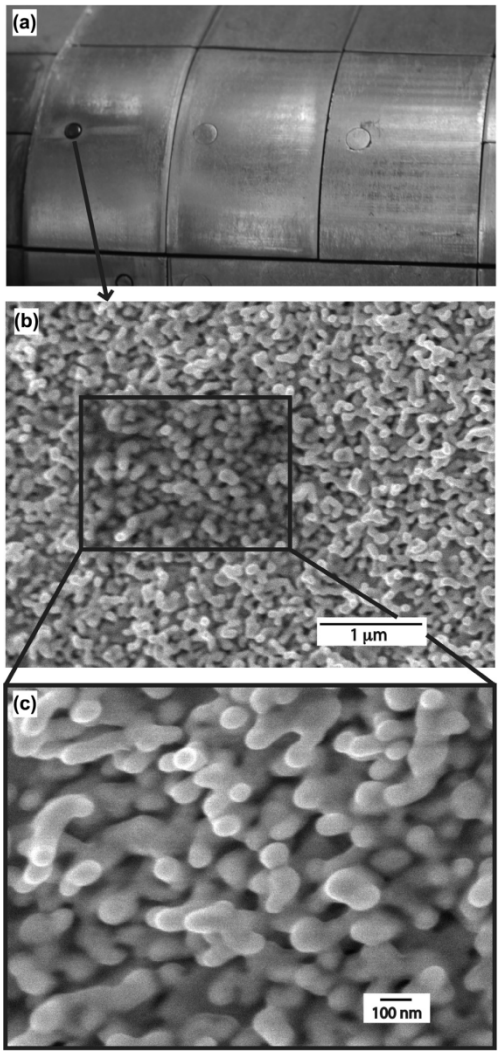

Fig. 17: (a) The ramped Mo tiles and W probe upon removal from Alcator C-Mod, (b) SEM image of the W probe surface showing nano-tendrils on the surface, and (c) high magnification SEM image [570].

Sputtering yields of nano-fibers bombarded by Ar plasmas have been measured in the linear divertor plasma simulator PISCES-B [576]. The sputtering yields of both smooth, Y_{smooth}, and covered by nano-fibers (called fuzzy), Y_{fuzzy}, W surfaces are compared. The ion energy dependence is similar for Y_{smooth} and Y_{fuzzy} with the ratio, Y_{fuzzy} / Y_{smooth}, of 0.15-0.2. As a cause of the reduction in the sputtering yield of nano-fibers, its porous structure could be considered. This observed trend of Y_{fuzzy} / Y_{smooth} is consistent with the change in (1 - p_{fuzz}), where p_{fuzz} is the porosity of nano-fiber layer. The equilibrium thickness of the surface nano-fiber layer is determined by the balance between the erosion rate and the growth rate, if the conditions exist for nano-fiber development in a steady-state plasma (surface temperature and energetic helium flux) [569].

Because the effective thermal conductivity of a nano-fiber layer is significantly lower compared to flat W surfaces, irradiation by pulsed heat and particle loads (e.g. ELMs) could lead to enhanced erosion by splashing and ejecting droplets. Kajita et al. [577] conducted systematic experiments using a pulsed laser (ruby laser, 694.3 nm, pulse width of ~0.6 ms) to observe blow-off of tungsten from the nano-fibers. Release of tungsten was monitored by WI line emission. When the laser pulse energy was greater than 0.5 MJm^{-2}, clear WI emission was observed from the He-irradiated surface. Sometimes the emission could be observed at a considerably lower pulse energy, although such an emission was not observed from the surface without damages due to He irradiation when the laser pulse energy was lower than 1 MJm^{-2}.

In contrast to pulsed heat, moderate heating of nano-fibers at temperatures well below the melting point of tungsten could bear a beneficial effect such as annealing without emission of tungsten atoms or clusters [578][579][580]. In these experiments, pre-formed nano-fibers were heat treated in-vacuo over periods of 45 min to maximum temperatures of 1900 K. In spite of the maximum temperature being well below the

melting point for W, all traces of nano-fibers are found to be absent from the target following the heat treatment without any observable mass change [579]. It was also stated that most of the He was desorbed below 1900 K, suggesting the nano-fibers were reintegrated with the bulk W after He desorption. This could indicate that high pressure He bubbles in nano-fibers play an important role in sustaining the structure.
Effects of transient heat pulses to nano-fibers, however, are very complicated and different observations were reported. Disappearance of nano-fibers (similar to the abovementioned annealing) was observed by ELM-like transient heat pulses in Pilot-PSI [568], while droplet formation was observed in a pulsed plasma gun [581]. Even nano-fiber growth by transient heat pulses during He plasma exposure was observed in PISCES [582]. These differences could be attributed to the pulse length and pulse energy density. For example, pulse length in Pilot-PSI is longer (~ 1 ms) than that of the plasma gun (~0.1 ms). Heating rate and duration as well as thickness of the nano-fiber layers, which are closely related to the temperature of nano-fibers and base W plates, could be a key for the fate of the nano-fibers.
One of the most severe concerns of the nano-fiber layer in response to transient loads is unipolar arcing in edge plasmas. Kajita et al. pointed out that unipolar arcing can be easily initiated on nano-fibers [577,583]. Irradiating a laser pulse to nano-fibers in the plasma initiates a unipolar arc, which continues for a period much longer than that of the laser pulse width (~0.6 ms). During the arcing, a strong emission of WI line was observed. This result suggests that nano-fibers could significantly change the ignition property of arcing and that ELMs could become a trigger of unipolar arcing, potentially an unfavourable intense impurity source in fusion devices. Kajita et al. also investigated conditions for arcing ignition [584]. Arcing was never ignited unless the target was sufficiently biased negatively, namely less than −60 V. Similar results were observed in PISCES-A experiments [585]. These findings suggest that sheath potential in front of W targets is important to initiate arcing. Therefore, at least for detached plasmas with a very low electron temperature (a few eV) and hence low sheath potential (several V), arcing may not be initiated.
This preferential arcing was observed also in a magnetic confinement devices DIII-D [573] and LHD [572]. In LHD, arcing was initiated without any pulsed heat loads (ELMs). In both cases, its impact on core plasmas is negligible partly because the area of nano-fiber surface was very small. Some rough estimation of W impurity released by arcing from the nano-fiber surface suggested impact of the W release on core plasma performance may not be negligible [544]. More research effort is required to clarify the effects of unipolar arcing on the core plasma performance.
The nano-fibers on tungsten produced by He plasma exposure are also observed on other transition metals. Extensive database of He exposure effects on materials were well compiled by Hammond [586]. Based on this comprising database, Takamura pointed out that nano-fibers are produced on stiff materials with a high shear modulus and low sputtering yields [587]. There seems to be no clear correlation with the crystal structure. For both, period 5 and period 6 transition metals, a good correlation of nano-fiber formation and shear modulus can be seen [546]. Young's and shear modulus are high from group 6 to group 9 transition metals, for which there are a large number of unpaired electrons in 4d (period 5) and 5d (period 6) orbitals. Young's modulus for these metals exceeds 300 GPa (at RT) and four transition metals among the tested (W, Re, Ir, and Mo) produce long nano-fibers from the base materials after He plasma exposure [546], see Fig. 18. On the other hand, transition metals with Young's modulus less than 200 GPa (at RT) do not produce long nano-fibers such as (Ta and Nb).
Density Functional Theory (DFT) calculation results show that helium atoms prefer to agglomerate in most of these transition metals. However, the helium binding energies of the group 6 elements are larger than those of the group 5 elements. Thus, helium can agglomerate easier in group 6 than group 5 elements. In addition, the normal stress increases approximately linearly with the number of helium atoms in the bubble. These values are close within the same group, and the normal stress of the group 6 elements is clearly larger than that of the group 5 elements. For stiff materials, as He pressure inside He bubbles is raised, the displacement of atoms around He bubbles is small. Therefore, normal stresses near the He bubbles in the material could become higher. This difference was clearly seen by DFT calculation on He-vacancy interaction [588,589].

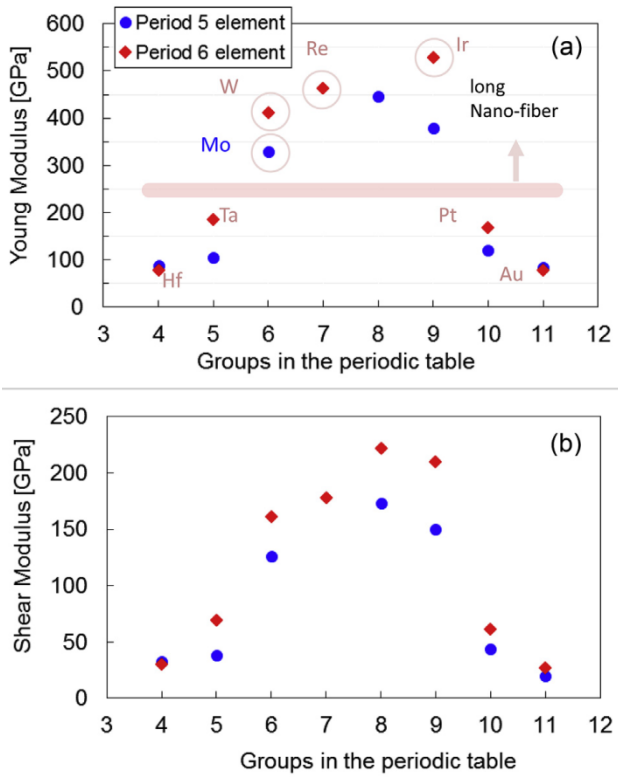

Fig. 18: Young's modulus (a) and shear modulus (b) for period 5 (Zr (Group 4) to Ag (Group11) and Period 6 (Hf (Group 5) to Au (Group 11)) elements at room temperature. Elements with long nano-fibers observed in our experiments are marked by circles.[546]

The formation mechanism of nano-fibers has been studied using several simulation techniques such as DFT for interatomic potential calculations, MD (Molecular Dynamics) for the dynamics of He atoms and defects, and KMC (Kinetic Monte Carlo) for He bubble dynamics [316,586,590–592]. A comprehensive review on these works is given in [586]. Although details on theoretical and simulation works are not described in this section, it is noted that growth mechanisms of nano-fibers to lengths larger than about several micrometers are not known yet. In order for nano-fibers to extend to such length, tungsten atoms need to migrate to the tips of nano-fibers or the whole nano-fiber structure needs to be pushed up from the substrate. But details of such migration or growth mechanisms are still under investigation.

Recently one interesting experimental result was reported by Kajita [593]. He showed enhanced growth of large-scale nano-fibers by precipitating additional metallic particles during helium plasma irradiation, see Fig. 19. The growth rate of the structures became orders of magnitude greater than conventional nano-fiber growth. Additional precipitation of metallic ions breaks the bottleneck diffusion process; moreover, further acceleration in the growth rate could have occurred, if the electric sheath shape was influenced by the grown structure and the electric field that formed around the structure started collecting ions. This novel finding indicates that effective deposition or migration of tungsten atoms to or around the nano-fiber tips is a key process in nano-fiber growth.

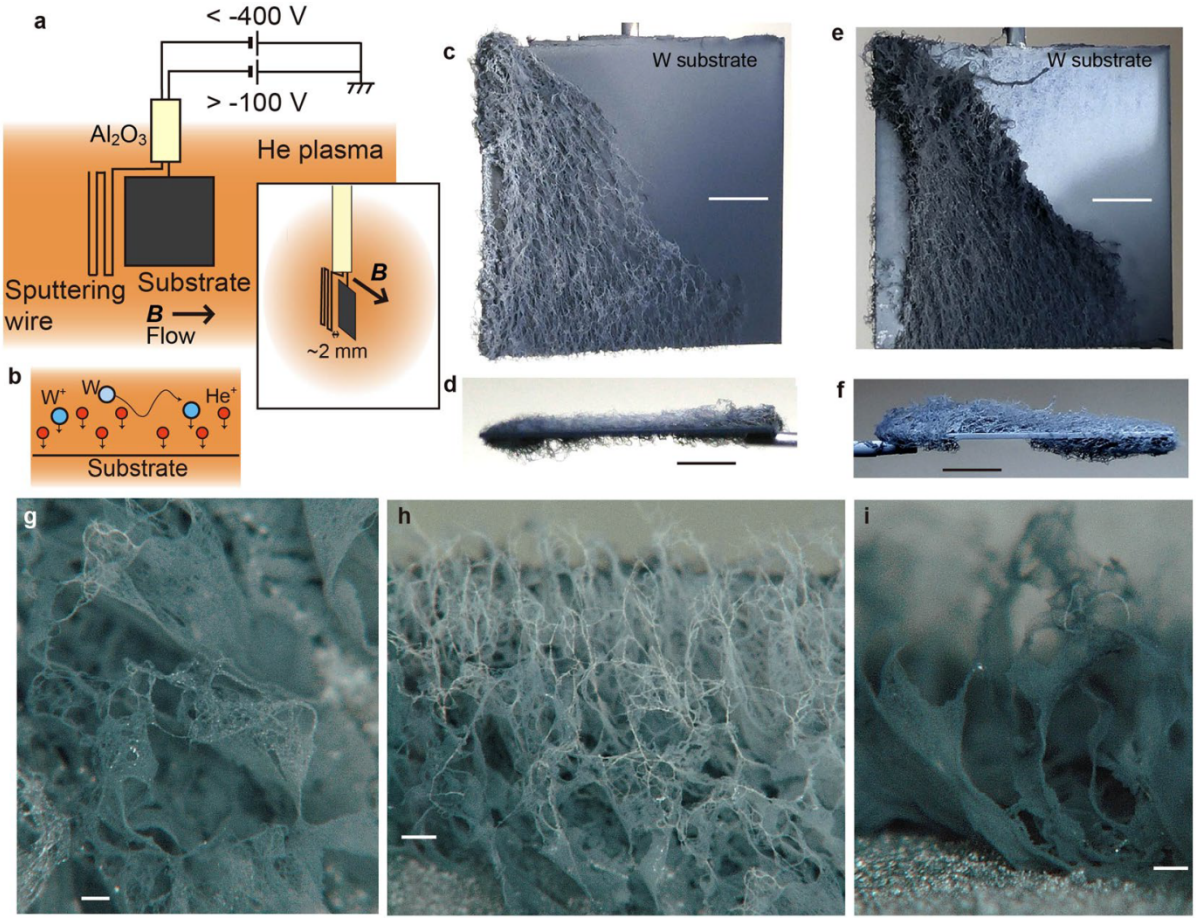

*Fig. 19: Schematics of the experiments and pictures and micrographs of fuzzy fur like materials. (**a**) Schematic of the experimental setup. (**b**) Schematic of the sample exposed to ions. (**c**,**d**) Pictures of W largescale nano-fibers on a W substrate after an irradiation time of 3600 s from top and side view. The sample temperature, T_s, the incident ion energy, E_i, and the ion fluence, Φ, were 1200 K, 70 eV, and 1.8 x 10^{25} m^{-2}, respectively. (**e**,**f**) Pictures of Mo large-scale nano-fibers. The irradiation conditions were T_s = 1250 K, E_i = 70 eV, and Φ = 2.0 x 10^{25} m^{-2}. (**g**–**i**) Optical microscope micrographs of W large-scale fuzzy nanostructures. The irradiation conditions were T_s = 1300 K, E_i = 70 eV, and Φ = 2.8 x 10^{25} m^{-2}. The scale bar in (**c**–**f**) and (**g**–**i**) represents 2 and 0.1 mm, respectively* [593].

5.2 Retention of hydrogen and its isotopes

Over the years there have been quite a few reviews addressing, at least in part, the issue of hydrogen isotope retention in tungsten[545,586,594–599]. These reviews cover a lot of experimental and modeling efforts for understanding the behavior of hydrogen isotopes in tungsten. In this section, we will try to describe the present understanding of hydrogen retention in tungsten, while referring readers to the detailed results described in the aforementioned reviews.

Before beginning, the term ‘retention’ needs a slight clarification. The total ‘retention’ during energetic particle exposure consists of both a static and a dynamic component. In this review, we will discuss static retention. Static retention refers to the hydrogen isotopes remaining in the material after the flux of particles to the surface is terminated. This component is typically referred to as trapped in the material and can, therefore, be measured by various techniques after the exposure. This is also the component that most concerns safety estimates [600] and tritium sustainability accounting [601]. The dynamic retention typically refers to the hydrogen isotopes that exist in the material during the particle flux exposure. This additional retention is responsible for establishing the concentration gradients that balance the flux of particles into the surface. Once the particle flux is removed this retention quickly escapes from the material.

In-situ diagnostics are required to measure the dynamically retained component. In-situ Nuclear Reaction Analysis (NRA) measurements have been made during plasma exposure [602], but these measurements are integrated over the entire depth range (approximately one micron) and required duration of 10

minutes of signal integration time. One would expect, however, the H isotope concentration to peak close to the stopping distance of the incoming plasma ions (typically a few nm) and for this concentration gradient to disappear quickly after the termination of the incoming ion flux. To date measurements of the dynamically retained component in the near surface region (defined below) are elusive during high flux plasma exposure of surfaces and so little can be definitively said about its magnitude, spatial profile or temporal behavior, hence it will not be the subject of this review. It should also be noted that static and dynamic retention exists in all plasma exposed surfaces and are not specific to tungsten.

When examining the depth profile of retained (i.e. statically trapped) deuterium in plasma-exposed tungsten, three regions generally become evident [603]. These regions are indicated on some experimental depth profiles as published by Alimov [604] in Fig. 20. In the near surface region (extending up to 100 nm into the material), very large concentrations of trapped D are found. Gao et al. [605] have found concentrations up to 10 % D/W in this narrow region. Recall that this is the retention remaining in the material after the exposure. The amount during the exposure must be larger than this value. Moving deeper into the bulk, a plateau with typical concentrations of ~0.1% is found, which can extend several microns into the bulk, depending on the exposure conditions. The thickness of this plateau region increases as the square root of the increasing plasma fluence [606]. Eventually, during the high-flux, steady-state operations expected in a fusion reactor, this plateau could be expected to extend throughout the extent of the plasma facing component. Finally, the deuterium concentration drops with increasing depth to values associated with intrinsic defects in the tungsten bulk.

The very high concentration in the near-surface region (the dynamically retained particles) is usually related to damage of the lattice induced by the plasma exposure. Since the flux of hydrogen ions to a plasma exposed surface is large and the stopping distance of those ions is short, the concentration of hydrogen in this region is well above the equilibrium solubility limit [597]. It is believed that the super-saturation of hydrogen in the near-surface region leads to plastic deformation of the tungsten and is assumed to result in the formation of bubbles and voids [595]. Recent investigations of tungsten surfaces exposed to deuterium plasma flux of 1.5 x 10^{24} $m^{-2}s^{-1}$ revealed a series of small bubbles formed in the near surface region [607].

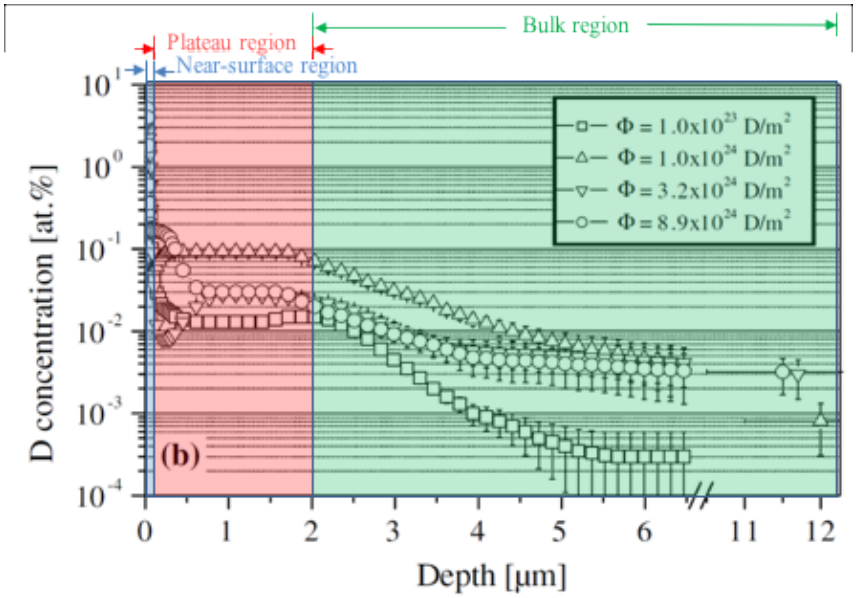

Fig. 20: When examining the depth profile of retained (i.e. statically trapped) deuterium in plasma-exposed tungsten, three regions generally become evident: near-surface, plateau, and bulk region [603]. *These regions are indicated on some experimental depth profiles as published by Alimov* [604].

In another experiment in a high-flux plasma, the dislocation density in the plateau region was seen to dramatically increase in both poly-crystalline and single-crystal tungsten samples exposed to deuterium plasma [608]. The super-saturation in the near-surface region spawns these dislocations that then propagate into the tungsten surface. Subsequently, the diffusion front of deuterium atoms loads deuterium into trap sites associated with the dislocations. As the deuterium concentration rises, additional

dislocations can be generated that propagate deeper into the tungsten and act as further trapping sites for diffusing deuterium atoms. Such a mechanism would explain the lack of saturation of deuterium retention in extremely large-fluence plasma exposures [609].
Another important effect of the large hydrogen content in the near surface of the material is embrittlement. The large amount of dislocations created and the presence of the hydrogen itself in the lattice will increase the hardness of the surface, leading to embrittlement. The plasma-facing surface can then exhibit an increased tendency to crack during transient heat loads (as will be discussed later).
Besides fluence, a second important parameter governing hydrogen isotope retention in tungsten is the temperature of the material during the exposure. Contrary to expectations, where one might assume at higher temperature, lower energy trap sites would not be populated and therefore retention would continuously decrease with temperature, a peak in retention in tungsten in the region around 400-700 K is measured (see Fig. 21) [610]. The exact temperature of the peak varies, but is likely dependent on the details of the microstructure of the tungsten being studied, sample preparation methodology, purity of material, etc.

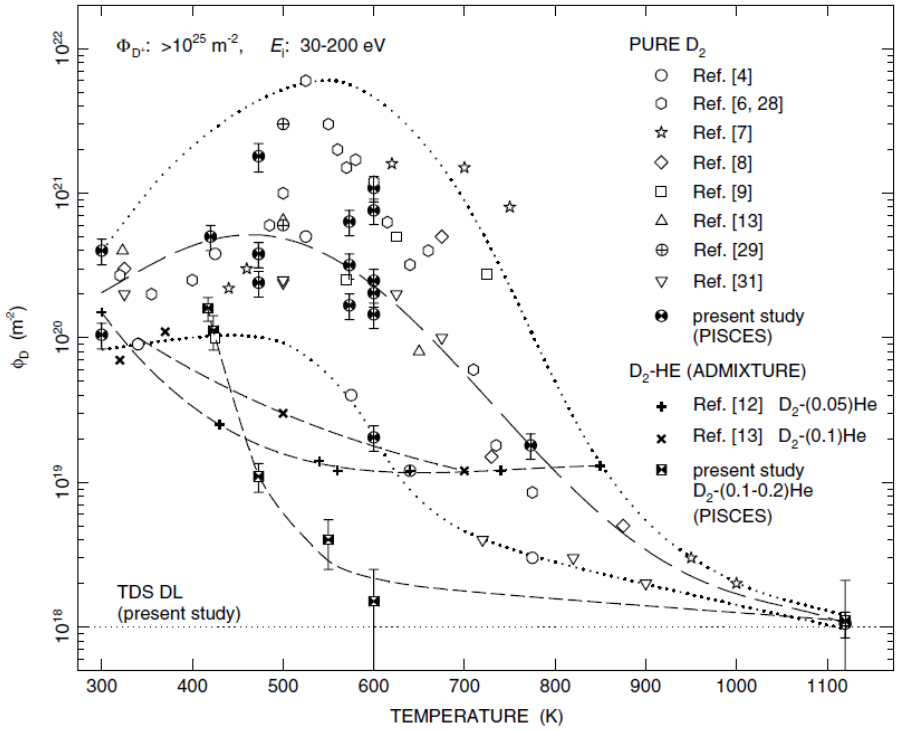

Fig. 21: Contrary to expectations, where one might assume at higher temperature, lower energy trap sites would not be populated and therefore retention would continuously decrease with temperature, a peak in retention in tungsten in the region around 400-700 K is measured [610].

The peak in retention is correlated to the empirical observation of blister formation in the tungsten surface. Some inter-grain blisters have been shown to elastically collapse back to the surface when the deuterium pressure below the blister cap is released [611]. Other blisters, which form predominantly at the interface between grains, have been shown to form subsurface cavities that deform the grain above. Such blister deformations then express themselves as a distortion on the surface that replicates the size and shape of the cavity below [612]. The details of the blister formation mechanisms are still being investigated, but their relationship to deuterium retention is clear.
As the temperature of the exposure increases above 400-700 K, deuterium diffusion also increases and the tendency for the surface to form blisters diminishes. However, an interesting aspect of blister formation has been revealed during higher flux plasma exposure. As the particle flux to the surface increases, the temperature window where blisters are observed widens [613]. At higher particle flux blisters are formed in surfaces which would have been blister-free at lower particle flux. This observation indicates that blister formation is related to the deuterium concentration in the surface. In any case at temperatures above that at which blisters form, deuterium retention in tungsten monotonically decreases. (Note: this could be

different under neutron irradiation due to the formation of high concentrations of cavities that may act as sinks for H isotope collection). Setting aside blisters and their impact on retention, the dependence of retention on incident flux appears to be opposite. In a study of the importance of ion flux, the maximum retention in samples exposed at lower flux was an order of magnitude higher than that observed at higher incident particle flux [614]. However, these measurements were done at a constant fluence and so the reduction may be related to the duration of the plasma exposure. At constant flux, retention is known to increase as the square root of the exposure time [609,615], so additional work in this area may be needed to understand the effect of incident flux.

The energy of the incident particles does not appear to be a significant factor in influencing retention, as long as the incident energy is low enough to not create defects due to collisional cascades during stopping of the incoming particles, yet high enough to penetrate into the surface [616].

In any operating fusion reactor based on the D/T fuel cycle, neutrons striking the surrounding armor and causing displacement damage will have a big impact on the hydrogen isotope retention in that material. A by-product of this neutron generating fusion reaction is the creation of helium ions within the burning plasma. These helium ions also interact with the surrounding armor. Therefore, before discussing neutron effects in tungsten, it is important to understand the interplay between hydrogen isotopes and helium reactions in tungsten.

As described in Section 5.1, exposure of tungsten to a large flux of energetic helium particles at temperatures below those that induce fuzz growth (<1000 K), results in the formation of a thin layer of nano-bubbles that occupy the top 20-40 nm of the surface. The impact of this nano-bubble layer on the retention of deuterium is dramatic. As can be seen in Fig. 21, factors of 100 to 1000 reductions in retention can be achieved near a temperature of 600 K. On the other hand, no change in retention is detected at temperatures close to room temperature.

The temperature dependence of the effect appears to be related to helium bubble growth. TEM imaging of tungsten samples exposed at a variety of temperatures to helium charge-exchange flux in LHD [553] showed little, if any, bubbles at 338 K. As the temperature increased to 463 K, bubbles became apparent with their size increasing above 813 K. Grazing Incidence Small Angle X-ray Scattering (GISAXS) measurements also do not show the presence of nano-bubbles after low temperature helium plasma exposure [617]. As the exposure temperature increases and the bubble layer becomes densely formed, the impact of the helium nano-bubble layer begins to appear and becomes quite dramatic. Miyamoto et al. [618] observed the first evidence of this effect during low-energy, high-flux plasma bombardment of tungsten samples at 573 K. Deuterium retention in tungsten after mixed D/He plasma, as compared to pure D plasma, was drastically suppressed by the simultaneous helium bombardment of the surface. At the same time, blisters that occurred during pure D plasma exposure, were seen to be absent from the mixed plasma exposed surface.

Subsequent measurements, utilizing TEM analysis of the surface cross-section, revealed the near surface contained a dense array of nanometer scale bubbles [552] extending a few tens of nanometers into the surface. TEM examination of the surface cross-section during somewhat higher temperature exposure (773 K), showed what appeared to be these bubbles interconnecting within the nano-bubble layer that could potentially provide direct connections for diffusing species to be released back to the surface. Two hypotheses to explain the reduction in retention grew from these measurements. In the first, interconnected porosity was responsible, in the second, the helium bubbles themselves provided some sort of diffusion barrier to permeating deuterium atoms in tungsten.

Measurements using in-situ analysis of ion beam interactions with tungsten [552], which invoked percolation theory, supported the idea of interconnected porosity. On the other hand, molecular dynamics modeling of deuterium in the presence of helium-filled bubbles seemed to support the idea of deuterium being trapped in the tungsten surrounding the bubbles [619]. The strain induced in the tungsten lattice surrounding the bubbles may alter the migration energy for diffusion [619]. Recent experiments in a plasma device determined that the primary mechanism responsible for the retention reduction was altered diffusion of deuterium in tungsten in the presence of helium-filled bubbles [620]. However, the best agreement between experimental results and modeling occurred when some amount of surface-connected porosity was also included in the model. The final bit of data indicating the importance of strain in the material was that by releasing some of the pressurized helium from the bubbles, the deuterium

permeability began to be recovered [620]. Similar reductions of permeation flux due to simultaneous deuterium and helium ion beam irradiation have also been measured [621].

6 Synergistic effects of neutron irradiation and plasma interaction

Along with helium generation in a burning D/T plasma, neutrons will also be generated and impinge on the plasma-facing materials. These neutrons will create collisional cascades within the lattice, leaving behind defects in the material. The measure of damage created by the collisional cascades is referred to as displacement per atom (dpa). Presently, there is no high-flux fusion neutron source available and so researchers have employed a variety of techniques to simulate the expected damage from neutron bombardment in order to investigate the effects of this damage on the material surrounding a burning plasma.

Two primary techniques have been employed to try to develop an understanding of the consequences of exposure of materials to a burning plasma. The first involves exposing samples to a neutron flux typically from fission reactors. While this approach creates collisional cascades that may more closely resemble those of fusion neutrons, it can create effects that may not exist when exposing samples to a fusion neutron spectrum. For example, the ratio of transmutations to damage created does not resemble that from fusion neutrons and the generation of helium and hydrogen in tungsten is not similar [622]. In addition, there are practical considerations for handling neutron irradiated tungsten samples which include long cooling off periods and extensive safety considerations when examining the irradiated samples. For these reasons, energetic ions beams are also used to mimic neutron irradiation effects. Like fission neutrons, energetic ions are not an ideal substitute for fusion neutrons [623]. Issues related to the type of ion and the ion energy all play a role in the damage created in tungsten samples. One practical limitation of ion beam irradiation is the damage is typically located only within a few microns of the irradiated surface, so interactions with high fluence plasma may be limited. In addition, the damage creation rate (or dose rate) is many orders of magnitude larger for ion beam irradiation, compared to neutrons, but the dose rate has recently been shown to not have a large influence on the retention of hydrogen isotopes in tungsten [624]. With all these details mentioned, this paper will gloss over the details related to creating damage in the material and focus on how the plasma interacts with damaged tungsten.

Damage induced in tungsten can have at least two profound effects. The first is related to an increase in the retention of hydrogen isotopes at the defects produced by the collisional cascades. The second effect is a change in the thermomechanical properties of the tungsten which may affect it desirability for use in a plasma-facing component. Each of these issues will be discussed in turn during the next part of this section.

In damaged tungsten, diffusing deuterium atoms typically become trapped in regions relating to the induced damage profile. The release of plasma atoms retained in the material has been correlated with different defect types as a function of damage dose, fluence and temperature [625]. It is, therefore, not surprising that retention increases as the dpa increases. The important issues to discuss are the saturation level of retention vs. dpa, any annealing of the incurred damage that may occur at elevated temperature and the types of traps created as compared to neutron damage.

There have been several ion beam studies that have observed a saturation of deuterium retention in tungsten with increasing damage level [626–629]. One of the examples for deuterium retention in damaged tungsten with high energy tungsten ions and neutrons is shown in Fig. 22. All of these publications agree that a saturation of retention with increasing damage occurs at a dose of 0.1-0.5 dpa. However, it should be noted that these levels of retention are obtained during deuterium loading after the damaging phase of the experiments are completed. Similar levels of damage saturation have also been calculated for other high-Z materials [630]. An open question exists as to whether or not damaging in the presence of hydrogen isotopes or helium atoms in tungsten results in the same level of saturation. In other words, does the presence of an atom in a trap location prevent annihilation of that defect during subsequent cascades in tungsten.

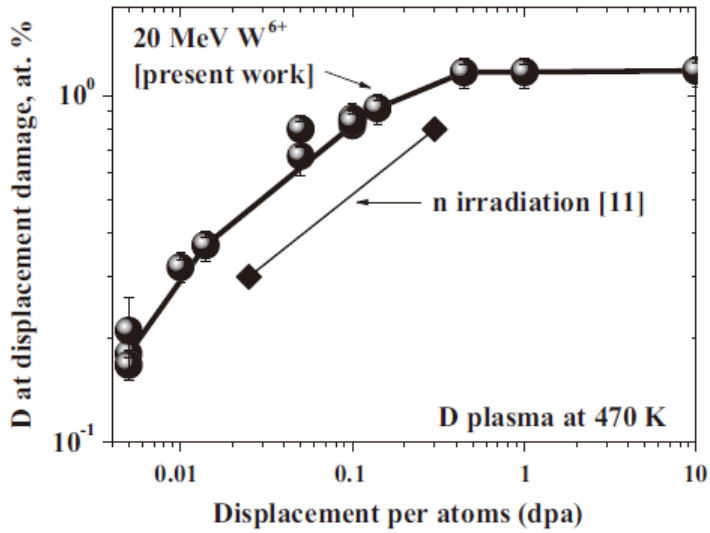

Fig. 22: Comparison of the deuterium concentration at radiation-induced defects in W created by neutron irradiation in the high-flux isotope reactor (HFIR) at Oak Ridge National Laboratory (ORNL) [631], *and by irradiation with 20 MeVW6+ and subsequently exposed to D plasma at sample temperature of 470 K* [627].

The wall temperature in any future fusion reactors is expected to be high for good power conversion efficiency. The question then arises as to the level of defects expected to survive at these elevated temperatures. Experiments have also addressed the annealing of damaged tungsten during different annealing temperatures [632–636]. As expected, as the temperature during the annealing process increases, the number of defects remaining in the material decreases. Full recovery has been reported at an annealing temperature of 1250-1300 K [633,636], with reduced recovery occurring at lower temperatures. The results from the annealing process agree well with the stages of damage recovery form neutron irradiated tungsten [133], showing at least qualitatively the similarities between ion beam and neutron damaged tungsten materials.

Measurements have shown that a similar level of damage, whether it be induced by heavy ion beams or fission neutrons, results in a similar value of retained deuterium at the location of the damage [626]. However, the deuterium release spectrum between the two types of energetic particles can be much different [631], indicating that the trapping of deuterium is occurring in much different types of defects. This might be expected due to the differences in the resulting cascades from the two types of incident particles [623]. Unfortunately, the little information available for fusion neutron irradiated tungsten does not resemble either heavy ion or fission neutron irradiated tungsten [637]. In addition, the deuterium retention in the fusion neutron irradiated tungsten was the same order of magnitude, yet the level of fusion neutron damage was on 2 x 10^{-7} dpa [637].

Although fusion neutron damage appears to be different than either fission or heavy ion beam damage, it is still possible to learn from surrogate irradiations of tungsten in anticipation of a high-fluence fusion neutron source. For example, it is possible to attribute certain release behavior to types of defects and to examine the annealing characteristics of that particular defect type. Also, the evolution of defects as a function of temperature or fluence can be evaluated. All the different types of irradiations should be pursued to gain as much valuable information as possible before a high-fluence neutron source becomes available.

The other area where damage to a material is important to the PMI with tungsten is with respect to changes in the thermo-mechanical properties of the material. Neutron irradiation of tungsten is well known to cause an increase in hardness and loss of ductility (embrittlement) of the material [531]. The hardness increase results from the creation of voids and dislocation loops within the material. Transmutation of tungsten into rhenium also increases the hardness. Both of these processes increase with increasing dpa. Another important effect of the large hydrogen content in the near surface of the material (discussed in the previous section) is embrittlement (in addition to that caused by neutron irradiation). The large amount of dislocations created and the presence of the hydrogen itself in the lattice will increase the hardness of

the surface, leading to embrittlement. The plasma-facing surface can then exhibit an increased tendency to crack during transient heat loads (see also Section 7).
A large amount of work in the area of changes to the mechanical properties of tungsten surfaces exposed to steady-state plasma loading, as well as transient power and particle loads has recently been reviewed by De Temmerman [599]. The interested reader is referred to that publication and to the references therein.
Besides altering the mechanical properties of the surface, the other significant effect that plasma exposure can have is alteration of the thermal transport characteristics of the material. One of the major functions of tungsten as a divertor target material is to remove the power deposited by the plasma. Changes to the thermal conductivity can result in additional thermal stresses in the materials, as well as premature melting of the surface during either steady-state or transient power loading.
To date, only a few measurements exist for changes due to plasma exposure. The thermal conductivity of helium plasma exposed tungsten, where the thin layer of helium nano-bubbles form within the top ~20 nm of the surface, showed a factor of 10-20 drop [638], see Fig. 23. Another measurement of helium-plasma exposed tungsten, which had formed a 3.5-micron thick fuzz layer, showed a factor of approximately 100 drop in the thermal conductivity of the nano-tendrils [639]. To date there appear to be no measurements from tungsten samples exposed to high-flux deuterium plasma.

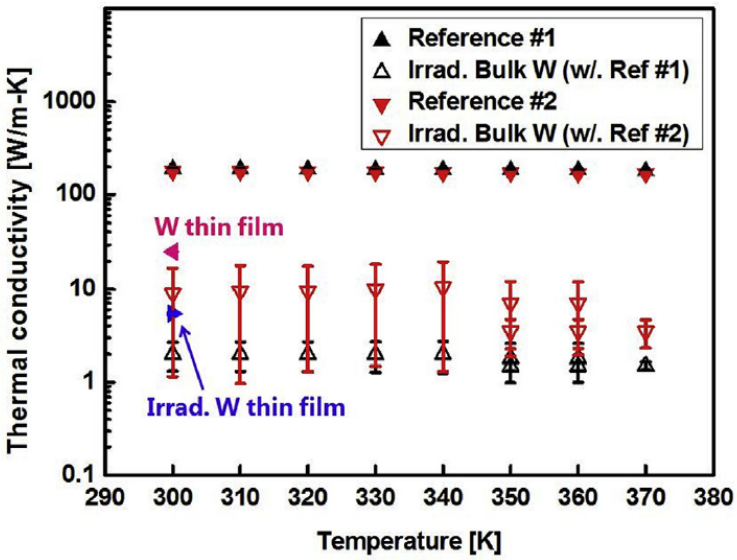

*Fig. 23: Thermal conductivity of pristine W and He p*lasma damaged W layer in bulk W, *along with that of thin film before and after irradiation.* The thermal conductivity *of the damaged film is at least one order of magni*tude lower than that of pristine *bulk W, and is nearly temperature independent,* suggesting the effect of defects *introduced during He plasma bombardment* [638].

Additional measurements exist, however, for changes in the thermal properties of damaged tungsten materials. The first measurements of a tungsten surface damaged by heavy ions to 0.2 dpa using a contact 3-ω measurement method found a 60% drop in the thermal conductivity of the damaged layer [640]. Additional measurements using an energetic helium ion beam and non-destructive laser techniques have been used to measure changes in thermal conductivity at a different damage level [641]. These measurements showed approximately a factor of ten reduction at 0.2 dpa and only a slight decrease in the thermal conductivity with increasing dpa. It should be pointed out that such saturation is similar to that observed in the hydrogen retention behavior of damaged tungsten mentioned previously.
Recent measurements, using the 3-ω technique and heavy ion damage, also show saturation of the thermal conductivity at about 40% of the value of pure tungsten with increasing damage [642]. These measurements also revealed recovery of the thermal conductivity to about 90% of the value for pure tungsten when the samples were damaged at 1000 K [642]. Again, this annealing of damage is similar to that observed for the retention properties of tungsten damaged at elevated temperature [636].

Finally, lanthanum-oxide doped tungsten was used to measure changes in thermal conductivity of fission-neutron irradiated samples [643]. A reduction of about 30% was measured at 0.2 dpa and again recovery of the thermal conductivity was observed at higher temperature.

7 High Heat Flux Effects on Tungsten

In recent studies, tungsten is considered as the most promising plasma facing material (PFM) for future fusion devices like ITER or DEMO [539,644]. Based on current tokamak designs, the most severe environmental conditions a PFM has to withstand during normal operation are in the divertor region. Beside high fluxes of low-energy particles (e.g. H, D, He, T, …) and neutron irradiation, tungsten will have to withstand repetitive and intense thermal loads with long discharge durations. These heat loads can be separated into a stationary and transient contribution. Experiments to investigate the performance and damage evolution of tungsten and tungsten components under these heat load conditions are performed with electron-beam, pulsed plasma, neutral beam, and powerful lasers devices [645–651].
Electron and neutral beam devices are the most common and flexible test devices today. They are capable to determine the stationary heat load performance of actively cooled plasma facing components (PFCs) as well as to simulate intensive transient events. Laser devices are used to apply intense transient events on a relatively small area. In combination with a linear plasma device this technique enables us to investigate synergistic effects between transient heat loads and plasma background. The major difference between electron and laser beam loading is the energy deposition in the bulk and near surface region, respectively, which does not have any qualitative influence on the thermal shock response of tungsten. Quasi stationary plasmas can provide intense pulses and allow the investigation of the influence of plasma pressure on the damage formation and melt motion. The most recent development is superimposed transient heat loads in plasma devices generated by a fast increase of the input power in the plasma source (capacitor bank). All of these simulation methods are addressing different aspects of fusion relevant heat loads and synergistic effects. The combination of all these methods is necessary to obtain a comprehensive picture of the expected material degradation during the operation of a fusion reactor. Hereafter, the focus will be the high heat load performance of tungsten and what are the important materials parameters influencing the damage response.
A schematic depiction of the temperature evolution during plasma discharges in a fusion device is shown by the red line in Fig. 24. The lower and upper limits for the surface temperature are defined by the ductile-to-brittle transition temperature (DBTT ≈ 373 K – 873 K [1]) and the recrystallization temperature (T_{recr} ≈ 1300 K – 1600 K [652,653]) of tungsten, which depend strongly on the material composition and the thermo-mechanical treatment during manufacturing.
The maximum expected stationary heat fluxes during the Deuterium-Tritium phase of ITER are 10 MW m^{-2} during normal steady state operation and a limited number of short duration (<10 s) slow transients of up to 20 MW m^{-2} [539]. These stationary heat loads in combination with the design of the plasma facing components and cooling parameters result in the base surface temperature (T_{base}).
The maximum T_{base} and the cyclic heating of the PFCs are mainly a concern for the formation of macro-cracks [416,437] and the joint between PFMs and heat sink [432,654–656]. For values above T_{recr}, recrystallisation of tungsten during the normal operation will take place and change its mechanical properties, such as a decrease in hardness and strength, which can facilitate the formation of deep macro-cracks [397,437]. Melting of large parts of the tungsten surface can lead to material erosion by melt layer loss, to plasma contamination, and to failure or to reduced power handling limits of PFCs. Furthermore, the pulsed operation causes damage accumulation and fatigue of the joint. Both effects could result in a delamination or detachment of the tungsten armor from the heat sink (e.g. a cooling pipe) and in overheating, melting and failure of the complete component [432,654–656].

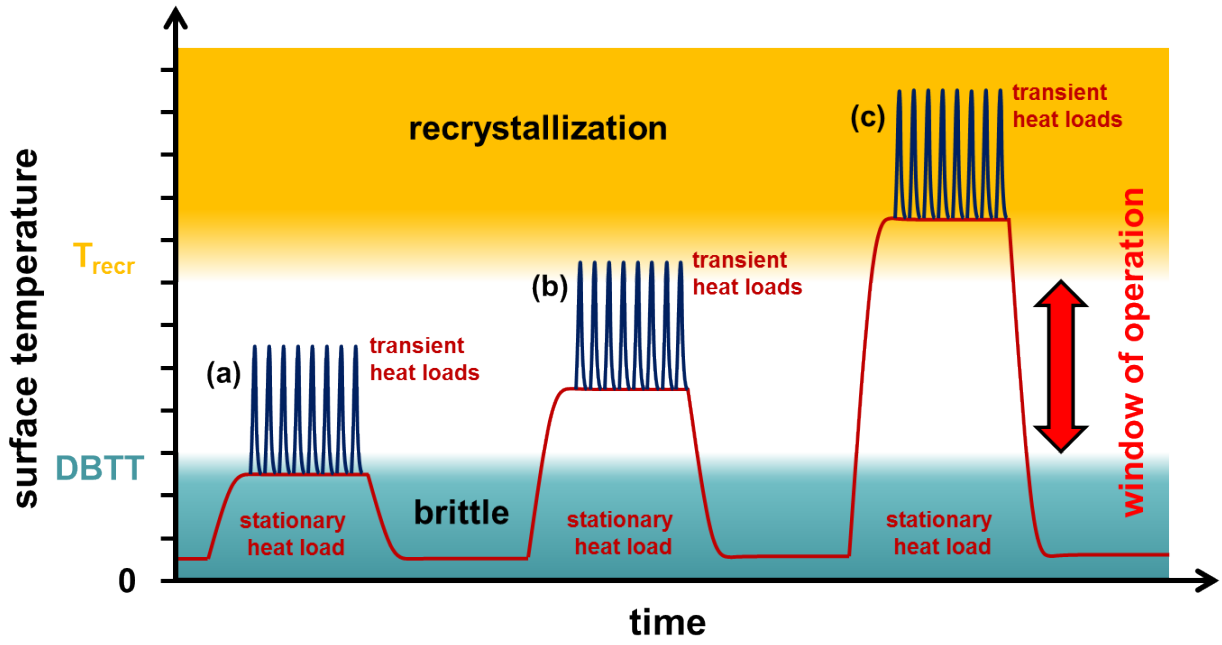

Fig. 24: Schematic depiction of the temperature evolution during plasma discharges in a fusion reactor with different stationary heat loads (red line, increasing from left to right) and the temperature rise during transient events (blue line) which cause an additional fast increase of the surface temperature. (a) temperature increase due to stationary heat loads below DBTT; (b) temperature increase due to stationary heat loads between DBTT and T_{recr}; (c) temperature increase due to stationary heat loads above T_{recr}.

In contrast to stationary heat loads, which provide a certain T_{base} with a shallow temperature gradient through the PFM, transient heat loads affect only the surface region with a steep temperature gradient in the scale of several hundred micrometers for a pulse length of ~1 ms. Several kinds of transient thermal events will occur during the operation of a fusion device. They can be divided into normal and off-normal events.

ELMs (edge localized modes) are expected during normal operation and are so-called off-normal events. They deposit in short (0.1–1 ms) but intense outbursts several percent of the plasma stored energy on the PFM. In a large device like ITER, ELMs deposit a maximum energy density of up to several MJ m^{-2} and occur with frequencies in the order of a few Hz [657]. In order to avoid melting of the tungsten divertor surface, the ELM energy density needs to be decreased to values below <1 MJ m^{-2}. This can be achieved by increasing the frequency to values of several ten Hz. However, this means more than 10^6 ELMs can easily be reached in the lifetime of a PFC [658–660]. The temperature development during such transient events is schematically shown by the blue lines in Fig. 24.

Beside ELMs, several less frequent (≥10^3) off-normal events such as plasma disruptions (30 MJ m^{-2} in 1–10 ms), vertical displacement events (VDEs, 60 MJ m^{-2} in 100–300 ms) and runaway electrons (50 MJ m^{-2} in <50 ms) might also occur [661] [662].

For a better comparison of thermal shock experiments performed in different facilities with different pulse durations, the heat flux factor ($F_{HF}= L\sqrt{\Delta t} = \frac{E}{\sqrt{\Delta t}}$ (L = power density, E = energy density, Δt = pulse duration)) is used. F_{HF} is directly proportional to the temperature increase at the surface during the transient event. However, it is valid only for constant (square pulse) and not for time dependent pulse shapes (e.g. triangular shape) [663].

The exposure of tungsten to frequent transient thermal loads results in a very fast thermal cycling of the first few hundred micrometers below the plasma facing surface. A wide range of surface modifications and damages is induced by these loading conditions. The surface modifications and damages are strongly influenced by the material properties and the microstructure but the underlying damage mechanisms are the same.

During the thermal shock, the heated surface area is subjected to thermal expansion, which is restricted by the colder surrounding material, generating compressive stresses. These stresses lead to plastic

deformation if they overcome the yield strength of the material. After the thermal shock, the material shrinks during the cooling down phase, but cannot return to its original state depending on the degree of plastic deformation, and thus the compressive stresses are converted into tensile stresses. Depending on the base temperature (below or above DBTT) these stresses can result in brittle cracks, which develop typically during the first couple of pulses, or in fatigue cracks, respectively [664–666].

Fatigue cracks are caused by the weakening of a material by repeatedly applied loads and by the accumulation of defects like dislocations. Therefore, it can be assumed that roughening due to plastic deformation is a precursor to crack formation. Once formed, these cracks constantly grow deeper into the material under further loading [664–666]. In contrast to fatigue cracks, brittle cracks are formed during the first couple of thermal shock pulses and do not change in crack density, width, or depth during further loading. They stop in a certain depth where the stresses (due to the thermal gradients) are insufficient to drive the cracks deeper into the material. Whether the fatigue crack depth saturates or continuously grows with increasing number of pulses cannot be answered yet.

Thermal shock tests are performed on different tungsten products with different absorbed power densities, base temperatures, pulse length and repetition rates in order to quantify the influence of certain materials properties and parameters on the damage response of tungsten. Based on the performed tests, damage mappings can be prepared (see Fig. 25). These show the response of the material (Fig. 25a pure tungsten produced by powder metallurgy + forging and Fig. 25b the same materials recrystallized in a vacuum furnace for 1 h at 1600 °C) to a low number of thermal shocks at different base temperatures. Induced surface modifications and damages are color and shape coded. The damage threshold is indicated by a green line while the red box indicates the mechanical properties of the material/samples obtained from tensile tests. This example shows clearly that the reduction of the mechanical strength (yield strength is smaller by a factor of about 3) after recrystallization leads to a significant drop of the damage threshold, which cannot be compensated by the increased ductility (fracture strain).

Thus, the thermal shock performance and damage evolution of tungsten depends strongly on its microstructure (grain size and orientation), mechanical properties (yield strength, ultimate tensile strength, ductility), and thermal properties (thermal conductivity, thermal expansion coefficient) [667]. Experiments have shown that for pure tungsten with ITER relevant grain orientation perpendicular to the loaded surface, the damage threshold is below 3 $MWm^{-2}s^{0.5}$ [665,666]. This is very low compared to the expected loading conditions in future fusion devices like ITER [539]. Grains oriented parallel to the loaded surface improve the mechanical strength (texture strengthening effect). The improved yield and ultimate tensile strength cause a higher resistance to surface modifications and cracking. However, this parallel grain orientation enhances the risk of parallel crack formation. These parallel cracks act as thermal barrier (reduced heat dissipation capability) and make the material more prone to overheating, melting, and to ejection of complete grains or parts of the surface. A reduced thermal conductivity due to the addition of alloying elements to improve the mechanical strength would lead to a smaller heat penetration depth and a smaller crack depth but also to a higher crack density to compensate the higher stresses at the surface. At high pulse numbers, small scale damages will accumulate and result in severe plastic deformation and cracking. Then small parts in the surface region will lose contact with the bulk material. This would cause a significant drop of the heat dissipation and results in overheating and melting of these structures. The loose contact of these structures to the bulk also poses the risk of enhanced erosion.

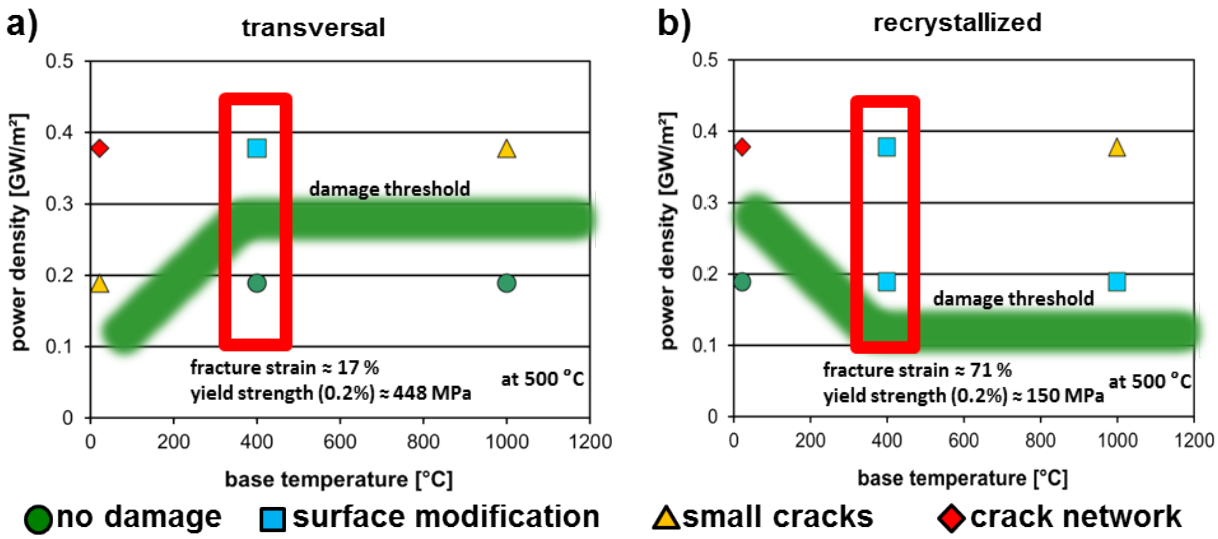

Fig. 25: Damage mappings of tungsten samples exposed to 100 ELM-like thermal shocks at different base temperatures and absorbed power densities with a pulse duration of 1ms and repetition frequency of 1 Hz [380]. *a) tungsten samples with grain oriented perpendicular to the loaded surface (transversal); b) same tungsten samples as in (a) but recrystallized at 1600 °C for 1 h before the thermal shock exposure. The green line indicates the damage threshold of the material while the red box indicates the mechanical properties (written below) obtained in tensile tests.*

During a plasma discharge, the maximum surface temperature results from a combination of T_{base} and the temperature rise during transient events as shown in Fig. 24. The surface temperature has significant influence on the properties of tungsten and is therefore of major importance for the performance of tungsten as PFM. A T_{base} between the DBTT and T_{recr} would be ideal in order to prevent brittle crack formation due to transient heat loads (see Fig. 24a) and recrystallization of tungsten during stationary exposure (see Fig. 24c). However, even for T_{base} within this window of operation, the temperature rise during transient event also needs to be considered (see Fig. 24b). Experiments have shown that recrystallization and grain growth of a large near surface zone occurs during transient heating due to the high repetition rates and large number of events [390,668,669].

Beside the plastic deformation and cracking of the PFM, recrystallization is one of the major concerns for the use of materials in a fusion reactor. Recrystallization is a time and temperature dependent process that strongly modifies the microstructure and mechanical properties of the material. It leads to a decreased strength, hardness, and cohesion between single grains. Due to the reduced mechanical strength of the recrystallized tungsten, the damage evolution is much faster and might lead to an earlier failure of a plasma facing component. The low cohesion leads to a predominantly intergranular cracking, which significantly increases the risk of overheating/melting and/or loss of complete grains, especially during long term operation of a fusion reactor. It can be stated that improved recrystallization behavior of tungsten would be beneficial for the application as plasma facing material and, in particular, it would have a positive impact on the high heat flux resistance (cyclic steady state loading). The reduction of mechanical strength and softening due to recrystallization deplete the thermal fatigue resistance of the material under identical loading conditions and therefore has a detrimental impact on the damage behavior and deformation of the material [388,437].

Furthermore, investigations like those in [381] show that molten and re-solidified tungsten surfaces exhibit a very similar damage behavior to recrystallized materials. It is not yet clear whether the thermal shock damages are a problem for the lifetime of a complete PFC. Nevertheless, high pulse number experiments [665,666] in combination with stationary heat load tests of PFCs [416,437] have demonstrated that continuous crack propagation under stationary loads and localized melting impose the risk of an increased tungsten release rate into the plasma.

Summarizing, it can be stated that the high heat flux and thermal shock performance of tungsten is a very complex interaction between a lot of parameters comprising among others the loading conditions itself, the thermal and mechanical properties, and the microstructure.

In addition to the pure thermal exposure of tungsten, high flux particle loading needs to be taken into account, too. H and He irradiation will change the mechanical and thermal properties of tungsten and hence have an influence on the thermal shock damage response. Due to H/He embrittlement, critical stresses for damage and crack formation will be lower and also lead to faster damage evolution [364,669]. As outlined in Section 5, He-induced bubble formation directly below the surface reduces the thermal conductivity and can result in higher surface temperatures. In addition, W-fuzz growth could lead to enhanced erosion of tungsten materials [578,581]. Unfortunately, the impact of high-energy neutrons on the performance of tungsten under transient heat loads, especially for high pulse number tests and simultaneous particle exposure, is not clear yet [147].
Beside the testing and characterization of commercially available tungsten products (see Fig. 25) a wide range of R&D activities focusses on new tungsten-based materials concept and manufacturing processes in order to improve the stationary and transient heat load performance. Some examples for these developments are microstructure stabilized/dispersion-strengthened tungsten alloys, self-passivating tungsten alloys, tungsten fiber-reinforced tungsten (W_f/W) composites and particle reinforced powder injection molding (PIM) tungsten [670] (an overview is given in Section 3). High heat flux tests of a wide range of different tungsten products have shown that the microstructure and the improvement of the mechanical strength are crucial points for new materials developments. The concept of W_f/W composites has already shown pseudo-ductile behavior and therefore overcome brittleness as one of the major problems of tungsten. However, the behavior under fusion relevant loads still needs to be investigated [671]. New tungsten grades manufactured by PIM have already been tested under fusion relevant heat loads. The results indicate an improved or at least similar stationary and thermal shock performance compared to industrially available tungsten grades [672].
The combination of this wide range of environmental conditions and new material developments makes the evaluation of tungsten and the prediction of possible damages and life-time very difficult and complex. However, it can be assumed that recrystallization and molten/re-solidified surface structures have a detrimental influence on the lifetime of PFM and components. Therefore, further investigations of tungsten as PFM for long term operation with high accumulated neutron doses and the study of the influence of pre-damaged surfaces on the plasma performance in existing tokamaks are presently important issues that will have to be addressed prior to the design of future fusion reactors.

8 Summary and Outlook

Without any doubt, research on tungsten materials have achieved by far the highest interest within the field of nuclear fusion research. Particularly, the International Thermonuclear Experimental Reactor (ITER) project was the main driver for an amazing increase in tungsten-related publications regarding irradiation and plasma interaction. Moreover, the world-wide ambitions towards a fusion demonstration reactor (DEMO) have initiated comprising plasma experiments and many irradiation studies.
Neutron irradiation induced defect formation and recovery experiments have been extensively performed on tungsten since the late 1950s. Therefore, activation energies on interstitial, vacancy, cluster formation and migration are probably the most studied and accurate data available for irradiated tungsten. Especially for the validation of modern atomistic modelling methods, these results have certainly been an invaluable source. On the other hand, macroscopic effects and mechanical properties have never been explored extensively. Irradiation induced void swelling, for example, has been explicitly studied in two experiments only: one for pure W and another one for W-25Re. And only a combination with unpublished data led later to a more complete picture. A comprising compilation of irradiation and engineering data on tungsten (and other refractory alloys) is given in [5], which represents the somewhat limited state of knowledge in the 1980s. With the upcoming ITER project and further nuclear fusion driven R&D programs, the demand for irradiation data on tungsten increased. As a consequence, basic mechanical post irradiation data (tensile, bending, hardness for relatively low doses) was produced, but also – very important for plasma-facing components – an irradiation microstructure map for the W-Re system [168] was established, which explains the Re precipitation morphology in tungsten. However, engineering data for a broader temperature and dose range, like for example fracture mechanics, fatigue, or creep data, is still not available.

Reliable databases of ion physical sputtering of metallic materials with energies down to about 40 eV and ion flux up to about 10^{21} m^{-2} were obtained since the 1950s. The energy regimes roughly correspond to those of plasma-facing materials and also include sputtering yields by hydrogen isotopes and helium ions, which are dominant in fusion applications. Therefore, these databases are important for the component design.

Hydrogen isotope behavior in metals has been also studied for a long time. Tungsten has a low hydrogen solubility and basic hydrogen isotope behavior is expressed by diffusion and trapping at defects. But high flux (high fluence) ion irradiation, a unique feature for plasma-facing materials in fusion devices, leads to oversaturation and to an associated increase in hydrogen isotope retention. Moreover, extensive studies on surface morphology changes by light ion bombardment were performed. Here, the focus was laid on blistering and He induced surface modification, like for example, the formation of surface He holes and nano-fibers. Such surface modifications could speed up the erosion of the armor parts in plasma-facing components significantly by sputtering, by pulsed load including melting and droplet ejection, and by unipolar arcing. Thus, the nature of blister and “fuzz” formation was (and still is) investigated thoroughly – also by applying modern simulation methods like density-functional theory, molecular dynamics, and kinetic Monte Carlo codes. However, some details on the specific formation mechanisms are still not known.

Hydrogen isotope retention in tungsten is an important safety issue in the design of future fusion reactors. Therefore, it not surprising that a lot of experimental and modeling efforts for understanding the behavior of hydrogen isotopes in tungsten have been made during the last decades [545,586,594–599]. Of interest are trapping sites, like dislocations, which could be multiplied by rising H/D/T concentrations and then propagate deeper into the material and act as further trapping sites. Such a mechanism would explain the lack of saturation of deuterium retention in extremely large-fluence plasma exposures. Another important effect related to the dislocation formation by the presence of hydrogen in the lattice is embrittlement. The plasma-facing surface can then exhibit an increased tendency to crack during transient heat loads. Measurements revealed a retention peak in the region around 400-700 K (contrary to expectations, where one might assume it to appear at higher temperatures), which is likely dependent on the details of the microstructure of the tungsten material, on the sample preparation methodology, on the purity of the material, and other details. This peak in retention is correlated to the empirical observation of blister formation in the tungsten surface. While the relationship to deuterium retention is clear, the understanding of the formation mechanisms requires still more investigations.

Among the least explored fields considered in this review are probably the synergistic effects of neutron irradiation and plasma interaction. Since there is no facility, which combines neutron irradiation with plasma exposure, experiments have to be performed sequentially (first irradiation, then plasma exposure), or neutron irradiation is replaced by ion or proton irradiation. However, it is rather difficult to meet all requirements (damage and transmutation rate, dose, H/He concentrations, etc.) for a specific case study, like for example, for a nuclear fusion relevant experiment. Nevertheless, neutron damage in tungsten can have at least two profound effects. The first is related to an increase in the retention of hydrogen isotopes at the defects produced by the collisional cascades. The second effect is a change in the thermomechanical properties of the tungsten material, which may affect its possible use in a plasma-facing component. Both topics were addressed mainly for lower dose levels within ITER-related experiments. Reliable (engineering) data for the design of a future nuclear fusion reactor (e.g. DEMO) is still not available.

Regarding high heat flux tests, electron and neutral beam devices are the most common and flexible test devices, while laser beams are used to apply intense transient events on a relatively small area. In combination with a linear plasma device this technique enables the investigation of synergistic effects between transient heat loads and a plasma background. The most recent development is superimposed transient heat loads in plasma devices generated by a fast increase of the input power in the plasma source by a capacitor bank. However, the combination of all these methods is required to obtain a comprehensive picture of the expected material degradation during the operation of a fusion reactor. So far, a broad range of load scenarios (stationary, transient), materials, component mock-ups, and parameter fields has been covered. It has been demonstrated that the high heat flux and thermal shock performance of tungsten and tungsten materials is a very complex interaction between a lot of parameters comprising among others the loading conditions itself, the thermal and mechanical properties, and the microstructure. In addition to the pure thermal exposure of tungsten, high flux particle loading needs to be considered, too. As mentioned

above, H and He irradiation changes the mechanical and thermal properties of tungsten and hence have an influence on the thermal shock damage response. Due to H/He embrittlement, critical stresses for damage and crack formation will be lower and also lead to faster damage evolution[364,669][364,668][364,668][372,668][372,668][364,668][364,668][364,667][365,668][370,665][362,665][362,665][362,665][369,664][360,663][360,663][368,663][368,663]. As outlined in Section 5, He-induced bubble formation directly below the surface reduces the thermal conductivity and can result in higher surface temperatures. In addition, W-fuzz growth could lead to enhanced erosion of tungsten materials. Unfortunately, the impact of high-energy neutrons on the performance of tungsten under transient heat loads, especially for high pulse number tests and simultaneous particle exposure, is not clear yet [147].

As repeatedly mentioned, nuclear fusion is the main tungsten-related R&D field in which irradiation and plasma interaction play a central role. This is certainly the reason why the interest in tungsten materials from a technological as well as a scientific viewpoint is currently as high as probably never before. As discussed and concluded, there are a number of open questions, which need to be answered in the course of a conceptual design phase towards DEMO. Interestingly, many of these are related to neutron irradiation and/or PSI effects, and it is rather likely that some of the recently completed campaigns will close one or another gap in the tungsten database. Currently more campaigns and R&D programs are in the planning stage and even more will be required to address all open questions. Therefore, the authors predict a bright future for the research field “irradiation behavior and plasma interaction of tungsten materials”. And certainly, the Journal of Nuclear Materials will further play an important role in this endeavor.

9 Acknowledgments

The authors are grateful to all colleagues worldwide who contributed to this exciting topic. Without their comprising R&D work and resulting publications this review would not have been possible. We want to emphasize that due to page limitations just a small selection of papers could be cited. In any case, this doesn’t mean that the other works are not considered as a valuable contribution to the topic.

Many thanks go also to Gary Was and Steve Zinkle who invited and encouraged the authors to this review. Finally, congratulations to the whole Journal of Nuclear Materials team - present and past - to the 60th (diamond) anniversary!

10 References

[1] E. Lassner, W.-D. Schubert, Kluwer Academic, New York, 1999.
[2] R.W. Fountain, J. Maltz, L.S. Richardson, eds., Gordon and Breach, New York, 1966.
[3] R.I. Jaffee, G.M. Ault, J. Maltz, M. Semchyshen, eds., Gordon and Breach, New York, 1967.
[4] W.D. Wilkinson, Gordon and Breach, New York, 1969.
[5] R.H. Cooper Jr., E.E. Hoffman, eds., in: Proc. a Symp. Held Oak Ridge, Tennessee August 10-11,1983, Tech. Inf. Center, Off. Sci. Tech. Information, United States Dep. Energy, 1984.
[6] J. Mathesius, (1564).
[7] F.X. Wurm, J. Franklin Inst. 70 (1860) 42–43. doi:10.1016/0016-0032(60)90572-X.
[8] T.H. Norton, J. Am. Chem. Soc. 19 (1897) 110. doi:10.1021/ja02076a003.
[9] S.J. De Benneville, J. Am. Chem. Soc. 16 (1894) 735–757. doi:10.1021/ja02109a004.
[10] S.J. De Benneville, J. Am. Chem. Soc. 16 (1894) 297–304. doi:10.1021/ja02103a002.
[11] W.H. Wahl, J. Franklin Inst. 134 (1892) 470–472.
[12] J. Waddell, Trans. R. Soc. Edinburgh. 33 (1887) 1–7. doi:10.1017/S008045680002545X.
[13] E.F. Smith, E.D. Desi, J. Franklin Inst. 139 (1895) 290–294.
[14] W.L. Hardin, J. Am. Chem. Soc. 19 (1897) 657–676. doi:10.1021/ja02082a006.
[15] G.E. Thomas, J. Am. Chem. Soc. 21 (1899) 373–381. doi:10.1021/ja02054a007.
[16] E. Desi, J. Am. Chem. Soc. 19 (1897) 213–242. doi:10.1021/ja02077a004.
[17] S. Rideal, J. Chem. Soc. Trans. 55 (1889) 41–45. doi:10.1039/CT8895500041.
[18] J.W. Mallet, J. Chem. Soc. 28 (1875) 1228–1233.
[19] I. Langmuir, Trans. Am. Inst. Electr. Eng. 32 (1913) 1913–1933. doi:10.1109/T-AIEE.1913.4765100.
[20] I. Langmuir, J.A. Orange, Trans. Am. Inst. Electr. Eng. 32 (1913) 1935–1954. doi:10.1109/T-AIEE.1913.4765101.
[21] I. Langmuir, J. Am. Chem. Soc. 35 (1913) 105–127. doi:10.1021/ja02191a001.
[22] I. Langmuir, J. Franklin Inst. 181 (1916) 426–427. doi:10.1016/S0016-0032(16)90275-8.
[23] I. Langmuir, J. Franklin Inst. 181 (1916) 706.
[24] I. Langmuir, Phys. Rev. 7 (1916) 302–330. doi:10.1103/PhysRev.7.302.
[25] K.B. Blodgett, I. Langmuir, Rev. Sci. Instrum. 5 (1934) 321–333. doi:10.1063/1.1751863.
[26] I. Langmuir, J.B. Taylor, Phys. Rev. 50 (1936) 68–87. doi:10.1103/PhysRev.50.68.
[27] I. Langmuir, Phys. Rev. 2 (1913) 450–486. doi:10.1103/PhysRev.2.450.
[28] I. Langmuir, K.H. Kingdon, Science (80-.). 57 (1923) 58–60.
[29] I. Langmuir, Phys. Rev. 21 (1923) 419–435. doi:10.1103/PhysRev.21.419.
[30] L. Tonks, H.M. Mott-Smith, I. Langmuir, Phys. Rev. 28 (1926) 104–128. doi:10.1103/PhysRev.28.104.
[31] L. Tonks, I. Langmuir, Phys. Rev. 29 (1927) 524–531. doi:10.1103/PhysRev.29.524.
[32] L. Tonks, I. Langmuir, Phys. Rev. 34 (1929) 876–922. doi:10.1103/PhysRev.34.876.
[33] I. Langmuir, Phys. Rev. 26 (1925) 585–613. doi:10.1103/PhysRev.26.585.
[34] I. Langmuir, J. Am. Chem. Soc. 34 (1912) 860–877. doi:10.1021/ja02208a003.
[35] I. Langmuir, J. Am. Chem. Soc. 34 (1912) 1310–1325. doi:10.1021/ja02211a004.
[36] I. Langmuir, G.M.J. Mackay, J. Am. Chem. Soc. 36 (1914) 1708–1722. doi:10.1021/ja02185a011.
[37] I. Langmuir, J. Am. Chem. Soc. 37 (1915) 417–458. doi:10.1021/ja02168a002.
[38] I. Langmuir, J. Franklin Inst. 182 (1916) 404–405. doi:10.1016/S0016-0032(16)90900-1.
[39] I. Langmuir, Ind. Eng. Chem. 19 (1927) 667–674. doi:10.1021/ie50210a009.
[40] I. Langmuir, Ind. Eng. Chem. 20 (1928) 332–336. doi:10.1021/ie50219a039.
[41] Wikipedia, Wikipedia. (2018). https://en.wikipedia.org/wiki/Irving_Langmuir.
[42] S. Oghi, J. Phys. Soc. Japan. 11 (1956) 593–598. doi:10.1143/JPSJ.11.593.
[43] J.R. Waters, J.E. Evans, B.B. Kinsey, G.H. Williams, Nucl. Phys. 12 (1959) 563–578. doi:10.1016/0029-5582(59)90098-7.
[44] G. Leliaert, J. Hoste, Z. Eeckhaut, Talanta. 2 (1959) 115–123. doi:10.1016/0039-9140(59)80049-7.
[45] M. Lindner, Phys. Rev. 84 (1951) 240–244. doi:10.1103/PhysRev.84.240.
[46] W. Selove, Phys. Rev. 84 (1951) 869–876. doi:10.1103/PhysRev.84.869.
[47] M. Lindner, J.S. Coleman, J. Am. Chem. Soc. 73 (1951) 1610–1611. doi:10.1021/ja01148a058.
[48] J.M. Cork, M.K. Brice, W.H. Nester, J.M. Leblanc, et al., Phys. Rev. 89 (1953) 1291–1292. doi:10.1103/PhysRev.89.1291.
[49] J.M. Cork, W.H. Nester, J.M. LeBlanc, M.K. Brice, Phys. Rev. 92 (1953) 119–120. doi:10.1103/PhysRev.92.119.
[50] M. Huaringa, Nature. 177 (1956) 85. doi:10.1038/177085a0.
[51] F.W.K. Firk, M.C. Moxon, Nucl. Phys. 12 (1959) 552–562. doi:10.1016/0029-5582(59)90097-5.
[52] J.F. Cosgrove, G.H. Morrison, Anal. Chem. 29 (1957) 1017–1019. doi:10.1021/ac60127a006.
[53] E.M. Bowey, Nucl. Phys. 3 (1957) 553–560. doi:10.1016/0029-5582(57)90020-2.
[54] K. Fajans, W.H. Sullivan, Phys. Rev. 58 (1940) 276. doi:10.1103/PhysRev.58.276.
[55] O. Minakawa, Phys. Rev. 57 (1940) 1189. doi:10.1103/PhysRev.57.1189.
[56] A.F. Clark, Phys. Rev. 61 (1942) 242–248. doi:10.1103/PhysRev.61.242.
[57] C.E. Mandeville, Phys. Rev. 64 (1943) 147–150. doi:10.1103/PhysRev.64.147.
[58] I. Nonaka, S. Tanabe, J. Phys. Soc. Japan. 5 (1950) 398–402. doi:10.1143/JPSJ.5.398.
[59] A.N. Phillips, L. Rosen, R.F. Taschek, Phys. Rev. 75 (1949) 919–922. doi:10.1103/PhysRev.75.919.
[60] M.J. Makin, E. Gillies, J. Inst. Met. 86 (1957) 108–112.
[61] M.W. Thompson, Philos. Mag. 3 (1958) 421–423. doi:10.1080/14786435808236828.
[62] G.H. Kinchin, M.W. Thompson, J. Nuc. Energy. 6 (1958) 275–284.
[63] M.J. Berger, S.M. Seltzer, Phys. Rev. C. 2 (1970) 621–631. doi:10.1103/PhysRevC.2.621.
[64] E. Storm, Phys. Rev. A. 5 (1972) 2328–2338. doi:10.1103/PhysRevA.5.2328.
[65] V. V. Verbinski, D.G. Costello, H.L. Moody, Nucl. Instruments Methods. 133 (1976) 131–136. doi:10.1016/0029-554X(76)90866-1.
[66] P.O. Nilsson, C.G. Larsson, Jpn. J. Appl. Phys. 17 (1978) 144–146. doi:10.7567/JJAPS.17S2.144.
[67] P.G. Kondev, A.P. Tonchev, K.G. Khristov, V.E. Zhuchko, Nucl. Inst. Methods Phys. Res. B. 71 (1992) 126–131. doi:10.1016/0168-

583X(92)95313-G.
[68] A.E.S. Von Wittenau, C.M. Logan, R.D. Rikard, Med. Phys. 29 (2002) 1797–1806. doi:10.1118/1.1494834.
[69] N.A. Abibullaev, K.K. Begimkulov, U.S. Salikhbaev, At. Energy. 92 (2002) 272–273. doi:10.1023/A:1016058300321.
[70] K. Kosako, K. Oishi, T. Nakamura, M. Takada, et al., J. Nucl. Sci. Technol. 48 (2011) 227–236. doi:10.1080/18811248.2011.9711696.
[71] K. Takahashi, H. Kikunaga, K. Tsukada, T. Muto, et al., in: IPAC 2016 - Proc. 7th Int. Part. Accel. Conf., 2016: pp. 1766–1768.
[72] V.K. Sakha, At. Energy. 120 (2016) 280–284. doi:10.1007/s10512-016-0130-y.
[73] P. Tothill, J. Phys. D. Appl. Phys. 1 (1968) 1093–1107. doi:10.1088/0022-3727/1/9/301.
[74] M.H. Unsworth, J.R. Greening, Phys. Med. Biol. 15 (1970) 621–630. doi:10.1088/0031-9155/15/4/001.
[75] N.Z. Noor Azman, S.A. Siddiqui, R. Hart, I.M. Low, Appl. Radiat. Isot. 71 (2013) 62–67. doi:10.1016/j.apradiso.2012.09.012.
[76] M.M. Nasseri, Nucl. Eng. Technol. 48 (2016) 795–798. doi:10.1016/j.net.2016.01.006.
[77] R. Birch, M. Marshall, L.H.J. Peaple, Phys. Med. Biol. 27 (1982) 1119–1129. doi:10.1088/0031-9155/27/9/003.
[78] J.G. Stears, J.P. Felmlee, J.E. Gray, Radiology. 160 (1986) 837–838. doi:10.1148/radiology.160.3.3737925.
[79] R.T. Mainardi, R.A. Barrea, Appl. Radiat. Isot. 46 (1995) 497–498. doi:10.1016/0969-8043(95)00068-2.
[80] S.G. Zhutyaev, G.I. Zhutyaev, A.B. Mishkinis, B.Y. Mishkinis, et al., Biomed. Eng. (NY). 35 (2001) 177–179. doi:10.1023/A:1012727215989.
[81] N.M. Vlasov, A.S. Gontar', V.A. Zaznoba, Fiz. i Khimiya Obrab. Mater. (2001) 56–61.
[82] E. Sato, H. Sugiyama, M. Ando, E. Tanaka, et al., Radiat. Phys. Chem. 75 (2006) 2008–2013. doi:10.1016/j.radphyschem.2005.11.019.
[83] J.M. Oduko, K.C. Young, O. Gundogdu, A. Alsager, 2008. doi:10.1007/978-3-540-70538-3_73.
[84] Y. Yang, X.-Q. Mou, H.-J. Yu, X. Chen, et al., Tien Tzu Hsueh Pao/Acta Electron. Sin. 38 (2010) 2285–2291.
[85] G.W.A. Newton, V.J. Robinson, M. Skarestad, J.D. Hemingway, J. Inorg. Nucl. Chem. 35 (1973) 1435–1441. doi:10.1016/0022-1902(73)80229-5.
[86] O.T. Inal, W.F. Sommer, J. Nucl. Mater. 99 (1981) 94–99. doi:10.1016/0022-3115(81)90142-2.
[87] I. Gavish Segev, E. Yahel, I. Silverman, G. Makov, J. Nucl. Mater. 496 (2017) 77–84. doi:10.1016/j.jnucmat.2017.09.024.
[88] D. Bulgadaryan, D. Sinelnikov, V. Kurnaev, S. Kajita, et al., Nucl. Instruments Methods Phys. Res. Sect. B Beam Interact. with Mater. Atoms. 434 (2018) 9–12. doi:10.1016/j.nimb.2018.07.038.
[89] A. Rakhman, W. Blokland, S. Rajic, M. Rennich, in: Opt. InfoBase Conf. Pap., 2018: pp. 6–7. doi:10.1364/ISA.2018.IM2B.6.
[90] I. Ipatova, R.W. Harrison, P.T. Wady, S.M. Shubeita, et al., J. Nucl. Mater. 501 (2018) 329–335. doi:10.1016/j.jnucmat.2017.11.030.
[91] J. Habainy, Y. Dai, Y. Lee, S. Iyengar, J. Nucl. Mater. 509 (2018) 152–157. doi:10.1016/j.jnucmat.2018.06.041.
[92] D.J. Farnum, W.F. Sommer, O.T. Inal, J. Nucl. Mater. 123 (1984) 996–1001. doi:10.1016/0022-3115(84)90208-3.
[93] C.E. Laird, D.H. Mullins, D.B. McGibney, J. Swartz, et al., Nucl. Sci. Eng. 130 (1998) 320–339. doi:10.13182/NSE98-A2009.
[94] S.A. Maloy, M.R. James, W. Sommer, G.J. Willcutt, et al., Mater. Trans. 43 (2002) 633–7. doi:10.2320/matertrans.43.633.
[95] B.M. Oliver, T.J. Venhaus, R.A. Causey, F.A. Garner, et al., J. Nucl. Mater. 307–311 (2002) 1418–1423. doi:10.1016/S0022-3115(02)01293-X.
[96] G.A. Greene, C.L. Snead Jr., C.C. Finfrock, A.L. Hanson, et al., in: Int. Meet. Nucl. Appl. Accel. Technol. Accel. Appl. a Nucl. Renaiss., 2003: pp. 881–892.
[97] W.F. Sommer, S.A. Maloy, M.R. Louthan, G.J. Willcutt, et al., Nucl. Technol. 151 (2005) 303–313. doi:10.13182/NT05-A3653.
[98] S.A. Maloy, M.R. James, W. Sommer, G.J. Willcutt, et al., J. Nucl. Mater. 343 (2005) 219–226. doi:10.1016/j.jnucmat.2004.12.018.
[99] R. Rayaprolu, S. Möller, C. Linsmeier, S. Spellerberg, Nucl. Mater. Energy. 9 (2016) 29–35. doi:10.1016/j.nme.2016.09.008.
[100] Y. Kasugai, M. Asai, A. Tanaka, H. Yamamoto, et al., J. Nucl. Sci. Technol. 31 (1994) 1248–1254. doi:10.1080/18811248.1994.9735287.
[101] I. Jun, M.A. Abdou, A. Kumar, Fusion Technol. 25 (1994) 51–83. doi:10.13182/FST94-A30236.
[102] C.H.M. Broeders, A.Y. Konobeyev, Nucl. Instruments Methods Phys. Res. Sect. B Beam Interact. with Mater. Atoms. 234 (2005) 387–411. doi:10.1016/j.nimb.2005.02.029.
[103] B. Han, B. Bednarz, Y. Danon, R. Block, et al., Nucl. Technol. 168 (2009) 576–579. doi:10.13182/NT09-A9246.
[104] P. Vorona, O. Kalchenko, V. Krivenko, in: 2nd Int. Conf. Curr. Probl. Nucl. Phys. At. Energy, NPAE 2008 - Proc., 2009: pp. 528–532.
[105] F. Luo, R. Han, Y. Nie, Z. Chen, et al., Fusion Eng. Des. 112 (2016) 355–359. doi:10.1016/j.fusengdes.2016.06.063.
[106] M. Rajput, S. Vala, P. V. Subhash, R. Srinivasan, et al., Fusion Eng. Des. 130 (2018) 114–121. doi:10.1016/j.fusengdes.2018.03.051.
[107] Y. Kasugai, M. Asai, A. Tanaka, H. Yamamoto, et al., J. Nucl. Sci. Technol. 31 (1994) 1248–1254. doi:10.1080/18811248.1994.9735287.
[108] D.G. Cepraga, G. Cambi, M. Frisoni, Fusion Eng. Des. 51–52 (2000) 747–752. doi:10.1016/S0920-3796(00)00222-2.
[109] S. Mirzadeh, F.Y. Lambrecht, R.M. Lambrecht, Appl. Radiat. Isot. 57 (2002) 637–640. doi:10.1016/S0969-8043(02)00177-X.
[110] B. Ponsard, J. Hiltunen, P. Penttilla, H. Vera Ruiz, et al., J. Radioanal. Nucl. Chem. 257 (2003) 169–174. doi:10.1023/A:1024730301381.
[111] K. Seidel, R. Eichin, R.A. Forrest, H. Freiesleben, et al., J. Nucl. Mater. 329–333 (2004) 1629–1632. doi:10.1016/j.jnucmat.2004.04.145.
[112] P. Batistoni, M. Angelone, L. Petrizzi, M. Pillon, J. Nucl. Mater. 329–333 (2004) 683–686. doi:10.1016/j.jnucmat.2004.04.191.
[113] C.H.M. Broeders, A.Y. Konobeyev, C. Villagrasa, J. Nucl. Mater. 342 (2005) 68–76. doi:10.1016/j.jnucmat.2005.03.012.
[114] C. Thomser, V. Bailescu, S. Brezinsek, J.W. Coenen, et al., 2012. doi:10.13182/FST12-A14103.
[115] G. Federici, W. Biel, M.R. Gilbert, R. Kemp, et al., Nucl. Fusion. 57 (2017). doi:10.1088/1741-4326/57/9/092002.
[116] M. Kaufmann, R. Neu, n.d. http://pubman.mpdl.mpg.de/pubman/item/escidoc:2143300/component/escidoc:2143299/kaufmann.pdf (accessed August 21, 2018).
[117] M.W. Thompson, Philos. Mag. 5 (1960) 278–296. doi:10.1080/14786436008235842.
[118] L.K. Keys, J.P. Smith, J. Moteff, Phys. Rev. 176 (1968) 851–856. doi:10.1103/PhysRev.176.851.
[119] S. Okuda, H. Mizubayashi, Phys. Rev. Lett. 34 (1975) 815–817. doi:10.1103/PhysRevLett.34.815.
[120] M.S. Anand., B.M. Pande, R.P. Agarwala, Radiat. Eff. 39 (1978) 149–155. doi:10.1080/00337577808234468.
[121] Y.W. Kim, J.M. Galligan, Acta Metall. 26 (1978) 379–390. doi:10.1016/0001-6160(78)90165-7.
[122] D.N. Seidman, Scr. Metall. 13 (1979) 251–257. doi:10.1016/0036-9748(79)90306-5.
[123] H. Mizubayashi, S. Okuda, Radiat. Eff. 54 (1981) 201–215. doi:10.1080/00337578108210049.
[124] V.I. Shcherbak, Phys. Chem. Mater. Treat. 22 (1988) 104–106.

[125] M.I. Zakharova, N.A. Artemov, V. V. Bogdanov, Inorg. Mater. 37 (2001) 786–789. doi:10.1023/A:1017979230262.
[126] J.C. He, G.Y. Tang, A. Hasegawa, K. Abe, Nucl. Fusion. 46 (2006) 877–883. doi:10.1088/0029-5515/46/11/001.
[127] T. Tanno, M. Fukuda, S. Nogami, A. Hasegawa, Mater. Trans. 52 (2011) 1447–1451. doi:10.2320/matertrans.MBW201025.
[128] M. Fukuda, T. Tanno, S. Nogami, A. Hasegawa, Mater. Trans. 53 (2012) 2145–2150. doi:10.2320/matertrans.MBW201110.
[129] L.K. Keys, J. Moteff, J. Appl. Phys. 40 (1969) 3866–3868. doi:10.1063/1.1658291.
[130] M. Fukuda, A. Hasegawa, T. Tanno, S. Nogami, et al., J. Nucl. Mater. 442 (2013). doi:10.1016/j.jnucmat.2013.03.058.
[131] M. Fukuda, A. Hasegawa, S. Nogami, K. Yabuuchi, J. Nucl. Mater. 449 (2014) 213–218. doi:10.1016/j.jnucmat.2013.10.012.
[132] C.N. Taylor, M. Shimada, B.J. Merrill, M.W. Drigert, et al., in: Phys. Scr., 2014. doi:10.1088/0031-8949/2014/T159/014055.
[133] J. Grzonka, Ł. Ciupiński, J. Smalc-Koziorowska, O.V. Ogorodnikova, et al., Nucl. Instruments Methods Phys. Res. Sect. B Beam Interact. with Mater. Atoms. 340 (2014) 27–33. doi:10.1016/j.nimb.2014.07.043.
[134] X. Hu, T. Koyanagi, M. Fukuda, Y. Katoh, et al., J. Nucl. Mater. 470 (2016) 278–289. doi:10.1016/j.jnucmat.2015.12.040.
[135] M. Fukuda, N.A.P. Kiran Kumar, T. Koyanagi, L.M. Garrison, et al., J. Nucl. Mater. 479 (2016) 249–254. doi:10.1016/j.jnucmat.2016.06.051.
[136] M. Klimenkov, U. Jäntsch, M. Rieth, H.C. Schneider, et al., Nucl. Mater. Energy. 9 (2016) 480–483. doi:10.1016/j.nme.2016.09.010.
[137] L.K. Keys, J. Moteff, J. Nucl. Mater. 34 (1970) 260–280. doi:10.1016/0022-3115(70)90193-5.
[138] D. Jeannotte, J.M. Galligan, Acta Metall. 18 (1970) 71–79. doi:10.1016/0001-6160(70)90070-2.
[139] J.T. Buswell, Philos. Mag. 22 (1970) 787–802. doi:10.1080/14786437008220947.
[140] J.T. Buswell, Philos. Mag. 23 (1971) 293–302. doi:10.1080/14786437108216385.
[141] S. Takamura, S. Okuda, R. Hanada, H. Kimura, J. Phys. Soc. Japan. 30 (1971) 1091–1095. doi:10.1143/JPSJ.30.1091.
[142] V.N. Bykov, G.A. Birzhevoi, M.I. Zakharova, V.A. Solov'ev, Sov. At. Energy. 33 (1972) 930–935. doi:10.1007/BF01666749.
[143] V.K. Sikka, J. Moteff, J. Appl. Phys. 43 (1972) 4942–4944. doi:10.1063/1.1661050.
[144] J. MOTEFF, M. HOCH, J. Met. 17 (1965) 1035-.
[145] R.C. Rau, J. Moteff, R.L. Ladd, J. Nucl. Mater. 24 (1967) 164–173. doi:10.1016/0022-3115(67)90005-0.
[146] X. Yongjun, W. Zhiqiang, Z. Jiazheng, T. Minamisono, et al., Mod. Phys. Lett. B. 17 (2003) 147–151. doi:10.1142/S0217984903004981.
[147] G. Pintsuk, J. Compan, T. Hirai, J. Linke, et al., in: Proc. - Symp. Fusion Eng., 2007. doi:10.1109/FUSION.2007.4337887.
[148] S.A. Maloy, R. Scott Lillard, W.F. Sommer, D.P. Butt, et al., J. Nucl. Mater. 431 (2012) 140–146. doi:10.1016/j.jnucmat.2011.11.052.
[149] A.I. Belyaeva, A.A. Savchenko, A.A. Galuza, I.V. Kolenov, AIP Adv. 4 (2014). doi:10.1063/1.4890594.
[150] J. Marsh, Y.S. Han, D. Verma, V. Tomar, Int. J. Plast. 74 (2015) 127–140. doi:10.1016/j.ijplas.2015.06.011.
[151] W. Van Renterghem, I. Uytdenhouwen, J. Nucl. Mater. 477 (2016) 77–84. doi:10.1016/j.jnucmat.2016.05.008.
[152] L.M. Garrison, Y. Katoh, L.L. Snead, T.S. Byun, et al., J. Nucl. Mater. 481 (2016) 134–146. doi:10.1016/j.jnucmat.2016.09.020.
[153] J.M. Steichen, J. Nucl. Mater. 60 (1976) 13–19. doi:10.1016/0022-3115(76)90112-4.
[154] P. Krautwasser, H. Derz, E. Kny, High Temp. - High Press. 22 (1990) 25–32.
[155] I. V GORYNIN, V.A. IGNATOV, V. V RYBIN, S.A. FABRITSIEV, et al., J. Nucl. Mater. 191 (1992) 421–425.
[156] J. Megusar, F.A. Garner, J. Nucl. Mater. 258–263 (1998) 940–944. doi:10.1016/S0022-3115(98)00274-8.
[157] M. Fujitsuka, B. Tsuchiya, I. Mutoh, T. Tanabe, et al., J. Nucl. Mater. 283–287 (2000) 1148–1151. doi:10.1016/S0022-3115(00)00170-7.
[158] V. Barabash, G. Federici, M. Rödig, L.L. Snead, et al., J. Nucl. Mater. 283–287 (2000) 138–146. doi:10.1016/S0022-3115(00)00203-8.
[159] M. Rödig, R. Duwe, W. Kühnlein, J. Linke, et al., Fusion Eng. Des. 56–57 (2001) 417–420. doi:10.1016/S0920-3796(01)00345-3.
[160] K. Farrell, T.S. Byun, J. Nucl. Mater. 296 (2001) 129–138. doi:10.1016/S0022-3115(01)00515-3.
[161] V.N. Bykov, G.A. Birzhevoi, M.I. Zakharova, Sov. At. Energy. 32 (1972) 365–366. doi:10.1007/BF01116968.
[162] J. Matolich, H. Nahm, J. Moteff, Scr. Metall. 8 (1974) 837–841. doi:10.1016/0036-9748(74)90304-4.
[163] R.K. Williams, F.W. Wiffen, J. Bentley, J.O. Stiegler, Metall. Trans. A, Phys. Metall. Mater. Sci. 14 A (1983) 655–666.
[164] R. Herschitz, D.N. Seidman, Nucl. Inst. Methods Phys. Res. B. 7–8 (1985) 137–142. doi:10.1016/0168-583X(85)90544-0.
[165] M. Fukuda, K. Yabuuchi, S. Nogami, A. Hasegawa, et al., J. Nucl. Mater. 455 (2014) 460–463. doi:10.1016/j.jnucmat.2014.08.002.
[166] A. Hasegawa, M. Fukuda, S. Nogami, K. Yabuuchi, Fusion Eng. Des. 89 (2014) 1568–1572. doi:10.1016/j.fusengdes.2014.04.035.
[167] X. Hu, T. Koyanagi, M. Fukuda, N.A.P.K. Kumar, et al., J. Nucl. Mater. 480 (2016) 235–243. doi:10.1016/j.jnucmat.2016.08.024.
[168] A. Hasegawa, M. Fukuda, K. Yabuuchi, S. Nogami, J. Nucl. Mater. 471 (2016) 175–183. doi:10.1016/j.jnucmat.2015.10.047.
[169] M.R. Gilbert, J.-C. Sublet, S.L. Dudarev, Nucl. Fusion. 57 (2017). doi:10.1088/1741-4326/aa5e2e.
[170] T. Koyanagi, N.A.P.K. Kumar, T. Hwang, L.M. Garrison, et al., J. Nucl. Mater. 490 (2017) 66–74. doi:10.1016/j.jnucmat.2017.04.010.
[171] G. Wei, F. Ren, W. Qin, W. Hu, et al., Comput. Mater. Sci. 148 (2018) 242–248. doi:10.1016/j.commatsci.2018.02.050.
[172] T. Hwang, A. Hasegawa, K. Tomura, N. Ebisawa, et al., J. Nucl. Mater. 507 (2018) 78–86. doi:10.1016/j.jnucmat.2018.04.031.
[173] M. Ekman, K. Persson, G. Grimvall, J. Nucl. Mater. 278 (2000) 273–276. doi:10.1016/S0022-3115(99)00241-X.
[174] G.A. Cottrell, J. Nucl. Mater. 334 (2004) 166–168. doi:10.1016/j.jnucmat.2004.07.001.
[175] T. Tanno, A. Hasegawa, J.-C. He, M. Fujiwara, et al., Mater. Trans. 48 (2007) 2399–2402. doi:10.2320/matertrans.MAW200722.
[176] T. Tanno, A. Hasegawa, M. Fujiwara, J.-C. He, et al., Mater. Trans. 49 (2008) 2259–2264. doi:10.2320/matertrans.MAW200821.
[177] T. Tanno, A. Hasegawa, J.C. He, M. Fujiwara, et al., J. Nucl. Mater. 386–388 (2009) 218–221. doi:10.1016/j.jnucmat.2008.12.091.
[178] A. Hasegawa, T. Tanno, S. Nogami, M. Satou, J. Nucl. Mater. 417 (2011) 491–494. doi:10.1016/j.jnucmat.2010.12.114.
[179] A. Hasegawa, M. Fukuda, T. Tanno, S. Nogami, Mater. Trans. 54 (2013) 466–471. doi:10.2320/matertrans.MG201208.
[180] M.E. Sawan, Fusion Sci. Technol. 66 (2014) 272–277. doi:10.13182/FST13-717.
[181] G.S. Was, J.T. Busby, T. Allen, E.A. Kenik, et al., J. Nucl. Mater. 300 (2002) 198–216. doi:10.1016/S0022-3115(01)00751-6.
[182] R. Rayaprolu, S. Möller, C. Linsmeier, S. Spellerberg, Nucl. Mater. Energy. 9 (2016) 29–35. doi:10.1016/j.nme.2016.09.008.
[183] F. Von Häussermann, Philos. Mag. 25 (1972) 561–581. doi:10.1080/14786437208228892.
[184] D. Pramanik, D.N. Seidman, Nucl. Instruments Methods Phys. Res. 209–210 (1983) 453–459. doi:10.1016/0167-5087(83)90838-4.
[185] O. El-Atwani, M. Efe, B. Heim, J.P. Allain, J. Nucl. Mater. 434 (2013) 170–177. doi:10.1016/j.jnucmat.2012.11.012.
[186] X. Yi, M.L. Jenkins, M. Briceno, S.G. Roberts, et al., Philos. Mag. 93 (2013) 1715–1738. doi:10.1080/14786435.2012.754110.
[187] C.E. Beck, S.G. Roberts, P.D. Edmondson, D.E.J. Armstrong, in: Mater. Res. Soc. Symp. Proc., 2013: pp. 99–104. doi:10.1557/opl.2013.356.
[188] F. Liu, S. Peng, H. Ren, Z. Long, et al., Fusion Eng. Des. 89 (2014) 2516–2522. doi:10.1016/j.fusengdes.2014.05.023.
[189] X. Yi, M.L. Jenkins, S.G. Roberts, M.A. Kirk, in: Mater. Res. Soc. Symp. Proc., 2014. doi:10.1557/opl.2014.732.

[190] X. Shu, B. Huang, J. Yang, D. Liu, et al., Fusion Sci. Technol. 66 (2014) 278–282. doi:10.13182/FST13-734.
[191] F. Liu, H. Ren, S. Peng, K. Zhu, Nucl. Instruments Methods Phys. Res. Sect. B Beam Interact. with Mater. Atoms. 333 (2014) 120–123. doi:10.1016/j.nimb.2014.04.004.
[192] O. V. Ogorodnikova, Y. Gasparyan, V. Efimov, Ciupiński, et al., J. Nucl. Mater. 451 (2014) 379–386. doi:10.1016/j.jnucmat.2014.04.011.
[193] N.J. Dutta, N. Buzarbaruah, S.R. Mohanty, J. Nucl. Mater. 452 (2014) 51–56. doi:10.1016/j.jnucmat.2014.04.032.
[194] W. Ni, Q. Yang, H. Fan, L. Liu, et al., J. Nucl. Mater. 464 (2015) 216–220. doi:10.1016/j.jnucmat.2015.04.045.
[195] C.H. Wu, E. Hechtl, J. Nucl. Mater. 196–198 (1992) 569–572. doi:10.1016/S0022-3115(06)80100-5.
[196] O. El-Atwani, S. Gonderman, S. Suslov, M. Efe, et al., Fusion Eng. Des. 93 (2015) 9–14. doi:10.1016/j.fusengdes.2015.02.001.
[197] O. El-Atwani, A. Suslova, T.J. Novakowski, K. Hattar, et al., Mater. Charact. 99 (2015) 68–76. doi:10.1016/j.matchar.2014.11.013.
[198] A. Xu, C. Beck, D.E.J. Armstrong, K. Rajan, et al., Acta Mater. 87 (2015) 121–127. doi:10.1016/j.actamat.2014.12.049.
[199] T. Hwang, M. Fukuda, S. Nogami, A. Hasegawa, et al., Nucl. Mater. Energy. 9 (2016) 430–435. doi:10.1016/j.nme.2016.06.005.
[200] Z. Zhang, E. Hasenhuetl, K. Yabuuchi, A. Kimura, Nucl. Mater. Energy. 9 (2016) 539–546. doi:10.1016/j.nme.2016.06.010.
[201] M.H. Cui, T.L. Shen, H.P. Zhu, J. Wang, et al., Fusion Eng. Des. 121 (2017) 313–318. doi:10.1016/j.fusengdes.2017.05.043.
[202] S. Cui, M. Simmonds, W. Qin, F. Ren, et al., J. Nucl. Mater. 486 (2017) 267–273. doi:10.1016/j.jnucmat.2017.01.023.
[203] E. Hasenhuetl, Z. Zhang, K. Yabuuchi, P. Song, et al., Nucl. Instruments Methods Phys. Res. Sect. B Beam Interact. with Mater. Atoms. 397 (2017) 11–14. doi:10.1016/j.nimb.2017.02.030.
[204] F. Kong, M. Qu, S. Yan, X. Cao, et al., Nucl. Instruments Methods Phys. Res. Sect. B Beam Interact. with Mater. Atoms. 409 (2017) 192–196. doi:10.1016/j.nimb.2017.04.006.
[205] M.T. Lessmann, I. Sudić, S. Fazinić, T. Tadić, et al., J. Nucl. Mater. 486 (2017) 34–43. doi:10.1016/j.jnucmat.2016.12.030.
[206] R. Sakamoto, T. Muroga, N. Yoshida, J. Nucl. Mater. 220–222 (1995) 819–822. doi:10.1016/0022-3115(94)00622-9.
[207] A. Xu, D.E.J. Armstrong, C. Beck, M.P. Moody, et al., Acta Mater. 124 (2017) 71–78. doi:10.1016/j.actamat.2016.10.050.
[208] M.A. de Lama, M. Balden, H. Greuner, T. Höschen, et al., Nucl. Mater. Energy. 13 (2017) 74–80. doi:10.1016/j.nme.2017.06.007.
[209] S. Gonderman, J.K. Tripathi, T.J. Novakowski, T. Sizyuk, et al., J. Nucl. Mater. 491 (2017) 199–205. doi:10.1016/j.jnucmat.2017.05.009.
[210] E. Hasenhuetl, Z. Zhang, K. Yabuuchi, A. Kimura, J. Nucl. Mater. 495 (2017) 314–321. doi:10.1016/j.jnucmat.2017.08.030.
[211] E. Hasenhuetl, R. Kasada, Z. Zhang, K. Yabuuchi, et al., Mater. Trans. 58 (2017) 749–756. doi:10.2320/matertrans.M2016437.
[212] E. Hasenhuetl, R. Kasada, Z. Zhang, K. Yabuuchi, et al., Mater. Trans. 58 (2017) 580–586. doi:10.2320/matertrans.ML201603.
[213] P. Sun, Y. Wang, M. Frost, C. Schönwälder, et al., J. Nucl. Mater. 510 (2018) 322–330. doi:10.1016/j.jnucmat.2018.07.062.
[214] M.Y. Xu, L.M. Luo, Y.F. Zhou, X. Zan, et al., Fusion Eng. Des. 132 (2018) 7–12. doi:10.1016/j.fusengdes.2018.05.015.
[215] O. El-Atwani, E. Esquivel, M. Efe, E. Aydogan, et al., Acta Mater. 149 (2018) 206–219. doi:10.1016/j.actamat.2018.02.035.
[216] J.S. Weaver, C. Sun, Y. Wang, S.R. Kalidindi, et al., J. Mater. Sci. 53 (2018) 5296–5316. doi:10.1007/s10853-017-1833-8.
[217] J. Megusar, F.A. Garner, J. Nucl. Mater. 258–263 (1998) 940–944. doi:10.1016/S0022-3115(98)00274-8.
[218] O. El-Atwani, J.S. Weaver, E. Esquivel, M. Efe, et al., J. Nucl. Mater. 509 (2018) 276–284. doi:10.1016/j.jnucmat.2018.06.023.
[219] M. Zhao, F. Liu, Z. Yang, Q. Xu, et al., Nucl. Instruments Methods Phys. Res. Sect. B Beam Interact. with Mater. Atoms. 414 (2018) 121–125. doi:10.1016/j.nimb.2017.09.002.
[220] S. Pathak, J.S. Weaver, C. Sun, Y. Wang, et al., 2018. doi:10.1007/978-3-319-67244-1_40.
[221] R.W. Harrison, J.A. Hinks, S.E. Donnelly, Scr. Mater. 150 (2018) 61–65. doi:10.1016/j.scriptamat.2018.02.040.
[222] H. Iwakiri, KURRI Prog. Rep. 283–287 (2000) 77.
[223] A.L. Suvorov, A.G. Zaluzhnyi, V.P. Babaev, A.A. Zaluzhnyi, J. Vac. Sci. Technol. A Vacuum, Surfaces, Film. 21 (2003) 2003–2006. doi:10.1116/1.1614273.
[224] H. Kurishita, S. Kobayashi, K. Nakai, T. Ogawa, et al., J. Nucl. Mater. 377 (2008) 34–40. doi:10.1016/j.jnucmat.2008.02.055.
[225] Y. Ueda, M. Fukumoto, J. Yoshida, Y. Ohtsuka, et al., J. Nucl. Mater. 386–388 (2009) 725–728. doi:10.1016/j.jnucmat.2008.12.300.
[226] R. Mateus, M. Dias, J. Lopes, J. Rocha, et al., J. Nucl. Mater. 442 (2013). doi:10.1016/j.jnucmat.2013.02.068.
[227] T. Funabiki, T. Shimada, Y. Ueda, M. Nishikawa, J. Nucl. Mater. 329–333 (2004) 780–784. doi:10.1016/j.jnucmat.2004.04.174.
[228] M. Ye, Plasma Sci. Technol. 7 (2005) 2828–2834. doi:10.1088/1009-0630/7/3/010.
[229] N. Ohno, S. Kajita, D. Nishijima, S. Takamura, J. Nucl. Mater. 363–365 (2007) 1153–1159. doi:10.1016/j.jnucmat.2007.01.148.
[230] M. Fukumoto, Y. Ohtsuka, Y. Ueda, M. Taniguchi, et al., J. Nucl. Mater. 375 (2008) 224–228. doi:10.1016/j.jnucmat.2007.11.005.
[231] N. Enomoto, S. Muto, T. Tanabe, J.W. Davis, et al., J. Nucl. Mater. 385 (2009) 606–614. doi:10.1016/j.jnucmat.2009.01.298.
[232] M. Sakamoto, T. Miyazaki, Y. Higashizono, K. Ogawa, et al., in: Phys. Scr. T, 2009. doi:10.1088/0031-8949/2009/T138/014043.
[233] D. Nunes, R. Mateus, I.D. Nogueira, P.A. Carvalho, et al., J. Nucl. Mater. 390–391 (2009) 1039–1042. doi:10.1016/j.jnucmat.2009.01.283.
[234] K. Tokunaga, T. Fujiwara, K. Ezato, S. Suzuki, et al., J. Nucl. Mater. 390–391 (2009) 916–920. doi:10.1016/j.jnucmat.2009.01.235.
[235] S. Takamura, T. Miyamoto, Plasma Fusion Res. 6 (2011). doi:10.1585/pfr.6.1202005.
[236] Y. Kikuchi, D. Nishijima, M. Nakatsuka, K. Ando, et al., J. Nucl. Mater. 415 (2011). doi:10.1016/j.jnucmat.2010.12.019.
[237] A.V. Arzhannikov, V.A. Bataev, I.A. Bataev, A.V. Burdakov, et al., J. Nucl. Mater. 438 (2013). doi:10.1016/j.jnucmat.2013.01.143.
[238] H.S. Kim, S.J. Noh, J.J. Kweon, C.E. Lee, J. Korean Phys. Soc. 63 (2013) 1422–1426. doi:10.3938/jkps.63.1422.
[239] S. Semsari, A. Zakeri, A. Sadighzadeh, S. Khademzadeh, et al., J. Fusion Energy. 32 (2013) 142–149. doi:10.1007/s10894-012-9540-6.
[240] S. Kajita, N. Ohno, M. Yajima, J. Kato, J. Nucl. Mater. 440 (2013) 55–62. doi:10.1016/j.jnucmat.2013.04.040.
[241] L.M. Garrison, G.L. Kulcinski, Fusion Sci. Technol. 64 (2013) 216–220.
[242] L. Gao, U. Von Toussaint, W. Jacob, M. Balden, et al., Nucl. Fusion. 54 (2014). doi:10.1088/0029-5515/54/12/122003.
[243] O. El-Atwani, S. Gonderman, M. Efe, G. De Temmerman, et al., Nucl. Fusion. 54 (2014). doi:10.1088/0029-5515/54/8/083013.
[244] L.M. Garrison, G.L. Kulcinski, in: Phys. Scr., 2014. doi:10.1088/0031-8949/2014/T159/014020.
[245] I.E. Garkusha, S.V. Malykhin, V.A. Makhlai, A.T. Pugachev, et al., Tech. Phys. 59 (2014) 1620–1625. doi:10.1134/S1063784214110097.
[246] S. Kajita, N. Yoshida, N. Ohno, Y. Hirahata, et al., Phys. Scr. 89 (2014). doi:10.1088/0031-8949/89/02/025602.
[247] T.J. Finlay, J.W. Davis, A.A. Haasz, J. Nucl. Mater. 463 (2015) 997–1000. doi:10.1016/j.jnucmat.2014.11.082.
[248] W. Hu, F. Luo, Z. Shen, L. Guo, et al., Fusion Eng. Des. 90 (2015) 23–28. doi:10.1016/j.fusengdes.2014.10.007.
[249] Y. Kikuchi, I. Sakuma, Y. Kitagawa, Y. Asai, et al., J. Nucl. Mater. 463 (2015) 206–209. doi:10.1016/j.jnucmat.2014.11.107.
[250] Y. Noiri, S. Kajita, N. Ohno, J. Nucl. Mater. 463 (2015) 285–288. doi:10.1016/j.jnucmat.2015.01.036.

[251] A. Al-Ajlony, J.K. Tripathi, A. Hassanein, J. Nucl. Mater. 466 (2015) 569–575. doi:10.1016/j.jnucmat.2015.08.036.
[252] A.M. Ito, A. Takayama, Y. Oda, T. Tamura, et al., J. Nucl. Mater. 463 (2015) 109–115. doi:10.1016/j.jnucmat.2015.01.018.
[253] L.M. Garrison, G.L. Kulcinski, J. Nucl. Mater. 466 (2015) 302–311. doi:10.1016/j.jnucmat.2015.07.025.
[254] K. Woller, D. Whyte, G. Wright, in: Proc. - Symp. Fusion Eng., 2016. doi:10.1109/SOFE.2015.7482349.
[255] Z. Chen, W. Han, J. Yu, L. Kecskes, et al., J. Nucl. Mater. 479 (2016) 418–425. doi:10.1016/j.jnucmat.2016.07.038.
[256] Y. Wu, L. Liu, B. Lu, W. Ni, et al., J. Nucl. Mater. 482 (2016) 294–299. doi:10.1016/j.jnucmat.2016.10.018.
[257] Y. Wu, W. Ni, H. Fan, L. Liu, et al., J. Nucl. Mater. 470 (2016) 164–169. doi:10.1016/j.jnucmat.2015.12.022.
[258] L. Liu, D. Liu, Y. Hong, H. Fan, et al., J. Nucl. Mater. 471 (2016) 1–7. doi:10.1016/j.jnucmat.2016.01.001.
[259] S. Saito, H. Nakamura, M. Tokitani, R. Sakaue, et al., Jpn. J. Appl. Phys. 55 (2016). doi:10.7567/JJAP.55.01AH07.
[260] A.A. Airapetov, L.B. Begrambekov, I.Y. Gretskaya, A.V. Grunin, et al., J. Phys. Conf. Ser. 748 (2016). doi:10.1088/1742-6596/748/1/012009.
[261] S. Saito, H. Nakamura, M. Tokitani, Jpn. J. Appl. Phys. 56 (2017). doi:10.7567/JJAP.56.01AF04.
[262] E. Bernard, R. Sakamoto, M. Tokitani, S. Masuzaki, et al., J. Nucl. Mater. 484 (2017) 24–29. doi:10.1016/j.jnucmat.2016.10.040.
[263] S. Kajita, H. Tanaka, N. Ohno, Jpn. J. Appl. Phys. 56 (2017). doi:10.7567/JJAP.56.030303.
[264] G. Valles, I. Martin-Bragado, K. Nordlund, A. Lasa, et al., J. Nucl. Mater. 490 (2017) 108–114. doi:10.1016/j.jnucmat.2017.04.021.
[265] X. Shu, B. Huang, D. Liu, H. Fan, et al., Fusion Eng. Des. 117 (2017) 8–13. doi:10.1016/j.fusengdes.2017.02.004.
[266] G. Sinclair, J.K. Tripathi, P.K. Diwakar, M. Wirtz, et al., Nucl. Mater. Energy. 12 (2017) 405–411. doi:10.1016/j.nme.2017.03.003.
[267] K. Tokunaga, O. Yoshikawa, K. Makise, N. Yoshida, J. Nucl. Mater. 307–311 (2002) 130–134. doi:10.1016/S0022-3115(02)01248-5.
[268] B.K. Rahadilov, M.K. Skakov, T.R. Tulenbergenov, 2017. doi:10.4028/www.scientific.net/KEM.736.46.
[269] Z. Shen, Z. Zheng, F. Luo, W. Hu, et al., Fusion Eng. Des. 115 (2017) 80–84. doi:10.1016/j.fusengdes.2017.01.001.
[270] F. Luo, L. Guo, D. Lu, J. Wang, et al., Fusion Eng. Des. 125 (2017) 463–467. doi:10.1016/j.fusengdes.2017.04.014.
[271] A. Al-Ajlony, J.K. Tripathi, A. Hassanein, J. Nucl. Mater. 488 (2017) 1–8. doi:10.1016/j.jnucmat.2017.02.029.
[272] J. Yu, W. Han, Z. Chen, K. Zhu, Nucl. Mater. Energy. 12 (2017) 588–592. doi:10.1016/j.nme.2016.10.001.
[273] S. Gonderman, J.K. Tripathi, G. Sinclair, T.J. Novakowski, et al., Nucl. Fusion. 58 (2018). doi:10.1088/1741-4326/aa9e9b.
[274] S. Wang, X. Zhu, L. Cheng, W. Guo, et al., J. Nucl. Mater. 508 (2018) 395–402. doi:10.1016/j.jnucmat.2018.05.082.
[275] D. Nishijima, M.Y. Ye, N. Ohno, S. Takamura, J. Nucl. Mater. 313–316 (2003) 97–101. doi:10.1016/S0022-3115(02)01368-5.
[276] M.Y. Ye, H. Kanehara, S. Fukuta, N. Ohno, et al., J. Nucl. Mater. 313–316 (2003) 72–76. doi:10.1016/S0022-3115(02)01349-1.
[277] T. Shimada, H. Kikuchi, Y. Ueda, A. Sagara, et al., J. Nucl. Mater. 313–316 (2003) 204–208. doi:10.1016/S0022-3115(02)01447-2.
[278] D. Nishijima, M.Y. Ye, N. Ohno, S. Takamura, J. Nucl. Mater. 329–333 (2004) 1029–1033. doi:10.1016/j.jnucmat.2004.04.129.
[279] S. O'hira, A. Steinér, H. Nakamura, R. Causey, et al., J. Nucl. Mater. 258–263 (1998) 990–997. doi:10.1016/S0022-3115(98)00315-8.
[280] S. Nagata, B. Tsuchiya, T. Sugawara, N. Ohtsu, et al., Nucl. Instruments Methods Phys. Res. Sect. B Beam Interact. with Mater. Atoms. 190 (2002) 652–656. doi:10.1016/S0168-583X(01)01242-3.
[281] M. Shimada, Y. Hatano, P. Calderoni, T. Oda, et al., J. Nucl. Mater. 415 (2011). doi:10.1016/j.jnucmat.2010.11.050.
[282] Y. Oya, M. Kobayashi, R. Kurata, N. Yoshida, et al., Fusion Eng. Des. 86 (2011) 1776–1779. doi:10.1016/j.fusengdes.2010.11.017.
[283] H.T. Lee, H. Tanaka, Y. Ohtsuka, Y. Ueda, J. Nucl. Mater. 415 (2011). doi:10.1016/j.jnucmat.2010.12.023.
[284] Y. Oya, M. Shimada, M. Kobayashi, T. Oda, et al., in: Phys. Scr. T, 2011. doi:10.1088/0031-8949/2011/T145/014050.
[285] Y. Li, W. Zhou, L. Huang, R. Ning, et al., Plasma Sci. Technol. 14 (2012) 624–628. doi:10.1088/1009-0630/14/7/13.
[286] Y. Hatano, M. Shimada, Y. Oya, G. Cao, et al., Mater. Trans. 54 (2013) 437–441. doi:10.2320/matertrans.MG201204.
[287] Y. Hatano, M. Shimada, T. Otsuka, Y. Oya, et al., Nucl. Fusion. 53 (2013). doi:10.1088/0029-5515/53/7/073006.
[288] Y. Hatano, M. Shimada, V.K. Alimov, J. Shi, et al., J. Nucl. Mater. 438 (2013). doi:10.1016/j.jnucmat.2013.01.018.
[289] Y. Sakoi, M. Miyamoto, K. Ono, M. Sakamoto, J. Nucl. Mater. 442 (2013). doi:10.1016/j.jnucmat.2012.10.003.
[290] Y. Nobuta, Y. Hatano, M. Matsuyama, S. Abe, et al., J. Nucl. Mater. 463 (2015) 993–996. doi:10.1016/j.jnucmat.2014.12.047.
[291] B.M. Oliver, R.A. Causey, S.A. Maloy, J. Nucl. Mater. 329–333 (2004) 977–981. doi:10.1016/j.jnucmat.2004.04.067.
[292] M. Shimada, G. Cao, T. Otsuka, M. Hara, et al., Nucl. Fusion. 55 (2015). doi:10.1088/0029-5515/55/1/013008.
[293] O. V. Ogorodnikova, V. V. Gann, M.S. Zibrov, Y.M. Gasparyan, in: Phys. Procedia, 2015: pp. 41–46. doi:10.1016/j.phpro.2015.08.309.
[294] T.J. Finlay, J.W. Davis, K. Sugiyama, V.K. Alimov, et al., in: Phys. Scr., 2016. doi:10.1088/0031-8949/T167/1/014042.
[295] H. Fujita, K. Yuyama, X. Li, Y. Hatano, et al., in: Phys. Scr., 2016. doi:10.1088/0031-8949/T167/1/014068.
[296] O. V. Ogorodnikova, J. Appl. Phys. 122 (2017). doi:10.1063/1.4996096.
[297] M. Shimada, Y. Oya, D.A. Buchenauer, Y. Hatano, Fusion Sci. Technol. 72 (2017) 652–659. doi:10.1080/15361055.2017.1347468.
[298] Y. Uemura, S. Sakurada, H. Fujita, K. Azuma, et al., J. Nucl. Mater. 490 (2017) 242–246. doi:10.1016/j.jnucmat.2017.04.041.
[299] T. Toyama, K. Ami, K. Inoue, Y. Nagai, et al., J. Nucl. Mater. 499 (2018) 464–470. doi:10.1016/j.jnucmat.2017.11.022.
[300] M. Shimada, Y. Oya, W.R. Wampler, Y. Yamauchi, et al., Fusion Eng. Des. (2018). doi:10.1016/j.fusengdes.2018.04.094.
[301] L.B. Begrambekov, A.S. Kaplevsky, S.S. Dovganyuk, A.E. Evsin, et al., in: J. Phys. Conf. Ser., 2018. doi:10.1088/1742-6596/941/1/012020.
[302] Q. Xu, N. Yoshida, T. Yoshiie, Mater. Trans. 46 (2005) 1255–1260. doi:10.2320/matertrans.46.1255.
[303] H.T. Lee, A.A. Haasz, J.W. Davis, R.G. Macaulay-Newcombe, J. Nucl. Mater. 360 (2007) 196–207. doi:10.1016/j.jnucmat.2006.09.013.
[304] H.T. Lee, A.A. Haasz, J.W. Davis, R.G. Macaulay-Newcombe, et al., J. Nucl. Mater. 363–365 (2007) 898–903. doi:10.1016/j.jnucmat.2007.01.111.
[305] Q. Xu, N. Yoshida, T. Yoshiie, J. Nucl. Mater. 367–370 A (2007) 806–811. doi:10.1016/j.jnucmat.2007.03.078.
[306] M. Fukumoto, H. Kashiwagi, Y. Ohtsuka, Y. Ueda, et al., J. Nucl. Mater. 390–391 (2009) 572–575. doi:10.1016/j.jnucmat.2009.01.107.
[307] Q. Xu, K. Sato, T. Yoshiie, J. Nucl. Mater. 390–391 (2009) 663–666. doi:10.1016/j.jnucmat.2009.01.184.
[308] W.R. Wampler, D.L. Rudakov, J.G. Watkins, C.J. Lasnier, J. Nucl. Mater. 415 (2011). doi:10.1016/j.jnucmat.2010.11.043.
[309] V.I. Dubinko, P. Grigorev, A. Bakaev, D. Terentyev, et al., J. Phys. Condens. Matter. 26 (2014). doi:10.1088/0953-8984/26/39/395001.
[310] S.I. Krasheninnikov, T. Faney, B.D. Wirth, Nucl. Fusion. 54 (2014). doi:10.1088/0029-5515/54/7/073019.
[311] R.D. Smirnov, S.I. Krasheninnikov, J. Guterl, J. Nucl. Mater. 463 (2015) 359–362. doi:10.1016/j.jnucmat.2014.10.033.
[312] M.A. Cusentino, K.D. Hammond, F. Sefta, N. Juslin, et al., J. Nucl. Mater. 463 (2015) 347–350. doi:10.1016/j.jnucmat.2014.10.043.
[313] J. Guterl, R.D. Smirnov, S.I. Krasheninnikov, B. Uberuaga, et al., J. Nucl. Mater. 463 (2015) 263–267.

doi:10.1016/j.jnucmat.2014.12.086.
[314] O. V. Ogorodnikova, V. Gann, J. Nucl. Mater. 460 (2015) 60–71. doi:10.1016/j.jnucmat.2015.02.004.
[315] R. Kobayashi, T. Hattori, T. Tamura, S. Ogata, J. Nucl. Mater. 463 (2015) 1071–1074. doi:10.1016/j.jnucmat.2014.12.049.
[316] B.D. Wirth, K.D. Hammond, S.I. Krasheninnikov, D. Maroudas, J. Nucl. Mater. 463 (2015) 30–38. doi:10.1016/j.jnucmat.2014.11.072.
[317] E.A. Hodille, X. Bonnin, R. Bisson, T. Angot, et al., J. Nucl. Mater. 467 (2015) 424–431. doi:10.1016/j.jnucmat.2015.06.041.
[318] D. Nguyen-Manh, S.L. Dudarev, Nucl. Instruments Methods Phys. Res. Sect. B Beam Interact. with Mater. Atoms. 352 (2015) 86–91. doi:10.1016/j.nimb.2014.11.097.
[319] E. Zarkadoula, D.M. Duffy, K. Nordlund, M.A. Seaton, et al., J. Phys. Condens. Matter. 27 (2015). doi:10.1088/0953-8984/27/13/135401.
[320] D. Kato, H. Iwakiri, Y. Watanabe, K. Morishita, et al., Nucl. Fusion. 55 (2015). doi:10.1088/0029-5515/55/8/083019.
[321] J. Boisse, C. Domain, C.S. Becquart, J. Nucl. Mater. 455 (2014) 10–15. doi:10.1016/j.jnucmat.2014.02.031.
[322] F. Hofmann, D. Nguyen-Manh, M.R. Gilbert, C.E. Beck, et al., Acta Mater. 89 (2015) 352–363. doi:10.1016/j.actamat.2015.01.055.
[323] D. Chernikova, K. Axell, A. Nordlund, H. Wirdelius, Ann. Nucl. Energy. 75 (2015) 219–227. doi:10.1016/j.anucene.2014.08.017.
[324] G. Valles, A. L. Cazalilla, C. Gonzalez, I. Martin-Bragado, et al., Nucl. Instruments Methods Phys. Res. Sect. B Beam Interact. with Mater. Atoms. 352 (2015) 100–103. doi:10.1016/j.nimb.2014.12.034.
[325] S. Saito, H. Nakamura, M. Tokitani, in: Proc. 2015 3rd Int. Conf. Adv. Electr. Eng. ICAEE 2015, 2016: pp. 121–124. doi:10.1109/ICAEE.2015.7506811.
[326] P. Grigorev, D. Matveev, A. Bakaeva, D. Terentyev, et al., J. Nucl. Mater. 481 (2016) 181–189. doi:10.1016/j.jnucmat.2016.09.019.
[327] D. Maroudas, S. Blondel, L. Hu, K.D. Hammond, et al., J. Phys. Condens. Matter. 28 (2016). doi:10.1088/0953-8984/28/6/064004.
[328] J.L. Barton, Y.Q. Wang, R.P. Doerner, G.R. Tynan, Nucl. Fusion. 56 (2016). doi:10.1088/0029-5515/56/10/106030.
[329] A.E. Sand, M.J. Aliaga, M.J. Caturla, K. Nordlund, Epl. 115 (2016). doi:10.1209/0295-5075/115/36001.
[330] A.E. Sand, J. Dequeker, C.S. Becquart, C. Domain, et al., J. Nucl. Mater. 470 (2016) 119–127. doi:10.1016/j.jnucmat.2015.12.012.
[331] K. Schmid, in: Phys. Scr., 2016. doi:10.1088/0031-8949/T167/1/014025.
[332] L. Hu, K.D. Hammond, B.D. Wirth, D. Maroudas, J. Appl. Phys. 115 (2014). doi:10.1063/1.4874675.
[333] P. Grigorev, D. Terentyev, G. Bonny, E.E. Zhurkin, et al., J. Nucl. Mater. 474 (2016) 143–149. doi:10.1016/j.jnucmat.2016.03.022.
[334] R. Alexander, M.C. Marinica, L. Proville, F. Willaime, et al., Phys. Rev. B. 94 (2016). doi:10.1103/PhysRevB.94.024103.
[335] N. Castin, A. Bakaev, G. Bonny, A.E. Sand, et al., J. Nucl. Mater. 493 (2017) 280–293. doi:10.1016/j.jnucmat.2017.06.008.
[336] T.D. Swinburne, P.W. Ma, S.L. Dudarev, New J. Phys. 19 (2017). doi:10.1088/1367-2630/aa78ea.
[337] A. De Backer, D.R. Mason, C. Domain, D. Nguyen-Manh, et al., Phys. Scr. 2017 (2017). doi:10.1088/1402-4896/aa9400.
[338] E. Marenkov, K. Nordlund, I. Sorokin, A. Eksaeva, et al., J. Nucl. Mater. 496 (2017) 18–23. doi:10.1016/j.jnucmat.2017.09.021.
[339] E.A. Hodille, A. Založnik, S. Markelj, T. Schwarz-Selinger, et al., Nucl. Fusion. 57 (2017). doi:10.1088/1741-4326/aa5aa5.
[340] S. Blondel, D.E. Bernholdt, K.D. Hammond, L. Hu, et al., Fusion Sci. Technol. 71 (2017) 84–92. doi:10.13182/FST16-109.
[341] G. Valles, I. Martin-Bragado, K. Nordlund, A. Lasa, et al., J. Nucl. Mater. 490 (2017) 108–114. doi:10.1016/j.jnucmat.2017.04.021.
[342] A. Eksaeva, E. Marenkov, D. Borodin, A. Kreter, et al., Nucl. Mater. Energy. 12 (2017) 253–260. doi:10.1016/j.nme.2017.03.014.
[343] D.R. Mason, X. Yi, M.A. Kirk, S.L. Dudarev, J. Phys. Condens. Matter. 26 (2014). doi:10.1088/0953-8984/26/37/375701.
[344] J.S. Wróbel, D. Nguyen-Manh, K.J. Kurzydłowski, S.L. Dudarev, J. Phys. Condens. Matter. 29 (2017). doi:10.1088/1361-648X/aa5f37.
[345] M.R. Gilbert, J.C. Sublet, S.L. Dudarev, Nucl. Fusion. 57 (2017). doi:10.1088/1741-4326/aa5e2e.
[346] J. Marian, C.S. Becquart, C. Domain, S.L. Dudarev, et al., Nucl. Fusion. 57 (2017). doi:10.1088/1741-4326/aa5e8d.
[347] F. Hofmann, D. Nguyen-Manh, D.R. Mason, M.R. Gilbert, et al., in: Procedia IUTAM, 2017: pp. 78–85. doi:10.1016/j.piutam.2017.03.040.
[348] N. Castin, G. Bonny, A. Bakaev, C.J. Ortiz, et al., J. Nucl. Mater. 500 (2018) 15–25. doi:10.1016/j.jnucmat.2017.12.014.
[349] M. Jin, C. Permann, M.P. Short, J. Nucl. Mater. 504 (2018) 33–40. doi:10.1016/j.jnucmat.2018.03.018.
[350] A.E. Sand, K. Nordlund, S.L. Dudarev, J. Nucl. Mater. 455 (2014) 207–211. doi:10.1016/j.jnucmat.2014.06.007.
[351] J. Boisse, A. De Backer, C. Domain, C.S. Becquart, J. Mater. Res. 29 (2014) 2374–2386. doi:10.1557/jmr.2014.258.
[352] Z. Wang, K. Zhao, W. Chen, X. Chen, et al., Appl. Therm. Eng. 73 (2014) 109–113. doi:10.1016/j.applthermaleng.2014.07.054.
[353] C. Sang, J. Sun, X. Bonnin, L. Wang, et al., Fusion Eng. Des. 89 (2014) 2214–2219. doi:10.1016/j.fusengdes.2014.01.040.
[354] T. Faney, S.I. Krasheninnikov, B.D. Wirth, Nucl. Fusion. 55 (2015). doi:10.1088/0029-5515/55/1/013014.
[355] C. Linsmeier, M. Rieth, J. Aktaa, T. Chikada, et al., Nucl. Fusion. 57 (2017). doi:10.1088/1741-4326/aa6f71.
[356] D. Stork, P. Agostini, J.L. Boutard, D. Buckthorpe, et al., J. Nucl. Mater. 455 (2014) 277–291. doi:10.1016/j.jnucmat.2014.06.014.
[357] M. Rieth, S.L. Dudarev, S.M. Gonzalez De Vicente, J. Aktaa, et al., J. Nucl. Mater. 432 (2013) 482–500. doi:10.1016/j.jnucmat.2012.08.018.
[358] M. Rieth, J.L. Boutard, S.L. Dudarev, T. Ahlgren, et al., J. Nucl. Mater. 417 (2011) 463–467. doi:10.1016/j.jnucmat.2011.01.075.
[359] N. Lemahieu, J. Linke, G. Pintsuk, G. Van Oost, et al., in: Phys. Scr., 2014. doi:10.1088/0031-8949/2014/T159/014035.
[360] C. Ruset, H. Maier, E. Grigore, G.F. Matthews, et al., in: Phys. Scr., 2014. doi:10.1088/0031-8949/2014/T159/014025.
[361] H. Maier, H. Greuner, M. Balden, B. Böswirth, et al., in: Phys. Scr., 2014. doi:10.1088/0031-8949/2014/T159/014019.
[362] P. Gavila, B. Riccardi, G. Pintsuk, G. Ritz, et al., Fusion Eng. Des. 98–99 (2015) 1305–1309. doi:10.1016/j.fusengdes.2014.12.006.
[363] N. Jaksic, H. Greuner, A. Herrmann, B. Böswirth, et al., Fusion Eng. Des. 98–99 (2015) 1333–1336. doi:10.1016/j.fusengdes.2015.03.030.
[364] M. Wirtz, S. Bardin, A. Huber, A. Kreter, et al., Nucl. Fusion. 55 (2015). doi:10.1088/0029-5515/55/12/123017.
[365] N. Lemahieu, H. Greuner, J. Linke, H. Maier, et al., Fusion Eng. Des. 98–99 (2015) 2020–2024. doi:10.1016/j.fusengdes.2015.06.051.
[366] G. De Temmerman, T.W. Morgan, G.G. Van Eden, T. De Kruif, et al., J. Nucl. Mater. 463 (2015) 198–201. doi:10.1016/j.jnucmat.2014.09.075.
[367] K. Arshad, D. Ding, J. Wang, Y. Yuan, et al., Nucl. Mater. Energy. 3–4 (2015) 32–36. doi:10.1016/j.nme.2015.05.001.
[368] T. Loewenhoff, S. Bardin, H. Greuner, J. Linke, et al., Nucl. Fusion. 55 (2015). doi:10.1088/0029-5515/55/12/123004.
[369] G. Pintsuk, M. Bednarek, P. Gavila, S. Gerzoskovitz, et al., Fusion Eng. Des. 98–99 (2015) 1384–1388. doi:10.1016/j.fusengdes.2015.01.037.
[370] I.E. Garkusha, V.A. Makhlaj, N.N. Aksenov, O. V. Byrka, et al., in: J. Phys. Conf. Ser., 2015. doi:10.1088/1742-6596/591/1/012030.
[371] Y. Lian, X. Liu, Z. Cheng, J. Wang, et al., J. Nucl. Mater. 455 (2014) 371–375. doi:10.1016/j.jnucmat.2014.07.021.

[372] S. Antusch, D.E.J. Armstrong, T. Ben Britton, L. Commin, et al., Nucl. Mater. Energy. 3–4 (2015) 22–31. doi:10.1016/j.nme.2015.04.002.
[373] A. Huber, M. Wirtz, G. Sergienko, I. Steudel, et al., Fusion Eng. Des. 98–99 (2015) 1328–1332. doi:10.1016/j.fusengdes.2015.01.028.
[374] Y. Patil, S.S. Khirwadkar, S.M. Belsare, R. Swamy, et al., Fusion Eng. Des. 95 (2015) 84–90. doi:10.1016/j.fusengdes.2015.04.036.
[375] M. Richou, M. Missirlian, E. Tsitrone, J. Bucalossi, et al., in: Phys. Scr., 2016. doi:10.1088/0031-8949/T167/1/014029.
[376] N. Lemahieu, H. Greuner, J. Linke, H. Maier, et al., in: Phys. Scr., 2016. doi:10.1088/0031-8949/T167/1/014008.
[377] W. Van Renterghem, I. Uytdenhouwen, T. Loewenhoff, M. Wirtz, Nucl. Mater. Energy. 9 (2016) 484–489. doi:10.1016/j.nme.2016.04.003.
[378] A.S. Arakcheev, A. V. Burdakov, A. Huber, A.A. Kasatov, et al., in: AIP Conf. Proc., 2016. doi:10.1063/1.4964218.
[379] N. Lemahieu, M. Balden, S. Elgeti, H. Greuner, et al., Fusion Eng. Des. 109–111 (2016) 169–174. doi:10.1016/j.fusengdes.2016.03.035.
[380] M. Wirtz, J. Linke, T. Loewenhoff, G. Pintsuk, et al., in: Phys. Scr., 2016. doi:10.1088/0031-8949/T167/1/014015.
[381] T. Loewenhoff, J. Linke, J. Matějíček, M. Rasinski, et al., Nucl. Mater. Energy. 9 (2016) 165–170. doi:10.1016/j.nme.2016.04.004.
[382] V.A. Makhlaj, I.E. Garkusha, N.N. Aksenov, B. Bazylev, et al., in: Phys. Scr., 2014. doi:10.1088/0031-8949/2014/T159/014024.
[383] V.A. Makhlai, I.E. Garkusha, J. Linke, S. V. Malykhin, et al., Nucl. Mater. Energy. 9 (2016) 116–122. doi:10.1016/j.nme.2016.04.001.
[384] X. Zhang, Q. Yan, S. Lang, M. Xia, et al., J. Fusion Energy. 35 (2016) 666–672. doi:10.1007/s10894-016-0082-1.
[385] Y. Yuan, J. Du, M. Wirtz, G.N. Luo, et al., Nucl. Fusion. 56 (2016). doi:10.1088/0029-5515/56/3/036021.
[386] I. Steudel, A. Huber, A. Kreter, J. Linke, et al., in: Phys. Scr., 2016. doi:10.1088/0031-8949/T167/1/014053.
[387] A. Calvo, C. Garcïa-Rosales, F. Koch, N. Ordïs, et al., Nucl. Mater. Energy. 9 (2016) 422–429. doi:10.1016/j.nme.2016.06.002.
[388] T. Hirai, S. Panayotis, V. Barabash, C. Amzallag, et al., Nucl. Mater. Energy. 9 (2016) 616–622. doi:10.1016/j.nme.2016.07.003.
[389] M. Wirtz, M. Berger, A. Huber, A. Kreter, et al., Nucl. Mater. Energy. 9 (2016) 177–180. doi:10.1016/j.nme.2016.07.002.
[390] I. Steudel, A. Huber, A. Kreter, J. Linke, et al., Nucl. Mater. Energy. 12 (2017) 1348–1351. doi:10.1016/j.nme.2017.03.016.
[391] A.A. Vasilyev, A.S. Arakcheev, I.A. Bataev, V.A. Bataev, et al., Nucl. Mater. Energy. 12 (2017) 553–558. doi:10.1016/j.nme.2016.11.017.
[392] X. Liu, Y.Y. Lian, H. Greuner, B. Boeswirth, et al., Nucl. Mater. Energy. 12 (2017) 1314–1318. doi:10.1016/j.nme.2017.01.018.
[393] V.A. Makhlaj, I.E. Garkusha, N.N. Aksenov, B. Bazylev, et al., in: Phys. Scr., 2014. doi:10.1088/0031-8949/2014/T161/014040.
[394] R. Neu, H. Maier, M. Balden, S. Elgeti, et al., Fusion Eng. Des. 124 (2017) 450–454. doi:10.1016/j.fusengdes.2017.01.043.
[395] O.V. Byrka, N.N. Aksenov, S.S. Herashchenko, V.A. Makhlaj, et al., Probl. At. Sci. Technol. 107 (2017) 115–118.
[396] L.N. Vyacheslavov, A.S. Arakcheev, A. V. Burdakov, I. V. Kandaurov, et al., Nucl. Mater. Energy. 12 (2017) 494–498. doi:10.1016/j.nme.2017.01.023.
[397] M. Wirtz, I. Uytdenhouwen, V. Barabash, F. Escourbiac, et al., Nucl. Fusion. 57 (2017). doi:10.1088/1741-4326/aa6938.
[398] E. Hoashi, S. Kuroyanagi, T. Okita, T. Maeji, et al., Fusion Eng. Des. (2018). doi:10.1016/j.fusengdes.2018.02.028.
[399] R. Neu, H. Maier, M. Balden, R. Dux, et al., J. Nucl. Mater. (2018). doi:10.1016/j.jnucmat.2018.05.066.
[400] I. Zammuto, M. Li, A. Herrmann, N. Jaksic, et al., Fusion Eng. Des. (2018). doi:10.1016/j.fusengdes.2018.04.066.
[401] G. Pintsuk, S. Antusch, T. Weingaertner, M. Wirtz, Int. J. Refract. Met. Hard Mater. 72 (2018) 97–103. doi:10.1016/j.ijrmhm.2017.11.039.
[402] M. Missirlian, G. Pintsuk, G.N. Luo, Q. Li, et al., Fusion Eng. Des. (2018). doi:10.1016/j.fusengdes.2018.02.063.
[403] M. Oane, D. Toader, N. Iacob, C.M. Ticoş, Nucl. Instruments Methods Phys. Res. Sect. B Beam Interact. with Mater. Atoms. 337 (2014) 17–20. doi:10.1016/j.nimb.2014.07.012.
[404] D. Rivera, T. Crosby, A. Sheng, N.M. Ghoniem, J. Nucl. Mater. 455 (2014) 500–506. doi:10.1016/j.jnucmat.2014.07.007.
[405] A. Huber, A. Arakcheev, G. Sergienko, I. Steudel, et al., in: Phys. Scr., 2014. doi:10.1088/0031-8949/2014/T159/014005.
[406] J.H. Yu, R.P. Doerner, T. Dittmar, T. Höschen, et al., in: Phys. Scr., 2014. doi:10.1088/0031-8949/2014/T159/014036.
[407] H. Greuner, H. Maier, M. Balden, B. Böswirth, et al., J. Nucl. Mater. 455 (2014) 681–684. doi:10.1016/j.jnucmat.2014.08.019.
[408] M. Li, J.H. You, Fusion Eng. Des. 101 (2015) 1–8. doi:10.1016/j.fusengdes.2015.09.008.
[409] Z. Sun, Q. Li, W. Wang, J.C. Wang, et al., Fusion Eng. Des. 121 (2017) 60–69. doi:10.1016/j.fusengdes.2017.06.009.
[410] K.M. Kim, H.T. Kim, J.H. Song, H.K. Kim, et al., IEEE Trans. Plasma Sci. 45 (2017) 519–522. doi:10.1109/TPS.2017.2650213.
[411] S. Nogami, M. Toyota, W. Guan, A. Hasegawa, et al., Fusion Eng. Des. 120 (2017) 49–60. doi:10.1016/j.fusengdes.2017.04.102.
[412] S. Nogami, W.H. Guan, T. Hattori, K. James, et al., in: Phys. Scr., 2017. doi:10.1088/1402-4896/aa864d.
[413] M. Li, J.H. You, Fusion Eng. Des. 124 (2017) 468–472. doi:10.1016/j.fusengdes.2017.01.015.
[414] Z.-X. Sun, Q. Li, W.-J. Wang, J.-C. Wang, et al., Hejubian Yu Dengliziti Wuli/Nuclear Fusion Plasma Phys. 37 (2017) 446–451. doi:10.16568/j.0254-6086.201704013.
[415] A. Lagoyannis, P. Tsavalas, K. Mergia, G. Provatas, et al., Nucl. Fusion. 57 (2017). doi:10.1088/1741-4326/aa6ec1.
[416] S. Panayotis, T. Hirai, V. Barabash, C. Amzallag, et al., Fusion Eng. Des. 125 (2017) 256–262. doi:10.1016/j.fusengdes.2017.08.009.
[417] T. Hirai, V. Barabash, F. Escourbiac, A. Durocher, et al., Fusion Eng. Des. 125 (2017) 250–255. doi:10.1016/j.fusengdes.2017.07.009.
[418] E. Visca, S. Roccella, P. Rossi, D. Candura, et al., Fusion Eng. Des. 124 (2017) 191–195. doi:10.1016/j.fusengdes.2017.03.012.
[419] M. Li, M. Sommerer, E. Werner, S. Lampenscherf, et al., Eng. Fract. Mech. 135 (2015) 64–80. doi:10.1016/j.engfracmech.2015.01.017.
[420] J.P. Gunn, S. Carpentier-Chouchana, R. Dejarnac, F. Escourbiac, et al., Nucl. Mater. Energy. 12 (2017) 75–83. doi:10.1016/j.nme.2016.10.005.
[421] A. Widdowson, E. Alves, A. Baron-Wiechec, N.P. Barradas, et al., Nucl. Mater. Energy. 12 (2017) 499–505. doi:10.1016/j.nme.2016.12.008.
[422] M. Li, F. Gallay, M. Richou, J.H. You, Fusion Eng. Des. 122 (2017) 124–130. doi:10.1016/j.fusengdes.2017.09.002.
[423] F. Crescenzi, E. Cacciotti, V. Cerri, H. Greuner, et al., Fusion Eng. Des. (2018). doi:10.1016/j.fusengdes.2018.03.023.
[424] K.M. Kim, H.T. Kim, H.C. Kim, S.H. Park, et al., Fusion Eng. Des. (2018). doi:10.1016/j.fusengdes.2018.01.055.
[425] F. Maviglia, S. Roccella, F. Crescenzi, E. Visca, et al., Fusion Eng. Des. (2018). doi:10.1016/j.fusengdes.2018.04.132.
[426] E. Visca, B. Böswirth, E. Cacciotti, V. Cerri, et al., Fusion Eng. Des. (2018). doi:10.1016/j.fusengdes.2018.05.064.
[427] T. Hirai, S. Carpentier-Chouchana, F. Escourbiac, S. Panayotis, et al., Fusion Eng. Des. 127 (2018) 66–72. doi:10.1016/j.fusengdes.2017.12.007.
[428] G. De Temmerman, T. Hirai, R.A. Pitts, Plasma Phys. Control. Fusion. 60 (2018). doi:10.1088/1361-6587/aaaf62.
[429] M. Tokitani, M. Miyamoto, S. Masuzaki, R. Sakamoto, et al., Fusion Eng. Des. (2018). doi:10.1016/j.fusengdes.2018.01.051.

[430] A. Herrmann, H. Greuner, N. Jaksic, M. Balden, et al., Nucl. Fusion. 55 (2015). doi:10.1088/0029-5515/55/6/063015.
[431] S. Huang, S. Liu, J. Fusion Energy. 37 (2018) 177–186. doi:10.1007/s10894-018-0164-3.
[432] T. Hirai, F. Escourbiac, V. Barabash, A. Durocher, et al., J. Nucl. Mater. 463 (2015) 1248–1251. doi:10.1016/j.jnucmat.2014.12.027.
[433] M. Li, E. Werner, J.H. You, J. Nucl. Mater. 457 (2015) 256–265. doi:10.1016/j.jnucmat.2014.11.026.
[434] K. Ezato, S. Suzuki, Y. Seki, H. Yamada, et al., Fusion Eng. Des. 109–111 (2016) 1256–1260. doi:10.1016/j.fusengdes.2015.12.049.
[435] K.M. Kim, H.T. Kim, J.H. Song, H.K. Kim, et al., in: Proc. - Symp. Fusion Eng., 2016. doi:10.1109/SOFE.2015.7482382.
[436] M. Li, J.H. You, Nucl. Mater. Energy. 9 (2016) 598–603. doi:10.1016/j.nme.2016.02.001.
[437] S. Panayotis, T. Hirai, V. Barabash, A. Durocher, et al., Nucl. Mater. Energy. 12 (2017) 200–204. doi:10.1016/j.nme.2016.10.025.
[438] S.W.H. Yih, C.T. Wang, Plenum Press, 1979. https://archive.org/details/Tungsten (accessed August 22, 2018).
[439] A. Bose, H. Zhang, P. Kemp, R.M. German, in: Adv. Powder Metall., 1990: pp. 401–413.
[440] J. Song, B. Yan, W. Wang, C. Liu, et al., in: World PM 2016 Congr. Exhib., 2016.
[441] R. Li, M. Qin, C. Liu, H. Huang, et al., Int. J. Refract. Met. Hard Mater. 62 (2017) 42–46. doi:10.1016/j.ijrmhm.2016.10.015.
[442] S. Antusch, J. Reiser, J. Hoffmann, A. Onea, Energy Technol. 5 (2017) 1064–1070. doi:10.1002/ente.201600571.
[443] X. Qu, J. Fan, B. Huang, in: ASM Proc. Heat Treat., 2000: pp. 985–988. http://www.scopus.com/inward/record.url?eid=2-s2.0-1442302747&partnerID=40&md5=92d407d176d369f11adac624a7a02e2a.
[444] I.H. Moon, Met. Powder Rep. 56 (2001) 39.
[445] C.M. Wang, J.J. Cardarella, K.R. Miller, C.L. Trybus, in: Adv. Powder Metall. Part. Mater., 2001: pp. 1616–1628.
[446] P. Suri, S. V. Atre, R.M. German, J.P. de Souza, Mater. Sci. Eng. A. 356 (2003) 337–344. doi:10.1016/S0921-5093(03)00146-1.
[447] J. Fan, B. Huang, X. Qu, J. Adv. Mater. 36 (2004) 72–74.
[448] A. Bose, R.J. Dowding, in: Adv. Powder Metall. Part. Mater. - 2005, Proc. 2005 Int. Conf. Powder Metall. Part. Mater. PowderMet 2005, 2005: pp. 72–83.
[449] B. Zeep, S. Rath, V. Piotter, P. Norajitra, et al., in: Proc. 6th Int. Conf. Tungsten, Refract. Hardmetals, 2006: pp. 312–320.
[450] W. Wang, J. Song, B. Yan, Y. Yu, Met. Powder Rep. 71 (2016) 441–444. doi:10.1016/j.mprp.2016.10.066.
[451] C. Ren, Z.Z. Fang, M. Koopman, B. Butler, et al., Int. J. Refract. Met. Hard Mater. 75 (2018) 170–183. doi:10.1016/j.ijrmhm.2018.04.012.
[452] E. Pink, L. Bartha, Elsevier, London, 1989.
[453] C. Yin, D. Terentyev, T. Pardoen, A. Bakaeva, et al., Int. J. Refract. Met. Hard Mater. 75 (2018). doi:10.1016/j.ijrmhm.2018.04.003.
[454] J. Riesch, T. Höschen, A. Galatanu, J.-H. You, in: ICCM Int. Conf. Compos. Mater., 2011: pp. 1–6.
[455] J. Riesch, T. Höschen, C. Linsmeier, S. Wurster, et al., in: Phys. Scr., 2014. doi:10.1088/0031-8949/2014/T159/014031.
[456] L. Zhang, Y. Jiang, Q. Fang, R. Liu, et al., Metals (Basel). 7 (2017) 249. doi:10.3390/met7070249.
[457] H. Gietl, J. Riesch, J.W. Coenen, T. Höschen, et al., Fusion Eng. Des. 124 (2017) 396–400. doi:10.1016/j.fusengdes.2017.02.054.
[458] J. Riesch, A. Feichtmayer, M. Fuhr, J. Almanstötter, et al., in: Phys. Scr., 2017: p. 7. doi:10.1088/1402-4896/aa891d.
[459] R. Neu, J. Riesch, A. V. Müller, M. Balden, et al., Nucl. Mater. Energy. 12 (2017) 1308–1313. doi:10.1016/j.nme.2016.10.018.
[460] H. Gietl, A. v. Müller, J.W. Coenen, M. Decius, et al., J. Compos. Mater. (2018). doi:10.1177/0021998318771149.
[461] Y. Mao, J.W. Coenen, J. Riesch, S. Sistla, et al., Compos. Part A Appl. Sci. Manuf. 107 (2018) 342–353. doi:10.1016/j.compositesa.2018.01.022.
[462] J.W. Coenen, Y. Mao, S. Sistla, J. Riesch, et al., Nucl. Mater. Energy. 15 (2018) 214–219. doi:10.1016/j.nme.2018.05.001.
[463] J. Riesch, J.Y. Buffiere, T. Höschen, M. Scheel, et al., Nucl. Mater. Energy. 15 (2018) 1–12. doi:10.1016/j.nme.2018.03.007.
[464] J. Reiser, M. Rieth, A. Möslang, B. Dafferner, et al., J. Nucl. Mater. 436 (2013) 47–55. doi:10.1016/j.jnucmat.2013.01.295.
[465] J. Reiser, P. Franke, T. Weingärtner, J. Hoffmann, et al., Int. J. Refract. Met. Hard Mater. 51 (2015) 264–274. doi:10.1016/j.ijrmhm.2015.04.032.
[466] J. Reiser, M. Rieth, A. Möslang, H. Greuner, et al., Adv. Eng. Mater. 17 (2015) 491–501. doi:10.1002/adem.201400204.
[467] L.M. Garrison, Y. Katoh, L.L. Snead, T.S. Byun, et al., J. Nucl. Mater. 481 (2016) 134–146. doi:10.1016/j.jnucmat.2016.09.020.
[468] J. Reiser, L. Garrison, H. Greuner, J. Hoffmann, et al., Int. J. Refract. Met. Hard Mater. 69 (2017) 66–109. doi:10.1016/j.ijrmhm.2017.07.013.
[469] T. Weissgaerber, B. Kloeden, B. Kieback, in: Proc.Powder Metall. World Congr. Exhib., 2010: pp. 377–83. https://www.mendeley.com/library/.
[470] N. Ordás, I. Iturriza, F. Koch, S. Lindig, et al., in: Proc. Int. Euro Powder Metall. Congr. Exhib. Euro PM 2012, 2012: pp. 1–6.
[471] P. López-Ruiz, N. Ordás, I. Iturriza, M. Walter, et al., J. Nucl. Mater. 442 (2013). doi:10.1016/j.jnucmat.2012.12.018.
[472] A. Calvo, C. Garcï¿½a-Rosales, F. Koch, N. Ordï¿½s, et al., Nucl. Mater. Energy. 9 (2016) 422–429. doi:10.1016/j.nme.2016.06.002.
[473] A. Litnovsky, T. Wegener, F. Klein, C. Linsmeier, et al., Nucl. Fusion. 57 (2017). doi:10.1088/1741-4326/aa6816.
[474] T. Wegener, F. Klein, A. Litnovsky, M. Rasinski, et al., Fusion Eng. Des. 124 (2017) 183–186. doi:10.1016/j.fusengdes.2017.03.072.
[475] F. Klein, T. Wegener, A. Litnovsky, M. Rasinski, et al., Nucl. Mater. Energy. 15 (2018) 226–231. doi:10.1016/j.nme.2018.05.003.
[476] A. Calvo, K. Schlueter, E. Tejado, G. Pintsuk, et al., Int. J. Refract. Met. Hard Mater. 73 (2018) 29–37. doi:10.1016/j.ijrmhm.2018.01.018.
[477] R.K. Ham, T.A. Place, J. Mech. Phys. Solids. 14 (1966) 271–276. doi:10.1016/0022-5096(66)90023-8.
[478] J.H. You, H. Bolt, J. Nucl. Mater. 307–311 (2002) 74–78. doi:10.1016/S0022-3115(02)01176-5.
[479] S. Guo, G. He, G. Liu, Z. Yang, et al., Mater. Des. 87 (2015) 901–904. doi:10.1016/j.matdes.2015.08.115.
[480] J. Hohe, S. Fliegener, C. Findeisen, J. Reiser, et al., J. Nucl. Mater. 470 (2016) 13–29. doi:10.1016/j.jnucmat.2015.11.056.
[481] Z. Yang, W. Zhe, Rare Met. Mater. Eng. 45 (2016) 2513–2518. doi:10.1016/S1875-5372(17)30025-5.
[482] V.E. Ivanov, A.I. Somov, Sov. Powder Metall. Met. Ceram. 9 (1970) 491–494. doi:10.1007/BF00802618.
[483] M.J. Bomford, A. Kelly, Fibre Sci. Technol. 4 (1971) 1–8. doi:10.1016/0015-0568(71)90007-8.
[484] K.K. Chawla, Metallography. 6 (1973) 155–169. doi:10.1016/0026-0800(73)90007-4.
[485] S. Ochiai, M. Mizuhara, Y. Murakami, J. Japan Inst. Met. 37 (1973) 208–215. doi:10.2320/jinstmet1952.37.2_208.
[486] K. Chawla, C.F. De Mendonca, Met. ABM. 29 (1973) 719–725.
[487] Y. Umakoshi, K. Nakai, T. Yamane, Metall. Trans. 5 (1974) 1250–1251. doi:10.1007/BF02644341.
[488] S. Ochiai, K. Osamura, Zeitschrift Fuer Met. Res. Adv. Tech. 77 (1986) 255–259.
[489] T. Ohira, T. Kishi, H. Miyashita, Y. Kagawa, et al., Trans. Japan Inst. Met. 27 (1986) 484–495. doi:10.2320/matertrans1960.27.484.
[490] R. Jedamzik, A. Neubrand, J. Rödel, J. Mater. Sci. 35 (2000) 477–486. doi:10.1023/A:1004735904984.
[491] O. Ozer, J.M. Missiaen, C. Pascal, S. Lay, et al., 2007. doi:10.4028/www.scientific.net/MSF.534-536.1569.
[492] F.L. Chong, J.L. Chen, Z.J. Zhou, J.G. Li, Fusion Sci. Technol. 53 (2008) 854–859. doi:10.13182/FST08-A1740.

[493] J.J. Raharijaona, J.M. Missiaen, R. Mitteau, A. Thomazic, 2009. doi:10.4028/www.scientific.net/MSF.631-632.279.
[494] J. McDonald, J. Hsieh, S. Satapathy, IEEE Trans. Plasma Sci. 39 (2011) 390–393. doi:10.1109/TPS.2010.2081383.
[495] P. Tian, Y. Feng, M. Xia, L. Zhao, et al., Rare Met. (2017) 1–8. doi:10.1007/s12598-017-0939-0.
[496] H. Salavati, H. Mohammadi, A. Yusefi, F. Berto, Theor. Appl. Fract. Mech. (2017). doi:10.1016/j.tafmec.2017.06.013.
[497] D.B. Miracle, O.N. Senkov, Acta Mater. 122 (2017) 448–511. doi:10.1016/j.actamat.2016.08.081.
[498] H.W. Yao, J.W. Qiao, M.C. Gao, J.A. Hawk, et al., Mater. Sci. Eng. A. 674 (2016) 203–211. doi:10.1016/j.msea.2016.07.102.
[499] O.N. Senkov, D. Isheim, D.N. Seidman, A.L. Pilchak, Entropy. 18 (2016) 1–13. doi:10.3390/e18030102.
[500] M.H. Tsai, J.W. Yeh, Mater. Res. Lett. 2 (2014) 107–123. doi:10.1080/21663831.2014.912690.
[501] G.H.H. Kinchin, M.W.W. Thompson, J. Nuc. Energy. 6 (1958) 275–284.
[502] H. Schultz, D. Erholung, S. Iii, A. Aktivierungsenergie, et al., Acta Metall. 12 (1964) 649–664. doi:10.1016/0001-6160(64)90037-9.
[503] M.K. Sinha, E.W. Müller, J. Appl. Phys. 35 (1964) 1256–1261. doi:10.1063/1.1713604.
[504] D.J. Littler, G.B.C.E.G. Board, Butterworths, 1962. https://books.google.de/books?id=j002AQAAIAAJ.
[505] H. Bowkett, J. Hren, B. Ralph, in: Third Eur. Reg. Conf. Electron Microsc. Vol. A, 1964: p. 191.
[506] M. Attardo, J.M. Galligan, Phys. Status Solidi. 16 (1966) 449–457. doi:10.1002/pssb.19660160209.
[507] D. Jeannotte, J.M. Galligan, Phys. Rev. Lett. 19 (1967) 232–233. doi:10.1103/PhysRevLett.19.232.
[508] L.K. Keys, J.P. Smith, J. Moteff, Scr. Metall. 1 (1967) 71–72. doi:10.1016/0036-9748(67)90017-8.
[509] L.K. Keys, J. Moteff, Phys. Lett. 29A (1969) 706–707. doi:10.1016/0375-9601(69)90217-5.
[510] L.K. Keys, J. Moteff, J. Nucl. Mater. 34 (1970) 260–280. doi:10.1016/0022-3115(70)90193-5.
[511] L.K. Keys, J.P. Smith, J. Moteff, J. Nucl. Mater. 33 (1969) 337–339. doi:10.1016/0022-3115(69)90032-4.
[512] D. Jeannotte, J.M. Galligan, Acta Metall. 18 (1970) 71–79. doi:10.1016/0001-6160(70)90070-2.
[513] H. Schultz, Mater. Sci. Eng. 3 (1968) 189–219. doi:10.1016/0025-5416(68)90013-X.
[514] K. Lacefield, J. Moteff, J.P. Smith, Philos. Mag. 13 (1966) 1079–1081. doi:10.1080/14786436608213157.
[515] R.C. Rau, Philos. Mag. 18 (1968) 1079–1084. doi:10.1080/14786436808227526.
[516] R.C. Rau, R.L. Ladd, J. Moteff, J. Nucl. Mater. 33 (1969) 324–327. doi:10.1016/0022-3115(69)90029-4.
[517] V.K. Sikka, J. Moteff, J. Appl. Phys. 43 (1972) 4942–4944. doi:10.1063/1.1661050.
[518] V.K. Sikka, J. Moteff, J. Nucl. Mater. 46 (1973) 217–219. doi:10.1016/0022-3115(73)90139-6.
[519] J. Matolich, H. Nahm, J. Moteff, Scr. Metall. 8 (1974) 837–841. doi:10.1016/0036-9748(74)90304-4.
[520] V.K. Sikka, J. Moteff, Met. Trans. 5 (1974) 1514–1517. doi:10.1007/BF02646643.
[521] F. Lee, J. Matolich, J. Moteff, Radiat. Eff. 60 (1982) 53–59. doi:10.1080/00337578208242775.
[522] J.M. Steichen, J. Nucl. Mater. 60 (1976) 13–19. doi:10.1016/0022-3115(76)90112-4.
[523] M. Kangilaski, Washington, D.C., 1971.
[524] M. Fukuda, N.A.P. Kiran Kumar, T. Koyanagi, L.M. Garrison, et al., J. Nucl. Mater. 479 (2016) 249–254. doi:10.1016/j.jnucmat.2016.06.051.
[525] R. Herschitz, D.. Seidman, Acta Metall. 32 (1984) 1141–1154. doi:10.1016/0001-6160(84)90121-4.
[526] C. Vitanza, T.E. Stien, J. Nucl. Mater. 139 (1986) 11–18. doi:10.1016/0022-3115(86)90158-3.
[527] I. V. Gorynin, V.A. Ignatov, V. V. Rybin, S.A. Fabritsiev, et al., J. Nucl. Mater. 191–194 (1992) 421–425. doi:10.1016/S0022-3115(09)80079-2.
[528] J.C. He, A. Hasegawa, K. Abe, J. Nucl. Mater. 377 (2008) 348–351. doi:10.1016/j.jnucmat.2008.03.014.
[529] T. Tanno, A. Hasegawa, J.C. He, M. Fujiwara, et al., J. Nucl. Mater. 386–388 (2009) 218–221. doi:10.1016/j.jnucmat.2008.12.091.
[530] A. Hasegawa, M. Fukuda, T. Tanno, S. Nogami, Mater. Trans. 54 (2013) 466–471. doi:10.2320/matertrans.MG201208.
[531] A. Hasegawa, M. Fukuda, S. Nogami, K. Yabuuchi, Fusion Eng. Des. 89 (2014) 1568–1572. doi:10.1016/j.fusengdes.2014.04.035.
[532] Y. Nemoto, A. Hasegawa, M. Satou, K. Abe, et al., J. Nucl. Mater. 324 (2004) 62–70. doi:10.1016/j.jnucmat.2003.09.007.
[533] M. Fujitsuka, B. Tsuchiya, I. Mutoh, T. Tanabe, et al., J. Nucl. Mater. 283–287 (2000) 1148–1151. doi:10.1016/S0022-3115(00)00170-7.
[534] M. Fujitsuka, I. Mutoh, T. Tanabe, B. Tsuchiya, et al., J. Nucl. Mater. 307–311 (2002) 426–430. doi:10.1016/S0022-3115(02)01099-1.
[535] M. Fukuda, N.A.P. Kiran Kumar, T. Koyanagi, L.M. Garrison, et al., J. Nucl. Mater. 479 (2016) 249–254. doi:10.1016/j.jnucmat.2016.06.051.
[536] X. Hu, T. Koyanagi, M. Fukuda, N.A.P.K. Kumar, et al., J. Nucl. Mater. 480 (2016) 235–243. doi:10.1016/j.jnucmat.2016.08.024.
[537] W. Van Renterghem, I. Uytdenhouwen, J. Nucl. Mater. 477 (2016) 77–84. doi:10.1016/j.jnucmat.2016.05.008.
[538] T. Toyama, K. Ami, K. Inoue, Y. Nagai, et al., J. Nucl. Mater. 499 (2018) 464–470. doi:10.1016/j.jnucmat.2017.11.022.
[539] R.A. Pitts, S. Carpentier, F. Escourbiac, T. Hirai, et al., J. Nucl. Mater. 438 (2013). doi:10.1016/j.jnucmat.2013.01.008.
[540] R. Behrisch, G. Federici, A. Kukushkin, D. Reiter, J. Nucl. Mater. 313–316 (2003) 388–392. doi:10.1016/S0022-3115(02)01580-5.
[541] Rainer Behrisch and Wolfgang Eckstein, ed., Springer-Verlag, Berlin Heidelberg, 2007.
[542] R.J. Hawryluk, K. Bol, N. Bretz, D. Dimock, et al., Nucl. Fusion. 19 (1979) 1307–1317. doi:10.1088/0029-5515/19/10/002.
[543] Y. Ueda, H.Y. Peng, H.T. Lee, N. Ohno, et al., J. Nucl. Mater. 442 (2013). doi:10.1016/j.jnucmat.2012.10.023.
[544] Y. Ueda, J.W. Coenen, G. De Temmerman, R.P. Doerner, et al., Fusion Eng. Des. 89 (2014). doi:10.1016/j.fusengdes.2014.02.078.
[545] Y. Ueda, K. Schmid, M. Balden, J.W. Coenen, et al., Nucl. Fusion. 57 (2017) 092006. doi:10.1088/1741-4326/aa6b60.
[546] Y. Ueda, N. Yamashita, K. Omori, H.T. Lee, et al., J. Nucl. Mater. 511 (2018) 605–609. doi:10.1016/j.jnucmat.2018.04.024.
[547] N. Yoshida, H. Iwakiri, K. Tokunaga, T. Baba, in: J. Nucl. Mater., 2005: pp. 946–950. doi:10.1016/j.jnucmat.2004.10.162.
[548] H. Iwakiri, K. Morishita, N. Yoshida, J. Nucl. Mater. 307–311 (2002) 135–138. doi:10.1016/S0022-3115(02)01178-9.
[549] M.S. Abd El Keriem, D.P. Van Der Werf, F. Pleiter, Phys. Rev. B. 47 (1993) 14771–14777. doi:10.1103/PhysRevB.47.14771.
[550] K. Ohsawa, J. Goto, M. Yamakami, M. Yamaguchi, et al., Phys. Rev. B - Condens. Matter Mater. Phys. 82 (2010) 1–6. doi:10.1103/PhysRevB.82.184117.
[551] M. Miyamoto, S. Mikami, H. Nagashima, N. Iijima, et al., J. Nucl. Mater. 463 (2015) 333–336. doi:10.1016/j.jnucmat.2014.10.098.
[552] M. Miyamoto, D. Nishijima, M.J. Baldwin, R.P. Doerner, et al., J. Nucl. Mater. 415 (2011) S657–S660. doi:10.1016/j.jnucmat.2011.01.008.
[553] E. Bernard, R. Sakamoto, N. Yoshida, H. Yamada, J. Nucl. Mater. 463 (2015) 316–319. doi:10.1016/j.jnucmat.2014.11.041.
[554] Q. Yang, D. Liu, H. Fan, X. Li, et al., Nucl. Instruments Methods Phys. Res. Sect. B Beam Interact. with Mater. Atoms. 325 (2014) 73–78. doi:10.1016/j.nimb.2014.02.011.
[555] S. Takamura, N. Ohno, D. Nishijima, S. Kajita, Plasma Fusion Res. 1 (2006) 051–051. doi:10.1585/pfr.1.051.

[556] M.J. Baldwin, R.P. Doerner, J. Nucl. Mater. 404 (2010) 165–173. doi:10.1016/j.jnucmat.2010.06.034.
[557] G.M. Wright, D. Brunner, M.J. Baldwin, R.P. Doerner, et al., Nucl. Fusion. 52 (2012). doi:10.1088/0029-5515/52/4/042003.
[558] M.Y. Ye, S. Takamura, N. Ohno, J. Nucl. Mater. 241–243 (1997) 1243–1247. doi:10.1016/S0022-3115(96)00707-6.
[559] S. Masuzaki, N. Ohno, S. Takamura, J. Nucl. Mater. 223 (1995) 286–293. doi:10.1016/0022-3115(94)00685-7.
[560] S. Kajita, S. Takamura, N. Ohno, D. Nishijima, et al., Nucl. Fusion. 47 (2007) 1358–1366. doi:10.1088/0029-5515/47/9/038.
[561] W. Sakaguchi, S. Kajita, N. Ohno, M. Takagi, J. Nucl. Mater. 390–391 (2009) 1149–1152. doi:10.1016/j.jnucmat.2009.01.276.
[562] S. Kajita, N. Ohno, W. Sakaguchi, M. Takagi, Plasma Fusion Res. 4 (2009) 004–004. doi:10.1585/pfr.4.004.
[563] M.J. Baldwin, R.P. Doerner, Nucl. Fusion. 48 (2008). doi:10.1088/0029-5515/48/3/035001.
[564] S. Kajita, W. Sakaguchi, N. Ohno, N. Yoshida, et al., Nucl. Fusion. 49 (2009). doi:10.1088/0029-5515/49/9/095005.
[565] S. Kajita, N. Yoshida, R. Yoshihara, N. Ohno, et al., J. Nucl. Mater. 418 (2011) 152–158. doi:10.1016/j.jnucmat.2011.06.026.
[566] M.J. Baldwin, R.P. Doerner, D. Nishijima, K. Tokunaga, et al., J. Nucl. Mater. 390–391 (2009) 886–890. doi:10.1016/j.jnucmat.2009.01.247.
[567] G.D.T.A. va. den B.S.L.J. va. der M.J.N. va. E.W.M.M. d. K.A.Z. van EmmichovenJ.J.Zielinski, Fusion Eng. Des. 88 (2013) 483–487.
[568] G. De Temmerman, K. Bystrov, R.P. Doerner, L. Marot, et al., J. Nucl. Mater. 438 (2013) S78–S83. doi:10.1016/j.jnucmat.2013.01.012.
[569] R.P. Doerner, M.J. Baldwin, P.C. Stangeby, Nucl. Fusion. 51 (2011). doi:10.1088/0029-5515/51/4/043001.
[570] G.M. Wright, D. Brunner, M.J. Baldwin, K. Bystrov, et al., J. Nucl. Mater. 438 (2013) S84–S89. doi:10.1016/j.jnucmat.2013.01.013.
[571] Y. Ueda, K. Miyata, Y. Ohtsuka, H.T. Lee, et al., J. Nucl. Mater. 415 (2011). doi:10.1016/j.jnucmat.2010.08.019.
[572] M. Tokitani, S. Kajita, S. Masuzaki, Y. Hirahata, et al., Nucl. Fusion. 51 (2011). doi:10.1088/0029-5515/51/10/102001.
[573] D.L. Rudakov, C.P.C. Wong, R.P. Doerner, G.M. Wright, et al., Phys. Scr. T167 (2016) 14055. doi:10.1088/0031-8949/T167/1/014055.
[574] S. Brezinsek, A. Hakola, H. Greuner, M. Balden, et al., Nucl. Mater. Energy. 12 (2017) 575–581. doi:10.1016/j.nme.2016.11.002.
[575] A. Kreter, S. Brezinsek, T. Hirai, A. Kirschner, et al., Plasma Phys. Control. Fusion. 50 (2008). doi:10.1088/0741-3335/50/9/095008.
[576] D. Nishijima, M.J. Baldwin, R.P. Doerner, J.H. Yu, J. Nucl. Mater. 415 (2011) 96–99. doi:10.1016/j.jnucmat.2010.12.017.
[577] S. Kajita, S. Takamura, N. Ohno, Nucl. Fusion. 49 (2009) 18–22. doi:10.1088/0029-5515/49/3/032002.
[578] S. Kajita, G. De Temmerman, T. Morgan, S. van Eden, et al., Nucl. Fusion. 54 (2014) 033005. doi:10.1088/0029-5515/54/3/033005.
[579] S. Takamura, T. Miyamoto, Plasma Fusion Res. 6 (2011) 6–7. doi:10.1585/pfr.6.1202005.
[580] S. Kajita, N. Ohno, M. Yajima, J. Kato, J. Nucl. Mater. 440 (2013) 55–62. doi:10.1016/j.jnucmat.2013.04.040.
[581] D. Nishijima, R.P. Doerner, D. Iwamoto, Y. Kikuchi, et al., J. Nucl. Mater. 434 (2013) 230–234. doi:10.1016/j.jnucmat.2012.10.042.
[582] J.H. Yu, M.J. Baldwin, R.P. Doerner, T. Dittmar, et al., J. Nucl. Mater. 463 (2015) 299–302. doi:10.1016/j.jnucmat.2014.10.035.
[583] S. Kajita, N. Ohno, S. Takamura, J. Nucl. Mater. 415 (2011) S42–S45. doi:10.1016/j.jnucmat.2010.08.030.
[584] S. Kajita, N. Ohno, N. Yoshida, R. Yoshihara, et al., Plasma Phys. Control. Fusion. 54 (2012) 035009 (9pp). doi:10.1088/0741-3335/54/3/035009.
[585] D.U.B. Aussems, D. Nishijima, C. Brandt, H.J. Van Der Meiden, et al., J. Nucl. Mater. 463 (2015) 303–307. doi:10.1016/j.jnucmat.2014.09.009.
[586] K.D. Hammond, Mater. Res. Express. 4 (2017) 104002. doi:10.1088/2053-1591/aa8c22.
[587] S. Takamura, Y. Uesugi, Appl. Surf. Sci. 356 (2015) 888–897. doi:10.1016/j.apsusc.2015.08.112.
[588] K. Omori, A.M. Ito, K. Shiga, N. Yamashita, et al., J. Appl. Phys. 121 (2017) 155301. doi:10.1063/1.4981128.
[589] K. Omori, A.M. Ito, I. Mun, N. Yamashita, et al., Nucl. Mater. Energy. 16 (2018) 226–229. doi:10.1016/j.nme.2018.07.003.
[590] A. Lasa, K.O.E. Henriksson, K. Nordlund, Nucl. Instruments Methods Phys. Res. Sect. B Beam Interact. with Mater. Atoms. 303 (2013) 156–161. doi:10.1016/j.nimb.2012.11.029.
[591] F. Sefta, K.D. Hammond, N. Juslin, B.D. Wirth, Nucl. Fusion. 53 (2013). doi:10.1088/0029-5515/53/7/073015.
[592] A.M. Ito, A. Takayama, Y. Oda, T. Tamura, et al., Nucl. Fusion. 55 (2015). doi:10.1088/0029-5515/55/7/073013.
[593] S. Kajita, S. Kawaguchi, N. Ohno, N. Yoshida, Sci. Rep. 8 (2018) 1–9. doi:10.1038/s41598-017-18476-7.
[594] T. Tanabe, Phys. Scr. T159 (2014) 014044. doi:10.1088/0031-8949/2014/T159/014044.
[595] J. Roth, K. Schmid, Phys. Scr. T. T145 (2011) 014031. doi:10.1088/0031-8949/2011/T145/014031.
[596] R.A. Causet, T.J. Venhaus, Phys. Scr. T94 (2001) 9. doi:10.1238/Physica.Topical.094a00009.
[597] G.H. Lu, H.B. Zhou, C.S. Becquart, Nucl. Fusion. 54 (2014) 086001. doi:10.1088/0029-5515/54/8/086001.
[598] K. Schmid, J. Bauer, T. Schwarz-Selinger, S. Markelj, et al., Phys. Scr. 2017 (2017) 014037. doi:10.1088/1402-4896/aa8de0.
[599] G. De Temmerman, T. Hirai, R.A. Pitts, Plasma Phys. Control. Fusion. 60 (2018). doi:10.1088/1361-6587/aaaf62.
[600] J. Roth, E. Tsitrone, A. Loarte, T. Loarer, et al., J. Nucl. Mater. 390–391 (2009) 1–9. doi:10.1016/j.jnucmat.2009.01.037.
[601] G.R. Tynan, R.P. Doerner, J. Barton, R. Chen, et al., Nucl. Mater. Energy. 12 (2017) 164–168. doi:10.1016/j.nme.2017.03.024.
[602] T. Watanabe, T. Kaneko, N. Matsunami, N. Ohno, et al., J. Nucl. Mater. 463 (2015) 1049–1052. doi:10.1016/j.jnucmat.2014.12.011.
[603] O. V. Ogorodnikova, J. Roth, M. Mayer, J. Appl. Phys. 103 (2008) 034902. doi:10.1063/1.2828139.
[604] V.K. Alimov, J. Roth, M. Mayer, J. Nucl. Mater. 337–339 (2005) 619–623. doi:10.1016/j.jnucmat.2004.10.082.
[605] L. Gao, W. Jacob, U. Von Toussaint, A. Manhard, et al., Nucl. Fusion. 57 (2017) 016026. doi:10.1088/0029-5515/57/1/016026.
[606] W.R. Wampler, R.P. Doerner, Nucl. Fusion. 49 (2009) 115023. doi:10.1088/0029-5515/49/11/115023.
[607] Y.Z. Jia, W. Liu, B. Xu, S.L. Qu, et al., Nucl. Fusion. 57 (2017) 034003. doi:10.1088/1741-4326/57/3/034003.
[608] D. Terentyev, A. Dubinko, A. Bakaeva, G. De Temmerman, Fusion Eng. Des. 124 (2017) 405–409. doi:10.1016/j.fusengdes.2017.02.043.
[609] R.P. Doerner, M.J. Baldwin, T.C. Lynch, J.H. Yu, Nucl. Mater. Energy. 9 (2016) 89–92. doi:10.1016/j.nme.2016.04.008.
[610] M.J. Baldwin, R.P. Doerner, W.R. Wampler, D. Nishijima, et al., Nucl. Fusion. 51 (2011) 103021. doi:10.1088/0029-5515/51/10/103021.
[611] M. Balden, A. Manhard, S. Elgeti, J. Nucl. Mater. 452 (2014) 248–256. doi:10.1016/j.jnucmat.2014.05.018.
[612] S. Lindig, M. Balden, V.K. Alimov, T. Yamanishi, et al., Phys. Scr. T. T138 (2009) 014040. doi:10.1088/0031-8949/2009/T138/014040.
[613] L. Buzi, G. De Temmerman, B. Unterberg, M. Reinhart, et al., J. Nucl. Mater. 455 (2014) 316–319. doi:10.1016/j.jnucmat.2014.06.059.
[614] L. Buzi, G. De Temmerman, D. Matveev, M. Reinhart, et al., J. Nucl. Mater. 495 (2017) 211–219. doi:10.1016/j.jnucmat.2017.08.026.
[615] O. V. Ogorodnikova, J. Roth, M. Mayer, J. Nucl. Mater. 313–316 (2003) 469–477. doi:10.1016/S0022-3115(02)01375-2.

[616] O. V. Ogorodnikova, S. Markelj, U. Von Toussaint, J. Appl. Phys. 119 (2016) 054901. doi:10.1063/1.4940678.
[617] C.S. Corr, S. O'Ryan, C. Tanner, M. Thompson, et al., Nucl. Mater. Energy. 12 (2017) 1336–1341. doi:10.1016/j.nme.2017.04.012.
[618] M. Miyamoto, D. Nishijima, Y. Ueda, R.P. Doerner, et al., Nucl. Fusion. 49 (2009) 065035. doi:10.1088/0029-5515/49/6/065035.
[619] N. Juslin, B.D. Wirth, J. Nucl. Mater. 438 (2013) S1221–S1223. doi:10.1016/j.jnucmat.2013.01.270.
[620] M.J. Baldwin, R.P. Doerner, Nucl. Fusion. 57 (2017) 076031. doi:10.1088/1741-4326/aa70b1.
[621] H.T. Lee, H. Tanaka, Y. Ohtsuka, Y. Ueda, J. Nucl. Mater. 415 (2011) S696–S700. doi:10.1016/j.jnucmat.2010.12.023.
[622] R. Rayaprolu, S. Möller, C. Linsmeier, S. Spellerberg, Nucl. Mater. Energy. 9 (2016) 29–35. doi:10.1016/j.nme.2016.09.008.
[623] S.J. Zinkle, L.L. Snead, Scr. Mater. 143 (2018) 154–160. doi:10.1016/j.scriptamat.2017.06.041.
[624] T. Schwarz-Selinger, Nucl. Mater. Energy. 12 (2017) 683–688. doi:10.1016/j.nme.2017.02.003.
[625] O. V. Ogorodnikova, J. Appl. Phys. 118 (2015) 074902. doi:10.1063/1.4928407.
[626] M.H.J. T'Hoen, B. Tyburska-Püschel, K. Ertl, M. Mayer, et al., Nucl. Fusion. 52 (2012) 023008. doi:10.1088/0029-5515/52/2/023008.
[627] O. V. Ogorodnikova, V. Gann, J. Nucl. Mater. 460 (2015) 60–71. doi:10.1016/j.jnucmat.2015.02.004.
[628] B. Tyburska, V.K. Alimov, O. V. Ogorodnikova, K. Schmid, et al., J. Nucl. Mater. 395 (2009) 150–155. doi:10.1016/j.jnucmat.2009.10.046.
[629] V.K. Alimov, Y. Hatano, B. Tyburska-Püschel, K. Sugiyama, et al., J. Nucl. Mater. 441 (2013) 280–285. doi:10.1016/j.jnucmat.2013.06.005.
[630] S.J. Zinkle, B.N. Singh, J. Nucl. Mater. 199 (1993) 173–191. doi:10.1016/0022-3115(93)90140-T.
[631] Y. Hatano, M. Shimada, T. Otsuka, Y. Oya, et al., Nucl. Fusion. 53 (2013) 073006. doi:10.1088/0029-5515/53/7/073006.
[632] M.H.J. T Hoen, M. Mayer, A.W. Kleyn, H. Schut, et al., Nucl. Fusion. 53 (2013) 043003. doi:10.1088/0029-5515/53/4/043003.
[633] O. V. Ogorodnikova, K. Sugiyama, J. Nucl. Mater. 442 (2013) 518–527. doi:10.1016/j.jnucmat.2013.07.024.
[634] E. Markina, M. Mayer, A. Manhard, T. Schwarz-Selinger, J. Nucl. Mater. 463 (2015) 329–332. doi:10.1016/j.jnucmat.2014.12.005.
[635] S. Sakurada, K. Yuyama, Y. Uemura, H. Fujita, et al., Nucl. Mater. Energy. 9 (2016) 141–144. doi:10.1016/j.nme.2016.06.012.
[636] M.J. Simmonds, Y.Q. Wang, J.L. Barton, M.J. Baldwin, et al., J. Nucl. Mater. 494 (2017) 67–71. doi:10.1016/j.jnucmat.2017.06.010.
[637] H. Fujita, K. Yuyama, X. Li, Y. Hatano, et al., Phys. Scr. 2016 (2016) 014068. doi:10.1088/0031-8949/T167/1/014068.
[638] S. Cui, M. Simmonds, W. Qin, F. Ren, et al., J. Nucl. Mater. 486 (2017) 267–273. doi:10.1016/j.jnucmat.2017.01.023.
[639] S. Kajita, T. Yagi, K. Kobayashi, M. Tokitani, et al., Jpn. J. Appl. Phys. 55 (2016) 056203. doi:10.7567/JJAP.55.056203.
[640] E. Dechaumphai, J.L. Barton, J.R. Tesmer, J. Moon, et al., J. Nucl. Mater. 455 (2014) 56–60. doi:10.1016/j.jnucmat.2014.03.059.
[641] S. Qu, Y. Li, Z. Wang, Y. Jia, et al., J. Nucl. Mater. 484 (2017) 382–385. doi:10.1016/j.jnucmat.2016.11.029.
[642] S. Cui, Submitt. to J. Nucl. Mater. 2015 (2017) 2015.
[643] M. Roedig, W. Kuehnlein, J. Linke, D. Pitzer, et al., J. Nucl. Mater. 329–333 (2004) 766–770. doi:10.1016/j.jnucmat.2004.04.176.
[644] R.A. Pitts, S. Carpentier, F. Escourbiac, T. Hirai, et al., J. Nucl. Mater. 415 (2011) S957–S964. doi:10.1016/j.jnucmat.2011.01.114.
[645] R. Duwe, W. Kühnlein, H. Münstermann, in: Fusion Technol. 1994, Elsevier, 1995: pp. 355–358. doi:10.1016/B978-0-444-82220-8.50057-1.
[646] P. Majerus, R. Duwe, T. Hirai, W. Kühnlein, et al., Fusion Eng. Des. 75–79 (2005) 365–369. doi:10.1016/j.fusengdes.2005.06.058.
[647] H. Greuner, B. Boeswirth, J. Boscary, P. McNeely, J. Nucl. Mater. 367–370 B (2007) 1444–1448. doi:10.1016/j.jnucmat.2007.04.004.
[648] I.E. Garkusha, V.A. Makhlai, N.N. Aksenov, B. Bazylev, et al., Fusion Sci. Technol. 65 (2014) 186–193. doi:10.13182/FST13-668.
[649] A. Schmidt, A. Börger, K. Dominiczak, S. Keusemann, et al., EBEAM 2010 Int. Conf. High-Power Electron Beam Technol. (Reno, NV). (2010) 571.
[650] G. De Temmerman, M.A. Van Den Berg, J. Scholten, A. Lof, et al., Fusion Eng. Des. 88 (2013) 483–487. doi:10.1016/j.fusengdes.2013.05.047.
[651] A. Kreter, C. Brandt, A. Huber, S. Kraus, et al., Fusion Sci. Technol. 68 (2015) 8–14. doi:10.13182/FST14-906.
[652] X.X. Zhang, Q.Z. Yan, C.T. Yang, T.N. Wang, et al., Rare Met. 35 (2016) 566–570. doi:10.1007/s12598-014-0315-2.
[653] J.. Davis, V.. Barabash, A. Makhankov, L. Plöchl, et al., J. Nucl. Mater. 258–263 (1998) 308–312. doi:10.1016/S0022-3115(98)00285-2.
[654] M. Roedig, R. Duwe, J. Linke, A. Schuster, et al., Japan, 1998. http://inis.iaea.org/search/search.aspx?orig_q=RN:29053488.
[655] T. Hirai, F. Escourbiac, S. Carpentier-Chouchana, A. Durocher, et al., Phys. Scr. T159 (2014). doi:10.1088/0031-8949/2014/T159/014006.
[656] S. Banetta, B. Bellin, P. Lorenzetto, F. Zacchia, et al., Fusion Eng. Des. 98–99 (2015) 1211–1215. doi:10.1016/j.fusengdes.2015.01.016.
[657] P.T. Lang, A. Loarte, G. Saibene, L.R. Baylor, et al., Nucl. Fusion. 53 (2013). doi:10.1088/0029-5515/53/4/043004.
[658] A.W. Leonard, A. Herrmann, K. Itami, J. Lingertat, et al., J. Nucl. Mater. 266–269 (1999) 109–117. doi:10.1016/S0022-3115(98)00522-4.
[659] V. Barabash, J. Nucl. Mater. 329–333 (2004) 156–160. doi:10.1016/j.jnucmat.2004.04.015.
[660] A.W. Leonard, Phys. Plasmas. 090501 (2014). doi:10.1063/1.4894742.
[661] H. Würz, S. Pestchanyi, B. Bazylev, I. Landman, et al., J. Nucl. Mater. 290–293 (2001) 1138–1143. doi:10.1016/S0022-3115(00)00478-5.
[662] H. Bolt, V. Barabash, G. Federici, J. Linke, et al., J. Nucl. Mater. 307–311 (2002) 43–52. doi:10.1016/S0022-3115(02)01175-3.
[663] J.H. Yu, G. De Temmerman, R.P. Doerner, M.A. Van Den Berg, Phys. Scr. 2016 (2016). doi:10.1088/0031-8949/T167/1/014033.
[664] G. Pintsuk, A. Prokhodtseva, I. Uytdenhouwen, J. Nucl. Mater. 417 (2011) 481–486. doi:10.1016/j.jnucmat.2010.12.109.
[665] T. Loewenhoff, J. Linke, G. Pintsuk, C. Thomser, Fusion Eng. Des. 87 (2012) 1201–1205. doi:10.1016/j.fusengdes.2012.02.106.
[666] M. Wirtz, J. Linke, T. Loewenhoff, G. Pintsuk, et al., Nucl. Mater. Energy. 12 (2017) 148–155. doi:10.1016/j.nme.2016.12.024.
[667] W.D. Callister, 9th ed., Wiley, John & Sons, Inc., 2014.
[668] A. Suslova, O. El-Atwani, D. Sagapuram, S.S. Harilal, et al., Sci. Rep. 4 (2014) 1–11. doi:10.1038/srep06845.
[669] G.G. Van Eden, T.W. Morgan, H.J. Van Der Meiden, J. Matejicek, et al., Nucl. Fusion. 54 (2014). doi:10.1088/0029-5515/54/12/123010.
[670] C. Linsmeier, M. Rieth, J. Aktaa, T. Chikada, et al., Nucl. Fusion. 57 (2017). doi:10.1088/1741-4326/aa6f71.
[671] J.W. Coenen, Y. Mao, J. Almanstötter, A. Calvo, et al., Fusion Eng. Des. 124 (2017) 964–968. doi:10.1016/j.fusengdes.2016.12.006.
[672] G. Pintsuk, S. Antusch, M. Rieth, M. Wirtz, Phys. Scr. 2016 (2016). doi:10.1088/0031-8949/T167/1/014056.

11 List of figures

Fig. 18: Young's modulus (a) and shear modulus (b) for period 5 (Zr (Group 4) to Ag (Group11) and Period 6 (Hf (Group 5) to Au (Group 11)) elements at room temperature. Elements with long nano-fibers observed in our experiments are marked by circles.[546]
Fig. 19: Schematics of the experiments and pictures and micrographs of fuzzy fur like materials. (**a**) Schematic of the experimental setup. (**b**) Schematic of the sample exposed to ions. (**c**,**d**) Pictures of W largescale nano-fibers on a W substrate after an irradiation time of 3600 s from top and side view. The sample temperature, T_s, the incident ion energy, E_i, and the ion fluence, Φ, were 1200 K, 70 eV, and 1.8 x 10^{25} m^{-2}, respectively. (**e**,**f**) Pictures of Mo large-scale nano-fibers. The irradiation conditions were T_s = 1250 K, E_i = 70 eV, and Φ = 2.0 x 10^{25} m^{-2}. (**g**–**i**) Optical microscope micrographs of W large-scale fuzzy nanostructures. The irradiation conditions were T_s = 1300 K, E_i = 70 eV, and Φ = 2.8 x 10^{25} m^{-2}. The scale bar in (**c**–**f**) and (**g**–**i**) represents 2 and 0.1 mm, respectively [593].
Fig. 20: When examining the depth profile of retained (i.e. statically trapped) deuterium in plasma-exposed tungsten, three regions generally become evident: near-surface, plateau, and bulk region [603]. These regions are indicated on some experimental depth profiles as published by Alimov [604].
Fig. 21: Contrary to expectations, where one might assume at higher temperature, lower energy trap sites would not be populated and therefore retention would continuously decrease with temperature, a peak in retention in tungsten in the region around 400-700 K is measured [610].
Fig. 22: Comparison of the deuterium concentration at radiation-induced defects in W created by neutron irradiation in the high-flux isotope reactor (HFIR) at Oak Ridge National Laboratory (ORNL) [631], and by irradiation with 20 MeVW6+ and subsequently exposed to D plasma at sample temperature of 470 K [627].
Fig. 23: Thermal conductivity of pristine W and He plasma damaged W layer in bulk W, along with that of thin film before and after irradiation. The thermal conductivity of the damaged film is at least one order of magnitude lower than that of pristine bulk W, and is nearly temperature independent, suggesting the effect of defects introduced during He plasma bombardment [638].
Fig. 24: Schematic depiction of the temperature evolution during plasma discharges in a fusion reactor with different stationary heat loads (red line, increasing from left to right) and the temperature rise during transient events (blue line) which cause an additional fast increase of the surface temperature. (a) temperature increase due to stationary heat loads below DBTT; (b) temperature increase due to stationary heat loads between DBTT and T_{recr}; (c) temperature increase due to stationary heat loads above T_{recr}.
Fig. 25: Damage mappings of tungsten samples exposed to 100 ELM-like thermal shocks at different base temperatures and absorbed power densities with a pulse duration of 1ms and repetition frequency of 1 Hz [380]. a) tungsten samples with grain oriented perpendicular to the loaded surface (transversal); b) same tungsten samples as in (a) but recrystallized at 1600 °C for 1 h before the thermal shock exposure. The green line indicates the damage threshold of the material while the red box indicates the mechanical properties (written below) obtained in tensile tests.

Yoshio Ueda completed his PhD at University of Tokyo in 1986, followed by postdoctoral studies from Princeton Plasma Physics Laboratory. Then he started to work at Osaka University in 1987. He has been serving as the professor of Graduate School of Engineering, Osaka University since 2006. His current research field is plasma surface intereactions in fusion devices, mainly studies on tungsten as plasma facing materials.

Russell Doerner received degrees from Texas A&M University (B.S. in Physics, 1981) and the University of Wisconsin-Madison (M.S. in Materials Science, 1984 and Ph.D. in Electrical Engineering, 1988). Since that time he has performed experiments in the edge and scrape-off layer plasma of confinement machines throughout the world and has been involved in fundamental plasma-material interaction measurements conducted in various linear plasma devices. He has worked extensively with the IAEA in numerous plasma-material interactions coordinated research projects and presently leads the plasma-material interaction research program in the PISCES Laboratory at UCSD, and the US-EU Bilateral Collaboration on Mixed-Material Research for ITER.

Akira Hasegawa is a professor in the Department of Quantum Science and Energy Engineering, Faculty of Engineering, Tohoku University, Japan, since 2007. He has been studying neutron irradiation effects on materials including Tungsten-, Molybdenum-, Vanadium-alloys, and SiC/SiC composites using various type of fission reactors in Tohoku University since 1992. He is also studying irradiation behavior of Tungsten, reduced-acitivation-ferric steels, austenitic stainless steels using accelerators. His main scientific interests are material development and material evaluation during and after irradiation for fusion and fission reactors applications.

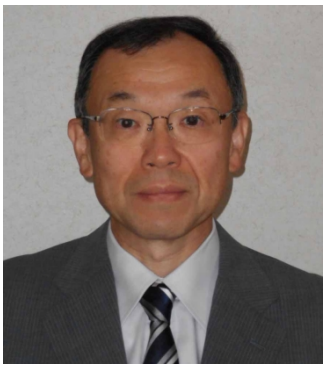

Michael Rieth is head of the department Metallic Materials in the Institute for Applied Materials, Karlsruhe Institute of Technology (KIT), Germany, since 2016. He received degrees from Karlsruhe University (M.S. in Electrical Engineering), Patras University (Ph.D. in Physics), started as senior scientist at KIT in 2002, and officiates various positions in the European Fusion Programme: co-chair of the EFDA Fusion Materials Group (2008-2013), leader of the EUROfusion Materials Project (2013-2016), leader of the Materials Irradiation Group (since 2016), member of the Scientific and Technical Advisory Committee (since 2019). His R&D topics address mainly applications in energy conversion and related large-scale projects (ITER, DEMO, concentrated solar power). This includes in particular the development of structural, high heat-flux and functional materials (steels, refractory alloys, beryllides, composites), materials technology (machining, joining, production routes), and irradiation defect studies (experiments, analysis, modelling).

Marius Wirtz is Head of High-Temperature Composite Materials section at the Forschungszentrum Jülich (FZJ), Microstructure and Properties of Materials (IEK-2) since 2016. He received degrees from University Bonn (M.S. in Physics), RWTH Aachen (Ph.D. in Physics) and started as postdoc research scientist at FZJ in 2012. His recent research topics in the field of refractory metals include transient high heat flux testing, hydrogen plasma loading, microstructure analysis, mechanical and thermo-physical characterization, and finite element modelling.